TGF-β Family Signaling in Tumor Angiogenesis

Eleftheriou, Nikolas

2017

Document Version:
Publisher's PDF, also known as Version of record

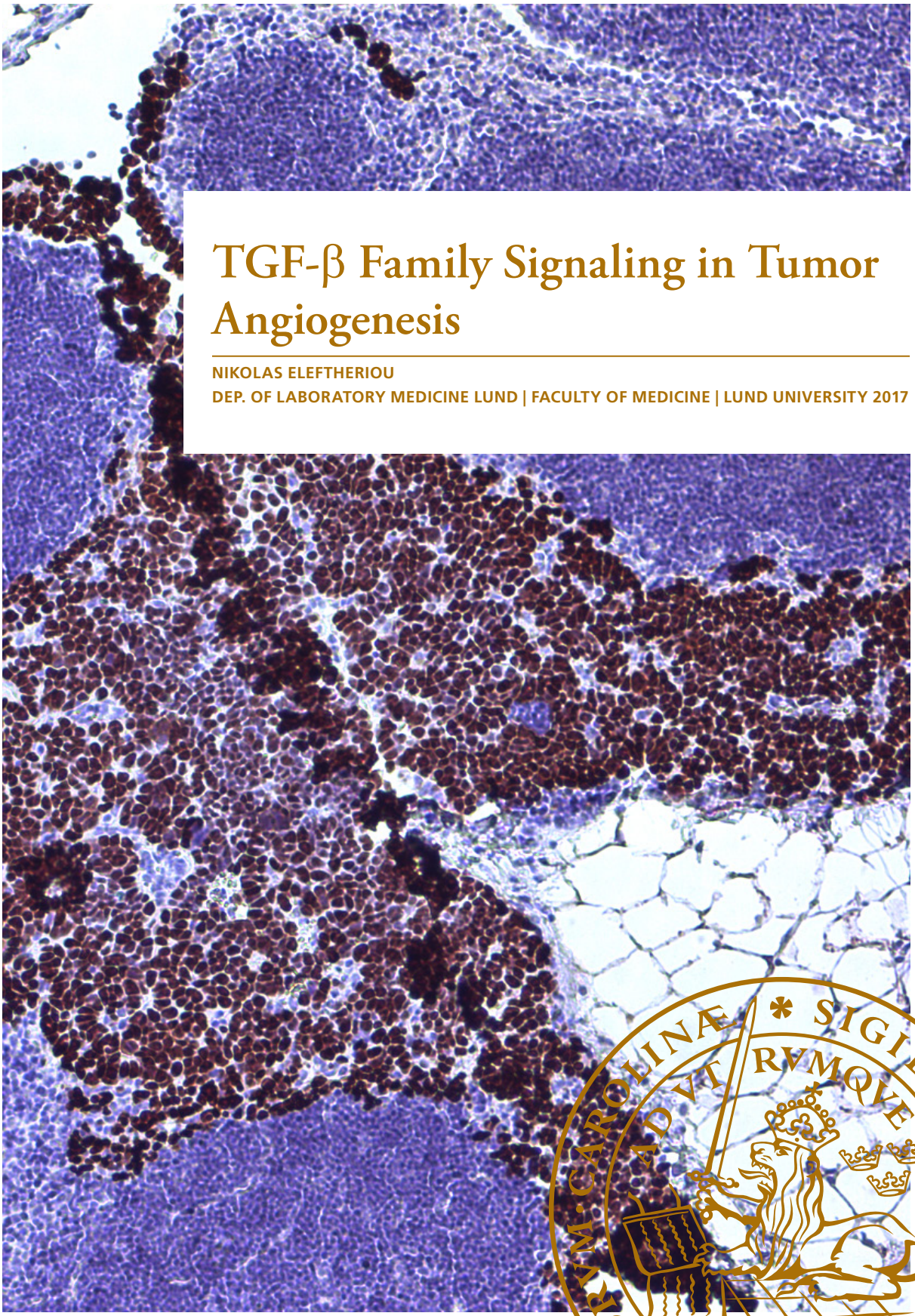

TGF-β Family Signaling in Tumor Angiogenesis

NIKOLAS ELEFTHERIOU
DEP. OF LABORATORY MEDICINE LUND | FACULTY OF MEDICINE | LUND UNIVERSITY 2017

TGF-β Family Signaling in Tumor Angiogenesis

TGF-β Family Signaling in Tumor Angiogenesis

Nikolas Eleftheriou

LUND
UNIVERSITY

DOCTORAL DISSERTATION
by due permission of the Faculty of Medicine, Lund University, Sweden.
To be defended at main lecture hall, Medicon Village, Lund.
Friday, 17th of March, 2017 at 13.00

Faculty opponent
Mariona Graupera
Institut d'Investigació Biomèdica de Bellvitge
Spain

Organization	Document name
LUND UNIVERSITY	DOCTORAL DISSERTATION
Faculty of Medicine Translational Cancer Research Lund	Date of issue 17th of March, 2017
Author(s) Nikolas Eleftheriou	Sponsoring organization

Title and subtitle TGF-β Family Signaling in Tumor Angiogenesis

Abstract

Angiogenesis provides growing tumors a source of nutrients and oxygen, and a route for metastatic dissemination. In recent years anti-angiogenic therapies that primarily target the vascular endothelial growth factor (VEGF) signaling cascade have entered the clinic. However in practice, these have encountered unexpected mechanisms of resistance in many solid tumors, highlighting the need for further understanding of the basic biology behind alternative signaling pathways that drive angiogenesis. The transforming growth factor (TGF)-β superfamily of ligands and receptors are critical for vascular development and are widely implicated in cancer. Here we investigate the TGF-β signaling activity through endothelial cells (EC), including their impact on tumor angiogenesis and metastatic dissemination, through genetic modification and therapeutic inhibition.

In papers I, II and IV we investigated the in vivo activing receptor-like kinase (ALK)1/bone morphogenetic protein (BMP)9 signaling axis in various mouse models of cancer. ALK1-Fc, a soluble ALK1 receptor domain ligand trap for BMP9 and BMP10, was evaluated in preclinical models of pancreatic and breast cancer, showing a decrease in angiogenesis, tumor growth and number of metastases. These reductions were enhanced when combined with chemotherapy. In the adjuvant setting, ALK1-Fc had fewer metastases in orthotopic breast cancer cell models following tumor resection. Combined deficiency of the genes encoding ALK1 and endoglin synergistically decreased the volume of pancreatic neuroendocrine tumors, whereas BMP9 knockout mice display decrease in primary tumor burden, but an increase in vessel hypersprouting and hepatic micrometastases.

In papers III and IV we investigated the roles of ALK5 and TGFBR2 in pancreatic neuroendocrine tumor models with genetic modifications limited to endothelial cells (EC). Mice undergo EC-specific recombination prior to the tumor angiogenic switch for deletion of TGFBR2, ALK5, or expression of a constitutively active ALK5 mutant. EC deletion of ALK5 induced blood vessel hypersprouting in tumors and increased lymph node metastases, whereas constitutive activation of ALK5 in ECs increased hepatic metastases. TGFBR2 deletion in ECs strongly inhibits tumorigenesis, decreasing the number of tumors and tumor volume, and tumors presented with highly irregular vasculature.

Our studies emphasize the impact of TGF-β signaling on tumor angiogenesis and metastatic dissemination, and this pathway presents potential targets in the development of clinical therapies. However the mechanism of action following pathway inhibition remains unclear, and further investigation is warranted.

Key words Angiogenesis, TGF-β, endothelial cells, metastasis, pancreatic neuroendocrine tumor

Classification system and/or index terms (if any)

Supplementary bibliographical information		Language English
ISSN and key title 1652-8220 Lund University, Faculty of Medicine Doctoral Dissertation Series 2017: 42		ISBN 978-91-7619-422-5
Recipient's notes	Number of pages 126	Price
	Security classification	

TGF-β Family Signaling in Tumor Angiogenesis

Nikolas Eleftheriou

LUND
UNIVERSITY

Coverphoto by Nikolas Eleftheriou

The image shows a tissue section of a lymph node in the RIP1-TAg2 mouse, displaying metastatic cells stained positive for T-antigen (brown). Cell nuclei are stained with hematoxylin (blue).

Faculty of Medicine
Department of Laboratory Medicine, Lund

ISBN 978-91-7619-422-5
ISSN 1652-8220

Printed in Sweden by Media-Tryck, Lund University
Lund 2017

“For 17 hours a day, I sat directly in front of at least two Marine Corps guards seated behind a one-way mirror. I was not allowed to lay down. I was not allowed to lean my back against the cell wall. I was not allowed to exercise.” –Chelsea Manning

Content

List of original papers

The thesis is based on the following papers, referred to in the text by their Roman numerals:

I. Endothelial ALK1 is a therapeutic target to block metastatic dissemination of breast cancer. Cunha SI, Bocci M, Lövrot J, **Eleftheriou N**, Roswall P, Cordero E, Lindström L, Basrtoschek M, Haller BK, Pearsall RS, Mulivor AW, Kumar R, Larsson C, Bergh J, Pietras K Cancer Res 75:2445-56 2015 Jun 15

II. Compound genetically engineered mouse models of cancer reveal dual targeting of ALK1 and endoglin as a synergistic opportunity to impinge on angiogenic TGF-β signaling. **Eleftheriou N**, Sjölund J, Bocci M, Cortez E, Lee S, Cunha S, Pietras K Oncotarget 2016 Oct 12 *Epublication*

III. Endothelial-specific genetic modifications of TGF-β receptors in mouse models of pancreatic neuroendocrine tumors. **Eleftheriou N**, Bocci M, Kurzejamska E, Cordero E, Pietras K. 2016 *Manuscript*

IV. Exploring novel targeting opportunities of endothelial TGF-β signaling during tumor angiogenesis. **Eleftheriou N**, Bocci M, Kurzejamska E, Cunha S, Cordero E, Pietras K. 2016 *Manuscript*

Abbreviations

AKT	Protein kinase B
ALK	Activin receptor-like kinase
ALK1-Fc	ALK1 fusion protein
BMP	Bone morphogenetic protein
DLL4	Delta-like ligand 4
EC	Endothelial cell
EMT	Epithelial-to-mesenchymal transition
EndMT	Endothelial-to-mesenchymal transition
FGF	Fibroblast growth factor
GDF	Growth differentiation factor
MAPK	Mitogen activated protein kinases
Nrp	Neuropilin
PanNET	Pancreatic neuroendocrine tumor
PDGF	Platelet differentiation growth factor
PI3K	phosphoinositide 3-kinase
SMAD	SMA- and MAD-related protein
TGF	Transforming growth factor
TKI	Tyrosine kinase inhibitor
VEGF	Vascular endothelial growth factor

Abstract

Angiogenesis provides growing tumors a source of nutrients and oxygen, and a route for metastatic dissemination. In recent years anti-angiogenic therapies that primarily target the vascular endothelial growth factor (VEGF) signaling cascade have entered the clinic. However in practice, these have encountered unexpected mechanisms of resistance in many solid tumors, highlighting the need for further understanding of the basic biology behind alternative signaling pathways that drive angiogenesis. The transforming growth factor (TGF)-β superfamily of ligands and receptors are critical for vascular development and are widely implicated in cancer. Here we investigate the TGF-β signaling activity through endothelial cells (EC), including their impact on tumor angiogenesis and metastatic dissemination, through genetic modification and therapeutic inhibition.

In papers I, II and IV we investigated the in vivo activing receptor-like kinase (ALK)1/bone morphogenetic protein (BMP)9 signaling axis in various mouse models of cancer. ALK1-Fc, a soluble ALK1 receptor domain ligand trap for BMP9 and BMP10, was evaluated in preclinical models of pancreatic and breast cancer, showing a decrease in angiogenesis, tumor growth and number of metastases. These reductions were enhanced when combined with chemotherapy. In the adjuvant setting, ALK1-Fc had fewer metastases in orthotopic breast cancer cell models following tumor resection. Combined deficiency of the genes encoding ALK1 and endoglin synergistically decreased the volume of pancreatic neuroendocrine tumors, whereas BMP9 knockout mice display decrease in primary tumor burden, but an increase in vessel hypersprouting and hepatic micrometastases.

In papers III and IV we investigated the roles of ALK5 and TGFBR2 in pancreatic neuroendocrine tumor models with genetic modifications limited to endothelial cells (EC). Mice undergo EC-specific recombination prior to the tumor angiogenic switch for deletion of TGFBR2, ALK5, or expression of a constitutively active ALK5 mutant. EC deletion of ALK5 induced blood vessel hypersprouting in tumors and increased lymph node metastases, whereas constitutive activation of ALK5 in ECs increased hepatic metastases. TGFBR2 deletion in ECs strongly inhibits tumorigenesis, decreasing the number of tumors and tumor volume, and tumors presented with highly irregular vasculature.

Our studies emphasize the impact of TGF-β signaling on tumor angiogenesis and metastatic dissemination, and this pathway presents potential targets in the development of clinical therapies. However the mechanism of action following pathway inhibition remains unclear, and further investigation is warranted.

Introduction

Cancer is the second highest cause of death of non-communicable diseases worldwide behind cardiovascular disease (1), and in recent years has become the leading cause of death in Canada and many western European countries (1, 2). Despite progress in diagnosis and therapy, death rates are on the rise for some cancers, especially pancreatic and hepatic cancers (3). Many traits allow tumors to grow, sustain themselves and spread to distant organs. Current curative measures are hindered by resistance to treatment and recurrence of tumor growth, and ultimately the metastatic spread is the primary cause of death (4).

Tumors arise from cells with genetic instability, where successive mutations lead to the high capacity for proliferation, and the escape of cell death signaling and growth suppression. These enabling properties of tumors, among others, are required for growth and dissemination and have been summated as the hallmarks of cancer (5). Beyond the intrinsic properties of cancer cells, tumors can sustain themselves through interactions with the native cells in their local environment. The surrounding environment, or tumor microenvironment, may consist of fibroblasts, immune cells, endothelial cells, pericytes and the extracellular-matrix (6). These cells can be recruited by the primary tumor, with the dichotomous capability to be antagonistic to tumor growth in earlier stages of tumor growth, such as the infiltration of T-cells, and later supportive towards cancer progressions, such as the provision of growth factors by cancer-associated fibroblasts (7, 8). The tumor microenvironment contributes to establishing the hallmarks of cancer, notably the metastatic potential and induction of angiogenesis.

Angiogenesis

Endothelial cells originate from the mesodermal germ layer via vasculogenesis in the early stages of embryonic development; afterwards all new endothelial cells formed during development and in adult derive from existing vessels, and angiogenesis is this process by which new vessels are formed (9). The growth of new blood and lymphatic vessels occurs in parallel with tissue and organ

development, to provide adequate and uniform coverage appropriate to the need of the local surrounding environment. Many factors are involved in the stimulation of blood-vessel growth, with the most potent inducer being vascular endothelial growth factor (VEGF)A and the associated family of ligands and receptors.

VEGFA is required for endothelial cell proliferation, assembly and vascular remodeling, and is expressed in response to low oxygen tension, mediated by hypoxia-inducible factor (HIF)-1, or can be upregulated by other major growth factors (10, 11). Sprouting angiogenesis occurs in response to VEGFA stimulation of VEGF receptor (VEGFR)2, where endothelial cells gain invasive properties and modulate endothelial cell junctions to become the leading tip cell of a new vessel branch, as the neighbouring cells form the growing stalk as the new vessel forms. The tip and stalk cell identities are maintained by the endothelial-cell expressed Notch receptor and delta-like- ligand 4 (DLL4), where the cell affected by the highest concentration gradient of VEGFA will transduce DLL4 to neighbouring cells (11). DLL4 activation of Notch inhibits expression of VEGFR2, decreasing the sensitivity to VEFGA and preventing these cells from assuming a tip cell identity. The flux of these factors between endothelial cells and the local environment creates dynamic competition for tip cell identity as the vessel grows in response to hypoxia and the vessel matures, or quiescent factors prevent further vessel growth through tip cell regression (12).

Other growth factors synergize with VEGF in inducing angiogenesis such as members of the fibroblast growth factor (FGF) protein family. FGF receptors are expressed on many cell types including tumor cells, endothelial cells and fibroblasts, and FGF expression can be induced by hypoxia (13, 14). FGF-1 and FGF-2 have roles in both neoangiogenesis and vessel maturation, by driving proliferation and differentiation, stabilization of cadherin junctions, and upregulation of VEGFA and VEGFRs (15). Also important to the maturation of capillary vessels is the recruitment of pericytes, which is primarily driven by platelet-derived growth factor (PDGF)-B, and will mobilize pericytes to stabilize and maintain neovasculature (16).

The transforming growth factor (TGF)-β superfamily of ligands and receptors is also implicit in endothelial development, and will be introduced in greater detail in the chapter TGF-β Family Signaling. Briefly, various TGF-β family receptors both unique to endothelial cells and ubiquitously expressed are depended on for vessel development. Furthermore, genetic mutations in the TGF-β family receptors activin-receptor-like kinase (ALK)1 and endoglin (ENG) are responsible for hereditarty haemorrhagic telangiectasia, a disease characterized by vessel malformations and chronic bleeding from vessel lesions (17).

Tumor Angiogenesis

Nutrients and oxygen are required to sustain tumors as they rapidly proliferate, thus the initiation of tumor angiogenesis becomes a requirement for many tumors to survive. The concept of targeting angiogenesis as a potential therapy against solid tumors was first stipulated by Judah Folkman in the 1970's, and since then tumor angiogenesis is recognized as a hallmark of cancer for its fundamental roles in shaping the tumor microenvironment and supporting metastatic dissemination (5). Angiogenesis is also implicit in liquid tumors, where the degree of bone marrow angiogenesis and the level of angiogenic factors in circulation correlate with poor prognosis and response to therapy (18).

Throughout development angiogenesis occurs together with tissue growth, but cancer cells lack the concerted signaling to develop a physiologically normal vessel bed coordinated with the growth of the bulk tumor. Growing tumors will typically trigger an angiogenic switch, which may be driven by oxygen deprivation and the hypoxic response, or from the consistent upregulation of growth factors by cancer and stromal cells (19). Following initiation of the angiogenic switch, vessels will grow toward and infiltrate the tumor from nearby pre-existing vessels in response to stimulation, but these vessels differ from physiologically normal vessels and are typically deformed, leaky, feature abnormal branching and lack sufficient pericyte coverage (20-22).

Beyond providing sustenance for tumors, blood and lymphatic vessels provide a route for metastatic dissemination. Cancer cells can gain mobility and escape into nearby vessels, travel through the blood and lymphatic systems, and then deposit into distant tissue sites as micrometastases (5). This feature of tumor angiogenesis emphasizes their critical function in the malignancy of tumors and the need to limit angiogenesis in treating cancer.

Inhibition of Tumor Angiogenesis

Anti-angiogenic therapies differ from cytotoxic chemotherapies in that they target genetically stable host endothelial cells, which are typically quiescent with the exception of wound healing and female reproductive cycling. The goal of anti-angiogenic therapies is not to directly eradicate tumor cells, but to induce regression by quenching supply of nutrients and oxygen to the tumors. Many current anti-angiogenic therapy schemes are developed as combination with traditional chemotherapy, targeting both neoangiogenesis and the bulk tumor mass.

Many inhibitors of angiogenesis are found endogenously in circulation, in balance with stimulatory factors to maintain a quiescent state in endothelial cells.

Endogenous inhibitors include thrombospondin-1 and -2, and protein fragments such as endostatin and angiostatin which inhibit cell proliferation and migration. Some of these inhibitors are further capable of destabilizing cell-cell adhesion, inducing apoptosis, and blocking FGF, VEGF or TGFβ signaling (18, 23, 24). Many endogenous inhibitors have shown strong tumor impairment in in vivo pre-clinical settings, but clinical applications have not been consistently positive (25). Current clinical trials in various stages include synthetic peptides based on the anti-angiogenic regions of endogenous inhibitors.

Clinical approval has been granted to a number of inhibitors of angiogenesis, the first of which was bevacizumab, an anti-VEGF monoclonal antibody. Bevacizumab will bind all VEGFA variants. Bevacizumab is approved in combination with chemotherapy for use against metastatic colorectal, cervical, ovarian and non-small cell lung cancers, as a monotherapy against glioblastoma, and in combination with interferon alfa against renal cell carcinoma (15, 26). Approval for the use of bevacizumab in metastatic breast cancer was revoked, as there were no improvements in overall survival and quality of life despite moderate reduction in tumor growth (15). Other approved therapies include receptor tyrosine-kinase inhibitors (TKIs) sorafenib, sunitinib, pazopanib (broad multi-kinase inhibitors against VEGFRs, PDGFRs and others), and axitinib (specific for VEGFRs) (27, 28). These TKIs are approved for treatment of renal cell carcinoma, hepatocellular carcinoma (sorafenib only) and neuroendocrine tumors (sunitinib only). Inhibitors of the serine/threonine kinase mTOR (temsirolemus and everolimus) also have potent anti-angiogenic properties and are approved against renal cell carcinoma and neuroendocrine tumors in the metastatic setting (28-30). The mechanism of action underlying the anti-angiogenic effects of thalidomide are not completely clear, however its clinical use has proven effective in managing multiple myeloma (28). The most common side effects across anti-angiogenic therapies are hemorrhaging and hypertension (31).

Resistance to Tumor Angiogenesis

The clinical applications of anti-angiogenic therapies have contributed to moderate improvements in the management of the disease and patient survival, but many clinical trials for inhibitors of angiogenesis have not realized the broad anti-tumorigenic utility imagined decades ago based on pre-clinical trials. Instead anti-angiogenic therapies brought to light how tumors inherently evade angiogenic inhibition and develop de novo mechanisms of resistance (32). Therapies targeting VEGF signaling, such as bevacizumab and TKIs, may encounter resistance through circumventing VEGFA-driven angiogenesis. Tumor cells and stromal cells may respond with compensatory upregulation of alternate pro-angiogenic growth factors, such as FGF (15, 33, 34). While multikinase inhibitors may be

more robust than bevacizumab in some settings as they can target multiple pro-angiogenic pathways, they are not sufficient to consistently evade resistance in solid tumors, as different mechanisms of resistance arise depending on the type of cancer (35).

The tumor microenvironment has proven crucial in providing innate resistance to chemotherapy, and can mediate resistance to VEGF-targeted therapy through infiltration of immature myeloid cells, endothelial progenitor cells and fibroblasts (35). Tumor growth may also be sustained by the tumor stroma independent of endothelial properties, as evidenced in pre-clinical models of glioblastoma following bevacizumab treatment (36). Anti-angiogenic therapy may be subverted by tumor adaptation to harsher conditions of low oxygen and nutrient levels or an increase in tumor aggressiveness and accelerated growth of metastases (35). Additional routes of VEGF-independent angiogenesis are possible through vessel co-option, where the tumor mass engulfs nearby vasculature, or vasculogenic mimicry, where the plasticity of tumor cells allow their physical incorporation into leaky vessels for liquid transport (32, 35).

The clinical application of anti-angiogenic therapies may benefit from molecular screening for predictive biomarkers (35). Screening validated biomarkers should help identify subgroups of responsive patients who are more likely to benefit than others, and to optimize the dosing and schedule of combination therapies (32). The failure to thoroughly understand tumor biology lead to underwhelming results in practice; understanding all mechanisms of angiogenesis and the tumor response to angiogenic inhibition are required to translate preclinical findings into successful clinical therapies.

TGF-β Family Signaling

The TGF-β superfamily is fundamental to nearly all developmental processes including regulation of proliferation, differentiation, apoptosis, migration and more, and in adults is crucial to mediating homeostasis (37). This signaling family includes over 30 ligands and receptors in humans, with orthologous pathways in even the most primitive metazoan species (38). The TGF-β family is multifunctional and can elicit diverse cellular responses, and expanding our knowledge of these signaling pathways has broad medical relevance. Underlying the multifunctional nature of TGF-β signaling is the complex, and at times opposing, roles that the pathways are responsible for, depending on the target cell type, receptors and other surrounding conditions; the TGF-β signaling response is contextual (39). The context defining TGF-β signaling is determined via: signal transduction by ligands, receptor subtypes, co-receptors, antagonists and crosstalk

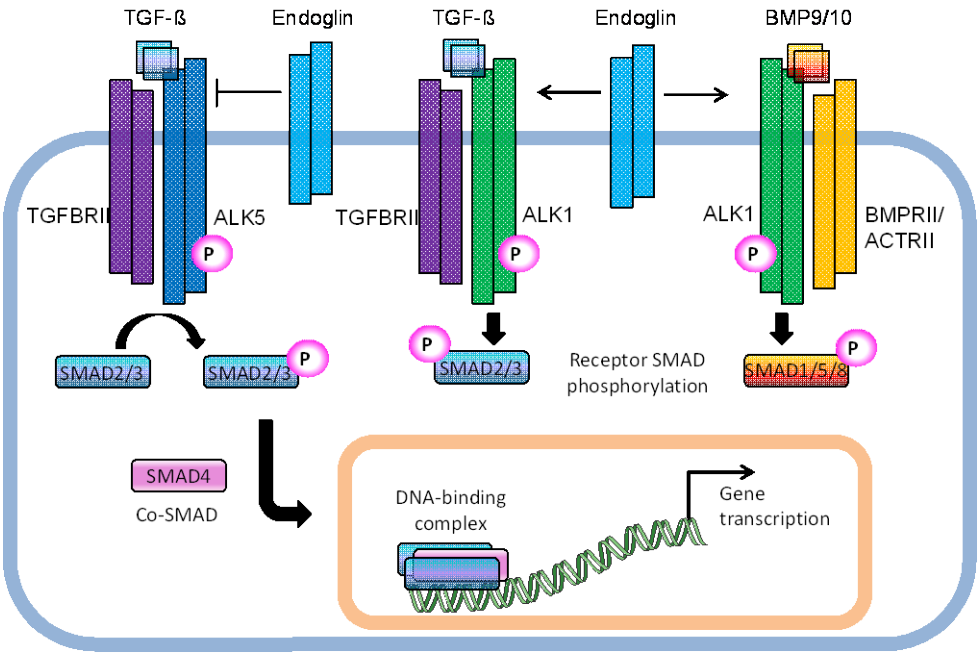

Figure 1. TGF-β signaling in endothelial cells
TGF-β and BMP9/10 bind and activate type I/II receptor complexes at the cell surface, and phosphorylate intracellular receptor SMADs. Type III receptors compliment or inhibit ligand-receptor interactions. Phosphorylated receptor SMADs form a complex with SMAD4. The SMAD complex binds DNA with transcription factors to regulate gene transcription.

between pathways; transcription by pluripotency and lineage regulators, and DNA-binding cofactors; and epigenetics (39). These cues, from the cell surface through to the nucleus, coexist to elicit a highly specific response.

The TGF-β family consists of dimeric ligands that can be divided into two subfamilies: one including TGF-β, activins, and Nodal, and the other bone morphogenetic proteins (BMPs) and growth differentiation factors (GDFs). These ligands bind to serine/threonine receptor complexes, consisting of two type I (signal propagating) and two type II (signal activating) receptors, and propagate signaling via SMAD substrate proteins that can bind DNA for transcriptional regulation (Figure 1). The isoforms of TGF-β (TGF-β1, -β2 and -β3) exclusively bind to the type I receptor activin receptor-like kinase (ALK)5 (also known as TGFBR1) and the type II receptor TGFBR2 (40). The activins, Nodal and BMPs commonly bind through the type II receptors activin receptor type 2A (ACVR2A) and ACVR2B, but can diversely bind a number of type I receptors. BMPs can also bind the type II receptor BMPR2, and readily engage the type I receptors ALK3 and ALK6. BMP9 and BMP10 are the primary binding partners to ALK1, however ALK1 may also be activated by high concentrations of TGF-β (41).

There are also co-receptors (type III receptors) that lack the intracellular kinase domain, and instead modulate type I/II complexes (42). These include betaglycan (also known as TGFBR3), which is required for TGF-β2 signaling, and endoglin, which is highly expressed by, but not limited to, endothelial cells and can interact with TGF-β1, TGF-β3, BMP9 and BMP10 (42, 43). The ligand subtypes have differing receptor affinities, and the extracellular ligand gradient, antagonist ligands and combination of receptors being expressed are crucial in processes such as embryogenesis.

The central conduit for TGF-β family signal transduction is through receptor-regulated SMA- and MAD-related proteins (SMAD)phosphorylated by the type I receptors; BMPs activate SMAD1, SMAD5 and SMAD8, and TGF-β, activins and Nodal activate SMAD2 and SMAD3 (40). The phosphorylated RSMADs partner with SMAD4, and this oligomeric complex binds DNA with transcription factors for transcriptional regulation. The SMAD proteins add another layer of regulation through interactions with transcriptional factors to modulate signal, and inhibitory SMADs (SMAD6 and SMAD7) can interrupt gene transcription and promote receptor degradation. Non-canonical signaling is mediated by type II receptors independent of SMAD signal transduction, and mediates signaling programs such as epithelial to mesenchymal transition (EMT), cell survival and proliferation (39). SMAD independent signaling pathways include mitogen activated protein kinases (MAPK), phosphoinositide 3-kinase/protein kinase B (PI3K/AKT), and Rho-like GTPase signaling (44).

Vascular Development

The most profound effects driven by the TGF-beta family, and likely reason for its highly conserved presence in the animal kingdom, is its roles in developmental biology. The TGF-beta family of ligands, particularly the BMPs and Nodal, tightly control stem cell fate commitment of embryonic stem cells, and their spatial and temporal regulation is highly specific throughout embryonic development (45). These ligands induce diverse cellular responses that include axis generation and patterning, and induction of germ layers. Differentiation into different tissue types is driven by a gradient of ligand activity which is interpreted by SMAD signaling.

TGF-β/ALK5 signaling mediates epithelial-to-mesenchymal transition (EMT), which functions uniquely in each of development, fibrosis and cancer. In development, EMT directs morphogenesis of epithelial cells through differentiation, changing cell polarity, remodeling cell-cell interactions and expression of mesenchymal markers, as required to form new tissue (46). EMT first occurs immediately following the blastocyst stage in germ line specification, and includes remodeling of the uterine vasculature to channel placental blood

supply to the fetus. As organs and tissue form, cells will undergo EMT and the reverse mesenchymal-to-epithelial transition (MET), and these transitions oscillate throughout development as necessary.

In vasculogenesis, TGF-β signaling mediates the differentiation of new endothelial cells from angioblasts to form the primary vascular plexus, and provides vessel muscularization by transforming recruited mesenchymal cells into pericytes or vascular smooth muscle cells (47). The importance of TGF-β signaling to the development of vasculature is further made evident in the phenotypes of mice containing genetic knockouts of various TGF-β family ligands and receptors, many of which display severe vascular and angiogenic defects. Mice with knockouts of *Tgfbr2* and *Alk5* are embryonic lethal, due to vasculogenic and angiogenic defects (47, 48). Specific deletions of *Tgfbr2* or *Alk5* in neural crest cell lineage have unique phenotypes distinct from each other, highlighting the non-redundant roles of these two receptors (49).

Knockout of *Tgfb1* in mice results in embryonic lethality due to vascular defects in certain mouse background strains, and otherwise mice die from post-natal autoimmune disease (47). *Tgfb2* knockouts have defects in the aortic arch and cardiac septum, whereas *Tgfb3* knockouts have defects in the cleft palate and delayed lung maturation, and die post-natally (47). Here TGF-β1 is the most potent angiogenic factor of the three TGF-β ligands, as it is localized in endothelial cells during embryogenesis, and absence of TGF-β2 and TGF-β3 do not display severe angiogenic defects, possibly indicating redundancy in the system.

ALK1 and Endoglin in Vascular Development

Unlike the primary receptor targets for TGF-β, ALK5 and TGFBR2, the roles of ALK1 and endoglin are almost exclusive to the endothelial compartment, though endoglin is transiently expressed in cardiac tissue during development (43). Mouse embryonic knockouts of *Acvrl1* (gene name for ALK1) or *Eng* are embryonic lethal, with a lack of vascular growth in the yolk sac and failure of vascular smooth muscle cell differentiation (47). Mutations in these genes are also linked to human vascular disease including hereditary hemorrhagic telangiectasia, characterized by abnormal blood vessels, vessel lesions and arteriovenous malformations.ALK1 mutations are also present in cases of pulmonary arterial hypertension (17).

The role of BMP9 in development is much less obvious, as knockout mice are viable and with no major abnormal phenotype (43). However, *Gdf2* (gene name for BMP9) knockout mice have higher detectable BMP10 in circulation, and in postnatal vascular remodeling of the retina, vessel hypersprouting was observed

only in *Gdf2* knockout mice also treated with anti-BMP10 antibody (50). These effects suggest BMP10 can compensate in development and in angiogenesis. Conversely, *Bmp10* knockout mice are embryonic lethal due to failure in cardiac development, and BMP9 is not compensating (51). BMP10 expression is restricted to the myocardium, and BMP9 and BMP10 are implicit in the development of the cardiovascular system, including the closure of the ductus arteriosus in the transition from fetal to neonatal circulation (52). The development of endocardial tissue requires the process of endothelial-to-mesenchymal transition (EndMT), such as formation of the A-V septum (46). Similar to EMT, EndMT transforms endothelial cells into motile, apolar cells required for tissue formation and cardiac fibrosis, with BMP10 and TGF-β2 being implicated in the process (46, 52).

During developmental lymphangiogenesis, BMP9/ALK1 signaling negatively regulates lymphatic vessel formation through inhibition of lymphatic endothelial cell proliferation (53). ALK1-depleted mice show enlarged lymphatic vessels in organs, whereas *Gdf2* deletion presents dilated lymphatic vessels due to the increased lymphatic endothelial cell proliferation. BMP9 negatively regulates lymphatic vessel differentiation during vasculogenesis by downregulating the lymphatic marker PROX1 (53).

Angiogenesis

Beyond development, TGF-β family signaling pathways maintain homeostatic regulation across various cell types, however the precise effects of BMP9 and TGF-β become difficult to parse when isolating or overexpressing single growth factors in vitro, given the high degree of synergy attributed to other concentration-dependent signaling molecules. TGF-β activity maintains anti-proliferative signaling in epithelial cells, and pro-proliferative signaling in fibroblasts, and can promote wound healing, tissue repair and fibrosis (46, 54). In endothelial cells, low levels of TGF-β1 is shown to promote cell proliferation and migration in the formation of new vessels in vitro, but at high levels induces extracellular matrix (ECM) component production and cytostasis that is attributed to mature vessels (47). VEGF induces endothelial cell pro-survival signals, but mediates TGF-β-enabled apoptosis in the formation of new vessels in embryoid body assays and in vivo (55). Similarly, expression of constitutively active ALK5 in endothelial cells has an anti-proliferative effect (42).

BMP9 and BMP10 are detected at low levels in adult circulation, and circulating active BMP9 is detected in excess of BMP10 (43). BMP9 is mostly expressed in the liver and to a lesser extent in the lung and brain, and BMP10 is expressed in the right atrium and at lower levels in the liver and lungs (43, 51, 56). BMP9 equilibrium is maintained by proteolytic degradation, hypothesized to provide low

level exposure to capillaries distant from the site of production (43). BMP9 and BMP10 have anti-angiogenic effects upon stimulating human umbilical vascular endothelial cells, human pulmonary artery endothelial cells, but pro-angiogenic effects in explant matrigel tube formation assays, conversely overexpression of endoglin induced endothelial cell proliferation in vitro (43).

The anti-angiogenic effects of BMP9/ALK1 signaling via inhibition of VEGF- and FGF-driven migration and proliferation suggests that BMP9 is a vascular quiescence factor (57). Inhibition of BMP9/ALK1 signaling produces hypersprouting in postnatal vascular remodeling of the retina, similar to DLL4-deficient mice that are unable to maintain a stalk cell phenotype (50, 58). Activation of BMP9/ALK1 upregulates downstream targets ID1 and ID3, and Notch targets including Hes1 and Hey1 (57). Synergy between Notch and BMP9/ALK1 signaling in endothelial cells to induce VEGFR1, and Hes1, Hey1 and Jagged1 actively suppress the tip cell phenotype (58). VEGF activation of sprouting angiogenesis and tip-cell identity is orchestrated through DLL4-mediated Notch activation in neighbouring cells via VEGFR2, suppressing neighbouring tip-cell activation. Neuropilin-1 (Nrp-1) also activates tip cell identity of endothelial cells through the inhibition of SMAD2/3 and SMAD1/5/8 (58, 59). Both ALK1/ALK5 canonical SMAD signaling and DLL4-mediated Notch signaling must be inactivated to elicit tip cell identity in sprouting angiogenesis. Increased activation of ALK1 and ALK5 signaling, similar to the anti-proliferative effects seen in various in vitro studies previously mentioned, reinforces the stalk cell identity (59). While the precise mechanism by which Nrp-1 interacts with and inhibits SMAD2/3 and SMAD1/5/8 signaling is unclear, the synergy between Notch and ALK1 models how TGF-β family signaling can maintain heterogeneity between neighbouring cells in angiogenesis.

Cancer

Given the pleiotropic effects of TGF-β signaling, the impact on tumor cells and the microenvironment is profound, but remains context dependent. In early stages of tumor growth, TGF-β is suppressive of pre-malignant cells, but in advanced stages enhances the proliferation, mobility and invasiveness of metastatic cells(39, 60). Increased expression of TGF-β is detected in many tumors including 68% of breast, 48% of lung and 47% of pancreatic cancers, and often mutations or deletions in *Tgfbr2*, *Alk5*, *Smad2*, *Smad3* and *Smad4* are detected (61). In preclinical tumor models transgenic mice containing constitutively active ALK5 expressed in granulosa cells was sufficient to instigate ovarian cancer, and drive tumor proliferation and angiogenesis (62). Similarly, deletion of BMP type I receptors ALK3 and ALK6, or deletion of SMAD1/5, from sex-cord stromal cells are also oncogenic. TGF-β signaling in cancer is unlike the finely-tuned and

highly coordinated regulation patterns witnessed in embryonic development created by generations of evolutionary pressure, but instead pathway regulation is chaotic, and given the context-dependent nature of TGF-β signaling makes deciphering these interactions in cancer a challenging task. What follows are several examples of the impact of TGF-β signaling in cancer and the tumor microenvironment (Figure 2).

Fibroblasts

TGF-β signaling through fibroblasts has shown to have both pro-tumorigenic and tumor suppressive capabilities. High levels of TGF-β in tumors correlate to high fibroblast activation and ECM collagen production, and fibroblasts from small cell lung carcinoma patients have enriched TGF-β gene signature that correlates with poor prognosis (63). Evidence suggests fibrosis and enhanced TGF-β signaling may facilitate tumor protection from radiotherapy (60). In mouse models of colon carcinoma overexpression of TGF-β in tumors linked to high activation of downstream target genes in fibroblasts, and increased rate of metastasis. Deletion of *Tgfbr2* in mouse fibroblasts results in tumor initiation of prostate neoplasms and squamous cell carcinoma, and deficiency of *Tgfbr2* in mammary fibroblasts enhanced proliferation and invasion of breast cancer cells (64, 65). In these instances loss of TGF-β responsiveness also contributed to an increase in tumor inflammation.

Epithelial-to-Mesenchymal Transition

TGF-β is a driver of EMT in cancer, and this process is one way tumor cells gain invasive properties. Activation of EMT imparts motility and metastatic potential on cancer cells through reactivation of embryonic and morphological gene expression programs (46). Cells that have undergone EMT can travel into the blood and lymphatic vasculature, and extravasate into distant organs and tissue to form nodes of metastases. Tumor cells with inactivated canonical TGF-β signaling displayed a reduced capability to colonize to distant organs in breast, head and neck and melanoma cancers (60). In preclinical models inhibition of SMAD2, SMAD3 and SMAD4 reduced the EMT potential, however non-canonical signaling through TGFBR2 promoted EMT invasion and metastasis in absence of SMAD signaling(60). Induction of EMT is not mandatory for metastatic dissemination, but has been linked to other pro-tumorigenic features such as maintaining a cancer stem cell-like population and chemoresistance (60, 66).

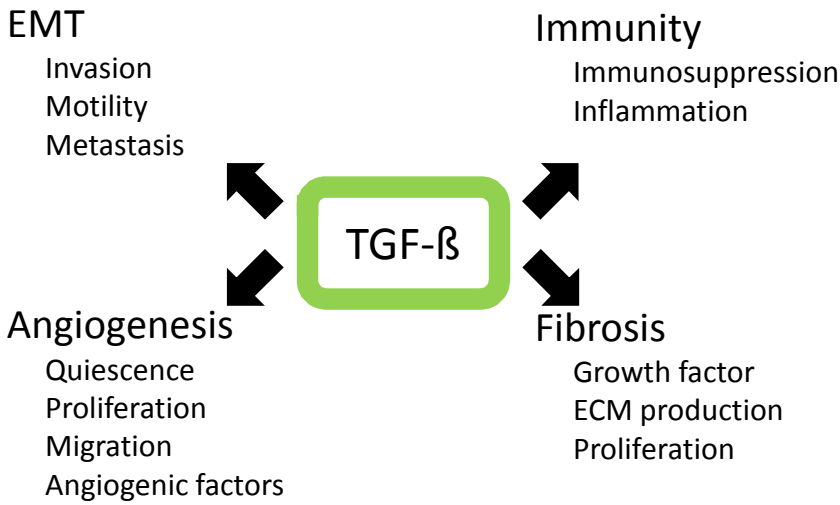

Figure 2. TGF-β signaling in cancer
The TGF-β family of ligands and receptors can suppress and promote tumor growth. TGF-β interacts with tumor cells and components of the tumor microenvironment, influencing the cellular programs listed above, among others.

Immune Response

TGF-β signaling contributes to the regulation of healthy immunosurveillance and inflammation, but in the tumor microenvironment deregulation of TGF-β signaling can lead to repressed immunosurveillance and pro-inflammatory response that support tumor progression. Defective TGF-β signaling in mice can lead to multifocal inflammatory disease, failed differentiation of neutrophils, T and B cells, and severe autoimmune reaction (47, 60). Deletion of *Tgfbr2* in mammary carcinoma cells increased recruitment of immature myeloid cells in mice, promoting tumor invasiveness and metastatic spread. Overexpression of TGF-β suppresses immunosurveillance by inhibiting proliferation of NK and T cells, and differentiation between T cell subtypes (60). The outcome is the protection of carcinoma survival pathways, suggesting that disruption of immune-cell signaling is pro-tumorigenic.

Tumor Angiogenesis

ALK1 has become a potential target for anti-angiogenic therapy for its role in tumor angiogenesis. In RIP1-TAg2 mice, a genetically engineered mouse model of pancreatic neuroendocrine tumors (PanNETs), increased expression of TGF-β and BMP9 correlate with the onset of tumor vascularization. This suggests that expression of these factors enable an angiogenic switch transforming hyperplastic

islets into angiogenic adenomas (67). BMP9 overexpression has similarly been detected in some human hepatocellular carcinomas, and ALK1 expression is detected in the vasculature of many tumors (43, 68, 69). While BMP9 and TGF-β can individually have anti-proliferative effects in endothelial cells, the combination of the two synergistically increased proliferation of human and mouse endothelial cells in vitro and in matrigel plug assays, which may be the underlying mechanism for the strong angiogenic response in tumorigenesis of RIP1-TAg2 mice.

RIP1-TAg2 mice deficient for *Acvrl1* have decreased tumor growth and angiogenesis. The effects of genetic deficiency were repeated with a therapeutic approach using a soluble ALK1 receptor domain ligand trap (ALK1-Fc) binding BMP9 and BMP10. ALK1-Fc decreased sprouting angiogenesis of endothelial cells in vitro, and RIP1-TAg2 mice treated with ALK1-Fc showed a decrease in tumor growth and angiogenesis similar to genetic deficiency of ALK1 (67). Profiling gene expression of endothelial cells isolated from tumors of RIP1-TAg2 mice revealed that genetic deficiency of *Acvrl1* and treatment with ALK1-Fc decreased the downstream regulation of both ALK1 and ALK5, further supporting their co-operation in promoting tumor angiogenesis.

In a similar study genetic deficiency of Eng in RIP1-TAg2 mice decreased the number of PanNETs, but did not decrease the combined tumor volume, and these tumors were fully vascularized (70). The endoglin deficiency also increased the number of hepatic micrometastases despite the decrease in the number of tumors. The perivascular niche of endoglin-deficient mice showed an increase in cells expressing mesenchymal markers, indicative of EndMT. In vitro cultures of Eng-deficient endothelial cells increased expression of Twist, a transcriptional regulator of EndMT, and increased permeability to tumor cells through a monolayer of endothelial cells (70). Furthermore, endothelial cells isolated from tumors of RIP1-TAg2 mice deficient for endoglin decreased expression of ALK1 targets but increased expression of ALK5 targets. These results suggest divergent roles for ALK1 and endoglin interactions with TGF-β/ALK5 signaling that can impact metastases, however these mechanisms require further investigation.

Inhibitors

Inhibitors of TGF-β signaling can be categorized into one of three groups: 1) antisense TGF-β molecules, 2) monoclonal antibodies and ligand traps, and 3) intracellular inhibitors of the signaling cascade (71). The inhibitors of TGF-β/ALK5 canonical signaling pathway that are in advanced clinical development are not designed to specifically inhibit angiogenesis, unlike inhibitors of ALK1 (dalantercept, PF-03446962) and endoglin (TRC105). Below are short descriptions

of TGF-β inhibitors in development, and description of the anti-angiogenic therapies against ALK1 and endoglin.

Two inhibtors of TGF-β translation include trabedersen and lucanix. Trabedersen is an antisense TGF-β2 molecule. Trabedersen was recently tested in a phase II clinical trial for high grade glioma. The results showed significant benefit over a 14-month period, however fell short on improvement at 6 months compared to the entire study population (72). The response to TGF-β2 inhibition showed alleviation of tumor-induced immune suppression overtime, differing from faster-acting cytotoxic agents, and contributing to long-term benefits (72). Lucanix is an anti-sense TGF-β2 allogeneic cancer cell vaccine, clinical details of which have not yet been published, however phase III trials for both trabedersen and lucanix have since been initiated (73).

Galunisertib is an inhibitor of ALK5, inhibiting phospho-SMAD2 and non-canonical pathway signaling. In preclinical models galunisertib showed improved efficacy when TGF-β overexpression occurred early in tumor development, including reduction in metastases (73). In phase II trials of advanced hepatocellular carcinoma, galunisertib improved time-to-tumor progression in patients with reduced circulating AFP, E-cadherin and TGF-β1 (74). AFP is a marker for poor prognosis in HCC, and galunsertinib may be of potential benefit in a difficult-to-treat populations (74). A phase II trial evaluated galunisertib as a monotherapy or in combination with chemotherapy against recurrent glioblastoma, however there was no added benefit compared to chemotherapy alone (75). Patients on galunisertib did exhibit a decrease in phospho-SMAD2, and patients who respond to treatment may be those with mesenchymal tumor phenotype, or dependent on the microenvironment or immune response (75).

Anti-Angiogenic Inhibitors

Dalantercept

Dalantercept is the human equivalent of RAP-041 (previously known as ACE-041), and is an ALK1 receptor fusion ligand trap that binds to BMP9 and BMP10 (76). Thus far two phase I and one phase II studies have been published, with various stages of phase I and II trials currently underway for hepatocellular and renal cell carcinomas, and multiple myeloma, including two combination trials with VEGFR TKIs sorafenib and axitinib (77). Phase II trials in pre-treated patients suffering advanced squamous cell carcinoma of the head and neck show that monotherapy of dalantercept was well-tolerated, but produced only modest improvement in progression-free survival (78). The safety profile of dalantercept was distinct from that of VEGF inhibitors, with the most common adverse effects being fatigue and anemia. Patients who developed telangiectasias had decreased

ALK1 and BMP9 levels, and had stable disease as the best response during therapy indicating active inhibition of ALK1 (78). A phase II trial of dalantercept in endometrial and ovarian cancers did not meet the clinical outcomes, however a phase I trial of dalantercept and axitinib for renal cell carcinoma was well tolerated and met the required overall response rate, and phase II trials have since started (79).

PF-03446962

PF-03446962 is an anti-ALK1 monoclonal antibody, binding to the ALK1 extracellular domain. PF-03446962 inhibits BMP9 signaling, SMAD1 phosphorylation, and endothelial cell sprouting in vitro, and improved tumor growth inhibition was observed when combined with VEGF inhibition in various in vivo models (77). Phase I clinical trials for PF-03446962 began in assorted advanced solid tumors, where results in hepatocellular carcinomas showed modest anti-tumor activity and acceptable safety profile (80, 81). However, phase II trials in refractory urothelial cancer and malignant mesothelioma did not result in observable anti-tumor activity (82, 83). Serum VEGF levels were increased in patients (a similar effect seen in the various clinical trials for dalantercept). Given the results of the phase II study, PF-03446962 as a monotherapy against urothelial cancer and mesothelioma was not recommended (82, 83). A phase I trial of PF-03446962 combined with reforafenib (TKI targeting VEGFR2-TIE2) against colorectal cancer is ongoing.

TRC105

TRC105 is a human/murine chimeric anti-endoglin monoclonal antibody. Several clinical trials are currently in phases I and II, many of which are in combination with VEGF-pathway inhibitors (42). In a phase I trial against advanced tumors, combination therapy of TRC105 and bevacizumab showed clinical activity in patients with disease refractory to VEGF inhibition, suggesting endoglin inhibition can counter the resistance to anti-VEGF therapy (84). TRC105 was administered as a monotherapy in a phase II trial against advanced or metastatic urothelial cancer in heavily pretreated patients. This trial did not show improvement of progression-free survival, however only 50% of patients expressed endoglin at varying intensities in tumor tissue, and variation in results suggest that only specific subsets may benefit in an endoglin-expression dependent manner (85). Sorafenib is the current treatment for advanced hepatocellular carcinoma; a phase II trial investigated the use of TRC105 treatment for a population of patients who have completed a sorafenib therapy regimen. However the efficacy of TRC105 in this clinical setting was modest and insufficient (86). A clinical trial for the concurrent combination of sorafenib and TRC105 in hepatocellular carcinoma is ongoing.

Mouse Models of Cancer

In the following papers mouse models of cancer are utilized to describe the effects of genetic modifications and anti-angiogenic therapy in a preclinical setting. They include two orthotopicallyimplanted syngeneic breast cancer cell lines (E0771 and 4T1), and transgenic mouse models of breast (MMTV-PyMT) and pancreatic (RIP1-TAg2) cancer.

Breast cancer cell lines are orthotopically implanted into the inguinal mammary fat pad to mimic the native microenvironment of the original tumor and improve clinical relevance, while remaining a simple procedure with little stress to the mice. E0771 is an estrogen receptor-positive medullary breast adenocarcinoma of C57Bl/6 mouse strain origin, which elicits an immunosuppressive response (87). 4T1 resembles highly tumorigenic and metastatic human mammary carcinoma, and is of BALB/c mouse strain origin (88). Both cell lines spontaneously develop pulmonary metastases, suitable for macroscopic quantification. In paper IV these cell lines are both used in a resection model mimicking clinical treatment; the tumor cells grow until they reach a threshold diameter, measured through the skin, and the mammary fat pad is then surgically removed. This procedure can be followed by a regimen of adjuvant therapy and the incidence of metastasis will be a measure of efficacy.

RIP1-TAg2 is a transgenic mouse model of pancreatic neuroendocrine cancer. The pancreatic β-cells express SV40 T-antigens (TAg) under the control of the rat insulin promoter (RIP) (89, 90). The SV40 T-antigen inhibits the tumor suppressor genes p53 and retinoblastoma. Islets of RIP1-TAg2 undergo multistage carcinogenesis, with hyperplastic islets forming during 4-8 weeks of age, followed by an angiogenic switch when islets become highly vascularized adenomas between 8-12 weeks. By 12 weeks of age, many angiogenic islets are solid tumors, and metastasis can be detected in the mesenteric lymph nodes or as hepatic micrometastases. In paper I the RIP1-TAg2 mouse is used to evaluate efficacy of ALK1-Fc anti-angiogenic therapy in advanced disease. In papers II-IV RIP1-TAg2 mice carry genetic modifications of various receptors or ligands to study the consequential effects on tumor growth and metastases. One limitation from this tumor model is that the cause of death is often due to the overproduction of insulin by the islets of Langerhans as they become increasingly tumorigenic, although this is partially remedied by the addition of glucose to their drinking water at 10 weeks of age.

MMTV-PyMT is a transgenic mouse model of multifocal mammary adenocarcinoma (91, 92). The polyomavirus middle T oncogene (PyMT) is expressed under the mouse mammary tumor virus (MMTV) promoter and enhancer. MMTV-PyMT mice have high oncogenic penetrance and rapidly

develop tumors. These mice develop vascularized tumors that are highly metastatic, including lymphatic and pulmonary metastases present in advanced disease. Papers I and IV investigate the role of anti-angiogenic therapy regimens in MMTV-PyMT mice, such as drug administration at different stages of tumor progression.

Specific Aims

Paper I – To investigate the utility of ALK1 inhibition as an anti-angiogenic therapy in vivo preclinical metastatic breast cancer

Paper II – To explore the contextual functions of the ligands and receptors in BMP9/ALK1 signaling, and how their activity drives tumor angiogenesis and metastasis

Paper III – To investigate changes to ALK5 signaling genetically limited to the endothelial cell compartment in angiogenic tumors

Paper IV – To understand the underlying biology in inhibiting tumor angiogenesis, through changes in the tumor microenvironment and metastatic progression related to TGF-β and ALK1 signaling pathways

Results

Paper I

Endothelial ALK1 Is a Therapeutic Target to Block Metastatic Dissemination of Breast Cancer

The degree of vascularity in breast cancer is a prognostic factor, however targeting angiogenesis in breast cancer has thus far not been successful (93, 94). Further knowledge on the molecular drivers that contribute to metastases is required. ALK1-Fc is a soluble receptor decoy of ALK1 (RAP-041, the mouse equivalent of dalantercept), binds to BMP9 and BMP10, and has previously shown anti-angiogenic and tumor suppressive properties (76). Here the therapeutic efficacy of ALK1 inhibition is evaluated in multiple metastatic mouse models of cancer, as well as exploring gene expression patterns of ALK1 signaling in metastatic breast cancer patients.

Key findings

The use of ALK1-Fc as an anti-angiogenic therapy was evaluated in several mouse models of cancer. In RIP1-TAg2 regression trial treatment with RAP-041 or IgG control began at 12 weeks of age, when tumors have fully developed, have metastatic potential and are well past angiogenic initiation. After four weeks of treatment, mice administered ALK1-Fc showed inhibition of tumor growth, hepatic metastases and angiogenesis, and had improved survival compared to the control cohort. Similar trials with ALK1-Fc were performed in MMTV-PyMT mice comparing treatment during 8-12 weeks of age (during tumor development), 11-15 weeks of age (advanced disease state past induction of metastatic dissemination), and in mice orthotopically implanted with E0771 cells for the duration of two weeks following tumor establishment. In all three trials ALK1-Fc managed to slow tumor growth, pulmonary metastases and tumor angiogenesis. The tumor grade of mammary tissue from MMTV-PyMT mice with or without ALK1-Fc therapy revealed a significantly smaller area of ALK1-Fc treated mice displayed features of late carcinoma. MMTV-PyMT mice were treated with ALK1-Fc combined with docetaxel, mimicking neoadjuvant therapy, synergistically decreasing the total tumor volume, incidence of pulmonary metastases and angiogenesis.

A nested case-control gene expression analysis of breast cancer patients with distant metastatic disease matched to control patients free from metastases revealed that high *ACVRL1* expression correlated with incidence of metastatic disease, and is independent prognostic indicator of poor survival.

Paper II

Compound genetically engineered mouse models of cancer reveal dual targeting of ALK1 and endoglin as a synergistic opportunity to impinge on angiogenic TGF-β signaling

ALK1 inhibition and genetic deficiency of *Acvrl1* reveal anti-angiogenic effects in mouse models of pancreatic and breast cancer, however Eng deficiency does not phenocopy these anti-angiogenic and tumor suppressive effects(70). To further understand the concerted roles of ALK1, endoglin and BMP9 signaling in tumor angiogenesis we investigated the combined deficiency of ALK1 and endoglin in RIP1-TAg2 mice, (RIP1-TAg2; $Acvrl1^{+/-}Eng^{+/-}$), and knockout of their primary ligand partner BMP9 (RIP1-TAg2; $Gdf2^{-/-}$) for changes in primary tumor burden, angiogenesis and metastatic dissemination. Additionally, we investigate the gene expression pattern of *ENG*, *ACVRL1* and *GDF2* in human and mouse datasets of pancreatic neuroendocrine cancer and their correlation to an endothelial metagene.

Key findings

Gene expression datasets of human pancreatic neuroendocrine tumors and metastases showed a high correlation of *ACVRL1* and *ENG* to each other, as well as to a combined endothelial metagene (*PECAM1*/*CDH5*/*CD34*), suggesting ALK1 and endoglin are closely tied to the degree of tumor angiogenesis. Similar analysis was completed for the pancreatic islets in various stages of tumor growth from RIP1-TAg2, where the correlation of *Acvrl1* and *Eng* to the endothelial metagene persisted. PanNETs from RIP1-TAg2; $Acvrl1^{+/-}Eng^{+/-}$ mice synergistically decreased tumor growth to a greater extent than the reduction in RIP1-TAg2; $Acvrl1^{+/-}$ mice, however the double heterozygous receptor knockdown did not recapitulate the anti-angiogenic effects of ALK1 deficiency alone.

Gene expression of *GDF2* and *BMP10* did not show any significant correlation to *ACVRL1* or *ENG* expression, or the endothelial metagene, in human datasets of PanNETs. *Gdf2* had a negative correlation to each *Acvrl1* and *Eng* in mouse PanNETs. RIP1-TAg2; $Gdf2^{-/-}$ mice developed fewer tumors and had a smaller total tumor volume compared to native RIP1-TAg2 mice. However, *Gdf2* knockout had an increase in the incidence of hepatic micrometastases, despite the

decreased primary tumor burden. The capillary bed of tumors from RIP1-TAg2; *Gdf2*$^{-/-}$ mice displayed a higher number of vessel junctions and junction density, and tumor endothelial cells overexpress Notch downstream target genes, suggesting deregulation of stalk cell identity and increase in vessel sprouting. Tumors from RIP1-TAg2; *Gdf2*$^{-/-}$ mouse have an increased population of mesenchymal cells in proximity to the tumor vasculature, similar to RIP1-TAg2; *Eng*$^{-/-}$ previously reported (70). The RIP1-TAg2; *Gdf2*$^{-/-}$ tumor phenotype is a combination of phenotypes from both RIP1-TAg2; *Acvrl1*$^{+/-}$ and RIP1-TAg2; *Eng*$^{+/-}$ mice.

Paper III

Endothelial-specific genetic modifications of TGF-β receptors in mouse models of pancreatic neuroendocrine tumors

ALK5 is ubiquitously expressed, and therefore difficult to isolate its effects on tumor angiogenesis in vivo. Genetically engineered RIP1-TAg2 mice with transgenes for the deletion of ALK5, or expression of a constitutively active ALK5 mutant, under the control of the Cre-ERT2 recombination system specific for endothelial cells (*Cdh5* promoter) or pericytes (*Ng2* promoter). Cre recombination is induced prior to the onset of tumor angiogenesis. This manuscript surveys the tumor properties induced from deletion and overexpression of ALK5 in the tumor microenvironment, and highlights the unique routes of metastatic dissemination observed.

Key findings

RIP1-TAg2 compound mice with conditional *Alk5* knockout or constitutively active ALK5 mutant in endothelial cells (simplified RIP1-TAg2; *Cdh5-Alk5*$^{-/-}$ and RIP1-TAg2; *Cdh5*-mut*Alk5*^{CA}, respectively) were induced with tamoxifen between 5 and 6 weeks of age to study the effects of the genetic modifications prior to tumor vascularization, and sacrificed at 12 weeks of age. Tumors from RIP1-TAg2; *Cdh5-Alk5*$^{-/-}$ mice displayed no changes in number of primary tumors or tumor volume, but increased tumor vascularity, including number of vessel endpoints and junctions in tumors. Tumors from RIP1-TAg2; *Cdh5*-mut*Alk5*^{CA} mice had a modest increase in tumor volume, but no changes in tumor vasculature. Quantifying the incidence of metastases showed that RIP1-TAg2; *Cdh5*-mut*Alk5*^{CA} mice had a higher incidence of hepatic micrometastases, whereas RIP1-TAg2; *Cdh5-Alk5*$^{-/-}$ mice had a higher incidence of mesenteric lymph node metastasis, which appear enlarged and red.

Similar compound mice were developed to observe the effects of *Alk5* knockout or expression of mut*Alk5*^{CA} in pericytes of RIP1-TAg2 mice (RIP1-TAg2; *Ng2-Alk5*$^{-/-}$ and RIP1-TAg2; *Ng2*-mut*Alk5*^{CA}, respectively). Preliminary results thus far show that RIP1-TAg2; *Ng2-Alk5*$^{-/-}$ mice produced fewer angiogenic islets with no changes in the number of tumors, tumor volume, or tumor vasculature. No changes in tumor burden have been detected in RIP1-TAg2; *Ng2*-mut*Alk5*^{CA} mice. Further characterization of four unique compound mouse models described in this manuscript is ongoing.

Paper IV

Exploring novel targeting opportunities of endothelial TGF-β signaling during tumor angiogenesis

Following up on the successful application of ALK1-Fc in preclinical mouse models of cancer in paper I, we sought to further characterize ALK1 inhibition in MMTV-PyMT mice. Dalantercept is currently being investigated in the clinical setting as a combination therapy with VEGF inhibitors. Here we combine ALK1-Fc treatment with DC101, an anti-VEGFR2 monoclonal antibody. We also investigated the efficacy of ALK1-Fc in an adjuvant setting, following surgical resection of metastatic E0771 and 4T1 orthotopically injected mammary tumors, and the impact of ALK1 inhibition on immune response in tumors from MMTV-PyMT mice.

TGFBR2 is ubiquitously expressed, whereas endoglin is largely expressed by endothelial cells and otherwise by monocytes and smooth muscle cells. To exclude the effects of genetic modifications outside of endothelial cells we generated compound mice for *Tgfbr2* and *Eng* deletion limited to endothelial cells in RIP1-TAg2 mice. We investigated the specific impact of receptor deletion prior to the tumor angiogenic switch, and report on the consequential results on PanNET growth and tumor angiogenesis.

Key findings

Expanding on the neoadjuvant trials described in paper I, MMTV-PyMT mice were treated with ALK1-Fc and DC101 from 8-12 weeks of age. MMTV-PyMT mice treated with ALK1-Fc or DC101 showed strong inhibition of tumor growth independently, however there was no additive benefit upon combining treatment. Adjuvant ALK1-Fc therapy was evaluated with two orthopically implanted breast cancer cell lines. E0771 cells were implanted in the fourth mammary fat pad of C57BL/6 mice and 4T1 cells were similarly implanted in BALB/c mice, until the longest tumor diameter grew to 13 mm or 4 mm, respectively. Tumors were then

surgically resected, and adjuvant ALK1-Fc treatment was administered for four weeks following one week of rest post-surgery. The number of lung macrometastases counted at sacrifice revealed that ALK1-Fc treated mice had a much lower incidence of metastasis in both E0771 and 4T1 tumor models.

Sections of mammary tumors from MMTV-PyMT mice treated with RAP-041 from 11-15 weeks of age were stained for several immune cell markers. Staining for markers of leukocytes (CD45) and macrophages (F4/80) revealed no noticeable changes between treated and untreated tissue. However tumors from ALK1-Fc treated mice have an increase infiltration of CD3+ T-cells. It remains unclear if ALK1 inhibition directly results in recruitment or activation of these cells, or if the increased influx of T-cells results from effects on the vasculature.

Compound RIP1-TAg2 mice were generated with floxed *Eng* and *Tgfbr2* genes under the control of *Cdh5*-CreERT2 recombination system (RIP1-TAg2; *Cdh5-Eng*$^{-/-}$ and RIP1-TAg2; *Cdh5-Tgfbr2*$^{-/-}$, respectively). Cre recombination was induced at 5 weeks of age, and mice were sacrificed at 12 weeks of age. RIP1-TAg2; *Cdh5-Eng*$^{-/-}$ mice generated fewer tumors compared with control RIP1-TAg2 mice, and did not have an effect on tumor volume, consistent with our previous work using global *Eng* knock-out mice(70). RIP1-TAg2; *Cdh5-Tgfbr2*$^{-/-}$ mice had fewer angiogenic islets, fewer tumors and smaller total tumor volume at 12 weeks. *Tgfbr2* deletion had a visible effect on the tumor vasculature, producing tumor vessels that appear deformed compared to the vessels in tumors from RIP1-TAg2 mice. Vessel analysis revealed that the average vessel length and number of vessel junctions are increased in tumors from RIP1-TAg2; *Cdh5-Tgfbr2*$^{-/-}$ mice. No discernable changes were observed in the rate of metastatic dissemination.

Discussion

Inhibition of ALK1 using ALK1-Fc ligand trap has proved effective in various preclinical models of cancer described in papers I and IV. ALK1-Fc has a strong anti-angiogenic and tumor suppressive effects in PanNETs and mammary tumors. The reduced incidence of metastasis persisted in both the neoadjuvant and adjuvant therapy regimens, suggesting ALK1 inhibition must have an effect independent of the primary tumor. ALK1 inhibition may alter extravasation of circulating tumor cells into the lungs, or prevent a pro-tumorigenic microenvironment following seeding of circulating tumor cells in the metastatic niche. We have also observed the increased presence of CD3+ T-cells in mammary tumors of MMTV-PyMT mice. CD3+ cell infiltration in tumor tissue from human breast cancer patients is correlated with improved treatment response, and may also be beneficial towards tumor growth suppression in the MMTV-PyMT mouse model (95, 96). Given the properties of ALK1 inhibition described here, RAP-041 may suppress metastatic colonization by modulating the angiogenic switch in lung lesions, but other microenvironment responses such as immune cell infiltration may also prevent metastatic growth. The conditions that benefit or suppress metastatic colonization are not thoroughly understood, and future investigation into the microenvironment of metastases may be clinically valuable.

Combination of ALK1-Fc and DC101 administered to MMTV-PyMT mice did not show an additive benefit from two anti-angiogenic therapies, however ongoing clinical trials for dalantercept include combination therapy with sorafenib or axitinib (VEGFR TKIs). The premise of combining anti-angiogenic therapies is to circumvent resistance to VEGF, as has been observed in clinical trials with bevacizumab (97). The reduction of tumor volume in the two monotherapy arms of the MMTV-PyMT trial with ALK1-Fc and DC101 were similar, but the MMTV-PyMT mice did not display signs of resistance to the anti-angiogenic therapy. A mouse model of cancer that generates resistance to VEGF inhibitors may be a better indicator of clinical relevance for the combination of ALK1-Fc and DC101.

The knockout of BMP9, the primary ligand partner of ALK1, was expected to phenocopy ALK1 deficiency and inhibition, and tumors from RIP1-TAg2; *Gdf2*$^{-/-}$ mice were similarly reduced in number and volume. However, RIP1-TAg2; *Gdf2*$^{-/-}$

mice had a higher incidence of hepatic metastasis, in part resembling earlier studies of genetic deficiency for endoglin and diverging from the phenotype observed in ALK1 inhibition. BMP9 and endoglin deficiencies share similar phenotypes resembling EndMT. EndMT is poorly understood in tumor biology, and it is unclear how it contributes to metastasis. Impairment of EndMT is linked to reduced ALK5 signaling. Endoglin deficiency in tumor endothelial cells increased downstream ALK5 activity, suggesting modulation of ALK5 signaling by endoglin is necessary in maintaining the endothelial phenotype (70).

The increased incidence of hepatic metastases observed in RIP1-TAg2; *Cdh5*-mut*Alk5*CA mice also coincides with previous observations of RIP1-TAg2; *Eng*+/- mice. *Eng* deficiency increased downstream ALK5 activity, as the inhibitory modulation of ALK5 signaling by endoglin is reduced. The expression of mut*Alk5*CA should similarly increase downstream ALK5 signaling. The degree of ALK5 upregulation here has yet to be evaluated, but has recently been described elsewhere for the initiation of ovarian cancer(62). RIP1-TAg2; *Eng*+/-, RIP1-TAg2; *Gdf2*-/- and RIP1-TAg2; *Cdh5*-mut*Alk5*CA mice have similar effects on metastatic dissemination, but the underlying mechanism has not yet been elucidated. Tracking the cell fate of endothelial cell populations that have reduced endoglin signaling or over-activity of ALK5 may reveal more information about tumor intravasation and determine whether EndMT is involved in tumor invasiveness.

The endothelial-specific deletion and constitutive activation of ALK5 in RIP1-TAg2 mice uniquely influence metastatic dissemination. RIP1-TAg2; *Cdh5-Alk5*$^{-/-}$ mice displayed an increase in lymph node metastasis and no change in hepatic metastasis, while RIP1-TAg2; *Cdh5*-mut*Alk5*^{CA} mice displayed an increase in hepatic micrometastases but no lymph node metastases. These effects present a switch in the route of metastases hinging on the activity of one receptor, and further investigation may provide insight on the mechanism of tumor cell intravasation. TGF-β and BMP9 signaling are known to inhibit lymphangiogenesis in development and in tumor models, and the overexpression of both of these factors likely contributes to the absence of lymphangiogenesis within tumors from RIP1-TAg2 mice (53). *Cdh5* is also expressed by lymphatic and blood endothelial cells, so the effects of *Alk5* deletion cannot yet be clearly attributed. Alternatively, tumors from RIP1-TAg2; *Cdh5-Alk5*$^{-/-}$ may have managed to co-opt nearby lymphatic vessels. The lymph nodes of RIP1-TAg2; *Cdh5-Alk5*$^{-/-}$ appear swollen and red, indicating that metastatic seeding likely occurs earlier than in control mice, and that the lymph node microenvironment was permissive to enabling angiogenesis.

RIP1-TAg2; *Cdh5-Tgfbr2*$^{-/-}$ mice displayed profound effects on tumor suppression, reducing angiogenic islets, number of tumors and tumor volume, and

no increase in metastatic incidence. Angiogenesis was clearly impacted, greatly affecting vessel morphology, but no reduction in the degree of angiogenesis is obvious in any way similar to ALK1 inhibition. The vessel functionality has not yet been evaluated, and it is unclear if the vessel morphology is directly responsible for the suppression of tumor growth. The knockout of *Tgfbr2* and *Alk5* in endothelial cells each resulted in unique phenotypes in tumors from RIP1-TAg2 mice, demonstrating non-redundancy in their function. *Tgfbr2* deletion should be expected to eliminate ALK5 activity, since TBFBR2 is the only type 2 receptor ALK5 is known to form a complex with, but TGFBR2 deletion does not phenocopy the increase in lymphatic metastases observed in RIP1-TAg2; *Cdh5-Alk5*$^{-/-}$ mice. TGFBR2 can complex with ALK1 in addition to ALK5, but TGF-β activation of TGBR2/ALK1 reportedly also activates SMAD2/3 signaling cascade (41). Other interactions regulated through endoglin modulation, non-canonical signaling, or other TGF-β familial ligands and receptors not considered here may be impaired by TGFBR2 deletion in endothelial cells.

Thus far there is only one inhibitor of TGFBR2 in clinical development. IMC-TR1 is an anti-TGFBR2 monoclonal antibody, and phase I trials in advanced solid tumors were recently completed (73). However, information regarding its in vivo effects or efficacy as a cancer treatment is unpublished at the time of writing. The deletion of *Tgfbr2* in endothelial cells has not been explored in the context of tumor biology. The RIP1-TAg2 mice generate highly angiogenic PanNETs with a low fibroblast population, and while the high response of RIP1-TAg2 tumors to anti-angiogenic therapies is valuable, other facets of targeting *Tgfbr2* may not be revealed. *Tgfbr2* knockout generated a prominent phenotype in endothelial cells of RIP1-TAg2 mice, however preclinical cancer models of other tissues are required to convincingly demonstrate the consistency of targeting TGFBR2, or understanding the conditions in which it is an effective therapeutic approach.

Mice generated to target ALK5 signaling in pericytes did not yet demonstrate as great a phenotype as the endothelial cell equivalents. Pancreas of RIP1-TAg2;*Ng2-Alk5*$^{-/-}$ mice had fewer angiogenic islets, which may be an indication of fewer islets activating the angiogenic switch. The in vitro effects of TGF-β signaling on pericytes have been difficult to evaluate, as these cells do not form stable cell lines. While further characterization is required, progression of PanNETs may not be dependent on TGF-β signaling in pericytes. Pericytes are imperative to developmental angiogenesis, and TGF-β is required to regulate pericyte function once they have been recruited to blood vessels. Their contribution to the stroma or value as a therapeutic target in tumors is being investigated.

Conclusions and Perspectives

The body of research surrounding TGF-β family signaling reveals context-specific signaling interactions that do not consistently translate from in vitro to in vivo experiments, or from developmental biology to disease. To specifically investigate the roles of signaling in the context of tumor angiogenesis, we've utilized various preclinical tumor models to evaluate the efficacy of ALK1 inhibition, and compound genetically engineered mice to restrict genetic modifications to the endothelial cell compartment. Modulation of the TGF- β family members can alter the angiogenic and metastatic profile of mouse tumors, and may be valuable to the future development of clinically relevant therapeutic strategies.

The work described in papers III and IV introduced various genetically modified compound mouse models of TGF-β receptors, the work of which is currently ongoing. In the immediate future we plan to fully characterize the changes in the PanNET microenvironment resulting from endothelial cell and pericyte-specific modifications of TGFBR2 and ALK5 signaling. This includes the detection of lymphatic vessels, pericyte coverage, mesenchymal cells and their contribution to tumorigenesis. Evaluating the extent of up- or down-regulation of downstream factors of ALK5/TGF-β and ALK1/BMP9 signaling from isolated tumor endothelial cells or pericytes will clarify how ALK5 and TGFBR2 signaling affect the stromal cell population, tumor growth and metastatic dissemination.

The drivers of angiogenesis engaged by ALK5 deletion and high ALK5 activity in endothelial cells creates two diverging paths in which to understand how angiogenesis contributes to metastasis. The role of TGF-β signaling in lymphangiogenesis is not as well described as vascular angiogenesis, however investigating these interactions may illuminate mechanisms behind metastatic dissemination to lymph nodes. This body of research attempts to describe the role of EndMT in metastatic initiation, however stronger evidence is required to demonstrate the activity of EndMT in PanNETs, and its contribution to metastases. This will include tracing the fate of endothelial cells with impaired endoglin or BMP9 activity, or high activity of ALK5.

The TGF-β family contains many promising targets for developing cancer therapies. Deletion of *Tgfbr2* was limited to endothelial cells but displayed strong anti-angiogenic and anti-tumorigenic effects, however these effects are so far limited to one preclinical model. Diverse preclinical models that resemble human

disease will better contribute to the understanding of mechanisms of resistance as they are met in the clinic.

Popular Science Summary

Tumors arise from uncontrolled growth of mutated cells in the body. In order for tumors to survive they require a connection the body's circulatory system, providing a growing tumor with oxygen and nutrition. The ability to build this connection through new blood vessels is an important step in cancer progression, and gives tumor cells a route to escape the primary tumor and form metastasis in a different body tissue. The biological mechanisms for creating new blood vessels, termed angiogenesis, are valuable to the creation of new treatments against cancer. Some treatments in the clinic already target the growth of new blood vessels, but in practice some patients become resistant to these therapies. To improve tumor therapies targeting the creation of new blood vessels, we investigate other biological mechanisms that drive blood vessel growth, and various methods of inhibiting these biological mechanisms from enabling cancer progression.

The transforming-growth factor (TGF)-β family of proteins is responsible for many biological programs from early human development to many adult diseases, and has a significant role in angiogenesis. We investigate the signaling of several ligands and receptors in the TGF-β family in endothelial cells of tumors. This includes the receptors ALK1 and endoglin binding to BMP9, and the receptors ALK5 and TGFBR2 binding to TGF-β. Inhibition of the receptor ALK1 in several preclinical mouse models of breast and pancreatic cancer consistently resulted in decreased tumor growth, metastatic growth and angiogenesis, and an increase in the number of immune cells were detected in breast tumors. Combining inhibition of ALK1 with chemotherapy improved the anti-tumorigenic effect. The combined genetic reduction of ALK1 and its co-receptor endoglin in pancreatic cancer suppressed tumor growth to a greater degree than either individual genetic reduction. Deletion of the BMP9 protein did not replicate the effect of ALK1 inhibition, showing reduced tumor growth but increased liver metastases.

In endothelial cells of pancreatic tumor-bearing mice, the receptor ALK5 was deleted, or an "always-on" mutant of ALK5 was activated. These genetic modifications increased the number of detected metastasis to the lymph nodes, and the liver, respectively, suggesting a role for TGF-β/ALK5 signaling in influencing the route of metastatic spread. The TGFBR2 receptor was also deleted from the endothelial cells of pancreatic tumor-bearing mice. This resulted in a decrease in the number and total volume of tumors, and tumor vessel appeared highly abnormal. Further investigation into the activity ALK5 and TGFBR2 in

endothelial cells is required to understand how the unique contributions to TGF-β signaling in tumors.

Acknowledgements

Thank you Kristian, you took a chance on me and gave me the once-in-a-lifetime opportunity to study in Sweden as a member of your research team. You have fostered a fantastic team dynamic with a group of people passionate about science, and I'm glad to have been a part of it. Thank you Eugenia, your contributions to the animal work and managing the lab have been a blessing. Thank you to all the KP group members past and present, I am grateful for the help as I bumble through lab work, and even more grateful for the lifelong friends I have made.

Special thanks to Sam, nothing was more reassuring of my decision to leave home than my closest friend making the same trek over to Europe as I did. Glad we kept up our adventures over these years.

References

1. Townsend N, et al. (2016) Cardiovascular disease in Europe: epidemiological update 2016. European heart journal 37(42):3232-3245.

2. Statistics CCSsACoC (2016) Canadian Cancer Statistics 2016. Canadian Cancer Society.

3. Siegel RL, Miller KD, & Jemal A (2016) Cancer statistics, 2016. CA: a cancer journal for clinicians 66(1):7-30.

4. Steeg PS & Theodorescu D (2008) Metastasis: a therapeutic target for cancer. Nature clinical practice. Oncology 5(4):206-219.

5. Hanahan D & Weinberg RA (2011) Hallmarks of cancer: the next generation. Cell 144(5):646-674.

6. Pietras K & Östman A (2010) Hallmarks of cancer: interactions with the tumor stroma. Experimental cell research 316(8):1324-1331.

7. Gajewski TF, Schreiber H, & Fu YX (2013) Innate and adaptive immune cells in the tumor microenvironment. Nature immunology 14(10):1014-1022.

8. Bhowmick NA, Neilson EG, & Moses HL (2004) Stromal fibroblasts in cancer initiation and progression. Nature 432(7015):332-337.

9. Drake CJ (2003) Embryonic and adult vasculogenesis. Birth defects research. Part C, Embryo today : reviews 69(1):73-82.

10. Ferrara N, Gerber HP, & LeCouter J (2003) The biology of VEGF and its receptors. Nature medicine 9(6):669-676.

11. Adams RH & Alitalo K (2007) Molecular regulation of angiogenesis and lymphangiogenesis. Nature reviews. Molecular cell biology 8(6):464-478.

12. Jakobsson L, et al. (2010) Endothelial cells dynamically compete for the tip cell position during angiogenic sprouting. Nature cell biology 12(10):943-953.

13. Compagni A, Wilgenbus P, Impagnatiello MA, Cotten M, & Christofori G (2000) Fibroblast growth factors are required for efficient tumor angiogenesis. Cancer research 60(24):7163-7169.

14. Pugh CW & Ratcliffe PJ (2003) Regulation of angiogenesis by hypoxia: role of the HIF system. Nature medicine 9(6):677-684.

15. Al-Husein B, Abdalla M, Trepte M, Deremer DL, & Somanath PR (2012) Antiangiogenic therapy for cancer: an update. Pharmacotherapy 32(12):1095-1111.

16. Lindahl P, Johansson BR, Levéen P, & Betsholtz C (1997) Pericyte loss and microaneurysm formation in PDGF-B-deficient mice. Science 277(5323):242-245.

17. McAllister KA, et al. (1994) Endoglin, a TGF-b binding protein of endothelial cells, is the gene for hereditary haemorrhagic telangiectasia type 1. Nature Genet 8(4):345-351.

18. Ribatti D (2009) Endogenous inhibitors of angiogenesis: a historical review. Leukemia research 33(5):638-644.

19. Baeriswyl V & Christofori G (2009) The angiogenic switch in carcinogenesis. Seminars in cancer biology 19(5):329-337.

20. McDonald DM & Choyke PL (2003) Imaging of angiogenesis: from microscope to clinic. Nature medicine 9(6):713-725.

21. Carmeliet P & Jain RK (2000) Angiogenesis in cancer and other diseases. Nature 407(6801):249-257.

22. Nagy JA, Chang SH, Dvorak AM, & Dvorak HF (2009) Why are tumour blood vessels abnormal and why is it important to know? British journal of cancer 100(6):865-869.

23. Folkman J (2006) Antiangiogenesis in cancer therapy--endostatin and its mechanisms of action. Experimental cell research 312(5):594-607.

24. Recouvreux MV, Camilletti MA, Rifkin DB, Becu-Villalobos D, & Diaz-Torga G (2012) Thrombospondin-1 (TSP-1) analogs ABT-510 and ABT-898 inhibit prolactinoma growth and recover active pituitary transforming growth factor-beta1 (TGF-beta1). Endocrinology 153(8):3861-3871.

25. Abdollahi A, et al. (2004) Endostatin's antiangiogenic signaling network. Molecular cell 13(5):649-663.

26. Rini BI, et al. (2010) Phase III trial of bevacizumab plus interferon alfa versus interferon alfa monotherapy in patients with metastatic renal cell carcinoma: final results of CALGB 90206. J Clin Oncol 28(13):2137-2143.

27. Hamberg P, Verweij J, & Sleijfer S (2010) (Pre-)clinical pharmacology and activity of pazopanib, a novel multikinase angiogenesis inhibitor. The oncologist 15(6):539-547.

28. Samant RS & Shevde LA (2011) Recent advances in anti-angiogenic therapy of cancer. Oncotarget 2(3):122-134.

29. Yao JC, et al. (2011) Everolimus for advanced pancreatic neuroendocrine tumors. The New England journal of medicine 364(6):514-523.

30. Houghton PJ (2010) Everolimus. Clinical cancer research : an official journal of the American Association for Cancer Research 16(5):1368-1372.

31. Shibuya M (2011) Vascular Endothelial Growth Factor (VEGF) and Its Receptor (VEGFR) Signaling in Angiogenesis: A Crucial Target for Anti- and Pro-Angiogenic Therapies. Genes & cancer 2(12):1097-1105.

32. Dey N, De P, & Brian LJ (2015) Evading anti-angiogenic therapy: resistance to anti-angiogenic therapy in solid tumors. American journal of translational research 7(10):1675-1698.

33. Bergers G & Hanahan D (2008) Modes of resistance to anti-angiogenic therapy. Nature reviews. Cancer 8(8):592-603.

34. Casanovas O, Hicklin DJ, Bergers G, & Hanahan D (2005) Drug resistance by evasion of antiangiogenic targeting of VEGF signaling in late-stage pancreatic islet tumors. Cancer Cell 8(4):299-309.

35. Vasudev NS & Reynolds AR (2014) Anti-angiogenic therapy for cancer: current progress, unresolved questions and future directions. Angiogenesis 17(3):471-494.

36. Ricard C, et al. (2013) Dynamic quantitative intravital imaging of glioblastoma progression reveals a lack of correlation between tumor growth and blood vessel density. PloS one 8(9):e72655.

37. Weiss A & Attisano L (2013) The TGFbeta superfamily signaling pathway. Wiley interdisciplinary reviews. Developmental biology 2(1):47-63.

38. Huminiecki L, et al. (2009) Emergence, development and diversification of the TGF-beta signalling pathway within the animal kingdom. BMC evolutionary biology 9:28.

39. Massague J (2012) TGFbeta signalling in context. Nature reviews. Molecular cell biology 13(10):616-630.

40. Moustakas A & Heldin CH (2009) The regulation of TGFbeta signal transduction. Development 136(22):3699-3714.

41. Pardali E, Goumans MJ, & ten Dijke P (2010) Signaling by members of the TGF-beta family in vascular morphogenesis and disease. Trends Cell Biol 20(9):556-567.

42. Jonker L (2014) TGF-beta & BMP receptors endoglin and ALK1: overview of their functional role and status as antiangiogenic targets. Microcirculation 21(2):93-103.

43. Li W, Salmon RM, Jiang H, & Morrell NW (2016) Regulation of the ALK1 ligands, BMP9 and BMP10. Biochemical Society transactions 44(4):1135-1141.

44. Zhang L, Zhou F, & ten Dijke P (2013) Signaling interplay between transforming growth factor-beta receptor and PI3K/AKT pathways in cancer. Trends in biochemical sciences 38(12):612-620.

45. Wu MY & Hill CS (2009) Tgf-beta superfamily signaling in embryonic development and homeostasis. Developmental cell 16(3):329-343.

46. Kovacic JC, Mercader N, Torres M, Boehm M, & Fuster V (2012) Epithelial-to-mesenchymal and endothelial-to-mesenchymal transition: from cardiovascular development to disease. Circulation 125(14):1795-1808.

47. ten Dijke P & Arthur HM (2007) Extracellular control of TGFbeta signalling in vascular development and disease. Nature reviews. Molecular cell biology 8(11):857-869.

48. Oshima M, Oshima H, & Taketo MM (1996) TGF-b receptor type II deficiency results in defects of yolk sac hematopoiesis and vasculogenesis. Dev Biol 179(1):297-302.

49. Wang J, et al. (2006) Defective ALK5 signaling in the neural crest leads to increased postmigratory neural crest cell apoptosis and severe outflow tract defects. BMC developmental biology 6:51.

50. Ricard N, et al. (2012) BMP9 and BMP10 are critical for postnatal retinal vascular remodeling. Blood 119(25):6162-6171.

51. Chen H, et al. (2004) BMP10 is essential for maintaining cardiac growth during murine cardiogenesis. Development 131(9):2219-2231.

52. Levet S, et al. (2015) BMP9 and BMP10 are necessary for proper closure of the ductus arteriosus. Proceedings of the National Academy of Sciences of the United States of America 112(25):E3207-3215.

53. Yoshimatsu Y, et al. (2013) Bone morphogenetic protein-9 inhibits lymphatic vessel formation via activin receptor-like kinase 1 during development and cancer progression. Proceedings of the National Academy of Sciences of the United States of America 110(47):18940-18945.

54. Hawinkels LJ, et al. (2016) Activin Receptor-like Kinase 1 Ligand Trap Reduces Microvascular Density and Improves Chemotherapy Efficiency to Various Solid Tumors. Clinical cancer research : an official journal of the American Association for Cancer Research 22(1):96-106.

55. Ferrari G, Cook BD, Terushkin V, Pintucci G, & Mignatti P (2009) Transforming growth factor-beta 1 (TGF-beta1) induces angiogenesis through vascular endothelial growth factor (VEGF)-mediated apoptosis. Journal of cellular physiology 219(2):449-458.

56. David L, et al. (2008) Bone morphogenetic protein-9 is a circulating vascular quiescence factor. Circulation research 102(8):914-922.

57. David L, Mallet C, Mazerbourg S, Feige JJ, & Bailly S (2007) Identification of BMP9 and BMP10 as functional activators of the orphan activin receptor-like kinase 1 (ALK1) in endothelial cells. Blood 109(5):1953-1961.

58. Larrivee B, et al. (2012) ALK1 signaling inhibits angiogenesis by cooperating with the Notch pathway. Developmental cell 22(3):489-500.

59. Aspalter IM, et al. (2015) Alk1 and Alk5 inhibition by Nrp1 controls vascular sprouting downstream of Notch. Nature communications 6:7264.

60. Tian M & Schiemann WP (2009) The TGF-beta paradox in human cancer: an update. Future Oncol 5(2):259-271.

61. Lebrun JJ (2012) The Dual Role of TGFbeta in Human Cancer: From Tumor Suppression to Cancer Metastasis. ISRN molecular biology 2012:381428.

62. Gao Y, et al. (2016) Constitutively active transforming growth factor beta receptor 1 in the mouse ovary promotes tumorigenesis. Oncotarget 7(27):40904-40918.

63. Pickup M, Novitskiy S, & Moses HL (2013) The roles of TGFbeta in the tumour microenvironment. Nature reviews. Cancer 13(11):788-799.

64. Bhowmick NA, et al. (2004) TGF-beta signaling in fibroblasts modulates the oncogenic potential of adjacent epithelia. Science 303(5659):848-851.

65. Cheng N, et al. (2005) Loss of TGF-beta type II receptor in fibroblasts promotes mammary carcinoma growth and invasion through upregulation of TGF-alpha-, MSP- and HGF-mediated signaling networks. Oncogene 24(32):5053-5068.

66. Zheng X, et al. (2015) Epithelial-to-mesenchymal transition is dispensable for metastasis but induces chemoresistance in pancreatic cancer. Nature 527(7579):525-530.

67. Cunha SI, et al. (2010) Genetic and pharmacological targeting of activin receptor-like kinase 1 impairs tumor growth and angiogenesis. J Exp Med 207(1):85-100.

68. Cunha SI & Pietras K (2011) ALK1 as an emerging target for antiangiogenic therapy of cancer. Blood 117(26):6999-7006.

69. Hu-Lowe DD, et al. (2011) Targeting Activin Receptor-Like Kinase 1 (ALK1) Inhibits Angiogenesis and Tumorigenesis Through a Mechanism of Action Complementary to Anti-VEGF Therapies. Cancer research 71(4):1362-1373.

70. Anderberg C, et al. (2013) Deficiency for endoglin in tumor vasculature weakens the endothelial barrier to metastatic dissemination. J Exp Med 210(3):563-579.

71. Sheen YY, Kim MJ, Park SA, Park SY, & Nam JS (2013) Targeting the Transforming Growth Factor-beta Signaling in Cancer Therapy. Biomolecules & therapeutics 21(5):323-331.

72. Bogdahn U, et al. (2011) Targeted therapy for high-grade glioma with the TGF-beta2 inhibitor trabedersen: results of a randomized and controlled phase IIb study. Neuro-oncology 13(1):132-142.

73. Neuzillet C, et al. (2015) Targeting the TGFbeta pathway for cancer therapy. Pharmacology & therapeutics 147:22-31.

74. Herbertz S, et al. (2015) Clinical development of galunisertib (LY2157299 monohydrate), a small molecule inhibitor of transforming growth factor-beta signaling pathway. Drug design, development and therapy 9:4479-4499.

75. Brandes AA, et al. (2016) A Phase II randomized study of galunisertib monotherapy or galunisertib plus lomustine compared with lomustine monotherapy in patients with recurrent glioblastoma. Neuro-oncology 18(8):1146-1156.

76. Mitchell D, et al. (2010) ALK1-Fc inhibits multiple mediators of angiogenesis and suppresses tumor growth. Molecular cancer therapeutics 9(2):379-388.

77. de Vinuesa AG, Bocci M, Pietras K, & Ten Dijke P (2016) Targeting tumour vasculature by inhibiting activin receptor-like kinase (ALK)1 function. Biochemical Society transactions 44(4):1142-1149.

78. Jimeno A, et al. (2016) A phase 2 study of dalantercept, an activin receptor-like kinase-1 ligand trap, in patients with recurrent or metastatic squamous cell carcinoma of the head and neck. Cancer 122(23):3641-3649.

79. Voss MH, et al. (2016) The DART Study: Results from the dose-escalation and expansion cohorts evaluating the combination of dalantercept plus axitinib in advanced renal cell carcinoma. Clinical cancer research : an official journal of the American Association for Cancer Research.

80. Goff LW, et al. (2016) A Phase I Study of the Anti-Activin Receptor-Like Kinase 1 (ALK-1) Monoclonal Antibody PF-03446962 in Patients with Advanced Solid Tumors. Clinical cancer research : an official journal of the American Association for Cancer Research 22(9):2146-2154.

81. Simonelli M, et al. (2016) Phase I study of PF-03446962, a fully human monoclonal antibody against activin receptor-like kinase-1, in patients with hepatocellular carcinoma. Annals of oncology : official journal of the European Society for Medical Oncology 27(9):1782-1787.

82. Necchi A, et al. (2014) PF-03446962, a fully-human monoclonal antibody against transforming growth-factor beta (TGFbeta) receptor ALK1, in pre-treated patients with urothelial cancer: an open label, single-group, phase 2 trial. Investigational new drugs 32(3):555-560.

83. Wheatley-Price P, et al. (2016) A Phase II Study of PF-03446962 in Patients with Advanced Malignant Pleural Mesothelioma. CCTG Trial IND.207. Journal of thoracic oncology : official publication of the International Association for the Study of Lung Cancer 11(11):2018-2021.

84. Gordon MS, et al. (2014) An open-label phase Ib dose-escalation study of TRC105 (anti-endoglin antibody) with bevacizumab in patients with advanced cancer. Clinical cancer research : an official journal of the American Association for Cancer Research 20(23):5918-5926.

85. Apolo AB, et al. (2016) A Phase II Clinical Trial of TRC105 (Anti-Endoglin Antibody) in Adults With Advanced/Metastatic Urothelial Carcinoma. Clinical genitourinary cancer.

86. Duffy AG, et al. (2015) A phase II study of TRC105 in patients with hepatocellular carcinoma who have progressed on sorafenib. United European gastroenterology journal 3(5):453-461.

87. Ewens A, Mihich E, & Ehrke MJ (2005) Distant metastasis from subcutaneously grown E0771 medullary breast adenocarcinoma. Anticancer research 25(6B):3905-3915.

88. Pulaski BA & Ostrand-Rosenberg S (2001) Mouse 4T1 breast tumor model. Current protocols in immunology Chapter 20:Unit 20 22.

89. Hanahan D (1985) Heritable formation of pancreatic beta-cell tumours in transgenic mice expressing recombinant insulin/simian virus 40 oncogenes. Nature 315(6015):115-122.

90. Eklund L, Bry M, & Alitalo K (2013) Mouse models for studying angiogenesis and lymphangiogenesis in cancer. Molecular oncology 7(2):259-282.

91. Taneja P, et al. (2009) MMTV mouse models and the diagnostic values of MMTV-like sequences in human breast cancer. Expert Rev Mol Diagn 9(5):423-440.

92. Guy CT, Cardiff RD, & Muller WJ (1992) Induction of mammary tumors by expression of polyomavirus middle T oncogene: a transgenic mouse model for metastatic disease. Mol Cell Biol 12(3):954-961.

93. Kumler I, Christiansen OG, & Nielsen DL (2014) A systematic review of bevacizumab efficacy in breast cancer. Cancer Treat Rev 40(8):960-973.

94. Mackey JR, et al. (2012) Controlling angiogenesis in breast cancer: a systematic review of anti-angiogenic trials. Cancer Treat Rev 38(6):673-688.

95. Hornychova H, et al. (2008) Tumor-infiltrating lymphocytes predict response to neoadjuvant chemotherapy in patients with breast carcinoma. Cancer investigation 26(10):1024-1031.

96. Gianni L, et al. (2005) Gene expression profiles in paraffin-embedded core biopsy tissue predict response to chemotherapy in women with locally advanced breast cancer. J Clin Oncol 23(29):7265-7277.

97. Delaloge S, et al. (2016) Paclitaxel plus bevacizumab or paclitaxel as first-line treatment for HER2-negative metastatic breast cancer in a multicenter national observational study. Annals of oncology : official journal of the European Society for Medical Oncology 27(9):1725-1732.

Paper I

Microenvironment and Immunology

Cancer Research

Endothelial ALK1 Is a Therapeutic Target to Block Metastatic Dissemination of Breast Cancer

Sara I. Cunha[1,2], Matteo Bocci[3], John Lövrot[4], Nikolas Eleftheriou[3], Pernilla Roswall[2], Eugenia Cordero[3], Linda Lindström[4], Michael Bartoschek[3], B. Kristian Haller[2], R. Scott Pearsall[5], Aaron W. Mulivor[5], Ravindra Kumar[5], Christer Larsson[3], Jonas Bergh[4], and Kristian Pietras[2,3]

Abstract

Exploration of new strategies for the prevention of breast cancer metastasis is justifiably at the center of clinical attention. In this study, we combined a computational biology approach with mechanism-based preclinical trials to identify inhibitors of activin-like receptor kinase (ALK) 1 as effective agents for blocking angiogenesis and metastasis in breast cancer. Pharmacologic targeting of ALK1 provided long-term therapeutic benefit in mouse models of mammary carcinoma, accompanied by strikingly reduced metastatic colonization as a monotherapy or part of combinations with chemotherapy. Gene-expression analysis of breast cancer specimens from a population-based nested case–control study encompassing 768 subjects defined endothelial expression of ALK1 as an independent and highly specific prognostic factor for metastatic manifestation, a finding that was corroborated in an independent clinical cohort. Overall, our results suggest that pharmacologic inhibition of endothelial ALK1 constitutes a tractable strategy for interfering with metastatic dissemination of breast cancer. *Cancer Res; 75(12); 2445–56. ©2015 AACR.*

Introduction

Exploration of new strategies for the prevention of breast cancer metastasis is justifiably at the center of clinical attention (1). The haematogenous dissemination of tumor cells is a multistep process requiring: (i) detachment of malignant cells from the primary tumor, (ii) intravasation into and extravasation from the blood stream, and (iii) colonization of the distant organ (2). However, we currently have limited knowledge on the molecular drivers contributing to each of the steps in the metastatic cascade in breast cancer, and thus efforts to target-specific signaling pathways involved in the systemic spread of the disease have largely been unsuccessful so far (3). In cases where breast tumors are found in early stages, the prognosis following adequate therapy is good with a 3-year overall survival (OS) rate reaching above 90% (4). Nevertheless, many women are not diagnosed until the tumor has reached advanced stages; tumor stage is an established factor for poor prognosis (4). Thus, novel treatment strategies to combat disseminated breast cancer, both for the neoadjuvant and the adjuvant setting, are sorely needed.

The angiogenic process is required for tumor progression from an indolent state (5). The vascular tree provides a tumor with its metabolic requirements, while simultaneously providing an escape route by which malignant cells can leave the primary tumor bulk. Indeed, in particular cases, high vascular density was demonstrated to be a prognostic factor for poor outcome in breast cancer, as well as in other malignancies (6, 7). The introduction of multitargeted agents incorporating antiangiogenic activity in clinical practice has led to improved disease control in terms of prolonged progression-free survival (PFS). Consequently, drugs targeting the vascular endothelial growth factor (VEGF) pathway are now included in the first line therapy for metastatic disease for a range of malignancies (8–11). However, attempts to target tumor angiogenesis in breast cancer has met with ambiguous success (12, 13). Although providing initial relief for metastatic breast cancer patients by improving response rates and prolonging PFS, no conclusive evidence for long-term benefit in OS has been provided to date (13). Consistent with this clinical reality, recent preclinical studies indicate that tumors in mice treated systemically with anti-VEGF therapy rapidly acquire resistance, coupled to recurring tumors that appear to be more locally invasive and have a higher propensity to seed distant metastases (14–16). Thus, the need for a mechanism-based and clinically relevant search for alternative angiogenic pathways that may serve as targets for more efficacious drugs without affecting disease stage in breast cancer is highly warranted.

ALK1 is a type I receptor in the large TGFβ family expressed selectively by endothelial cells (17). Pharmacologic targeting of ALK1 has demonstrable therapeutic efficacy in a diverse set of mouse models of cancer (18–20). Here, we investigate the utility of ALK1 inhibition as an antimetastatic therapy in breast cancer using a combined approach of preclinical testing of a clinically

[1]Ludwig Institute for Cancer Research, Uppsala, Sweden. [2]Division of Vascular Biology, Department of Medical Biochemistry and Biophysics, Karolinska Institutet, Stockholm, Sweden. [3]Division of Translational Cancer Research, Department of Laboratory Medicine, Medicon Village, Lund University, Lund, Sweden. [4]Department of Oncology and Pathology, Karolinska Institutet, Stockholm, Sweden. [5]Acceleron Pharma, Cambridge, Massachusetts.

Note: Supplementary data for this article are available at Cancer Research Online (http://cancerres.aacrjournals.org/).

Corresponding Author: Kristian Pietras, Lund University, Division of Translational Cancer Research, Medicon Village, Building 404:A3, SE-22381 Lund, Sweden. Phone: 46-709-209-709; E-mail: Kristian.Pietras@med.lu.se

doi: 10.1158/0008-5472.CAN-14-3706

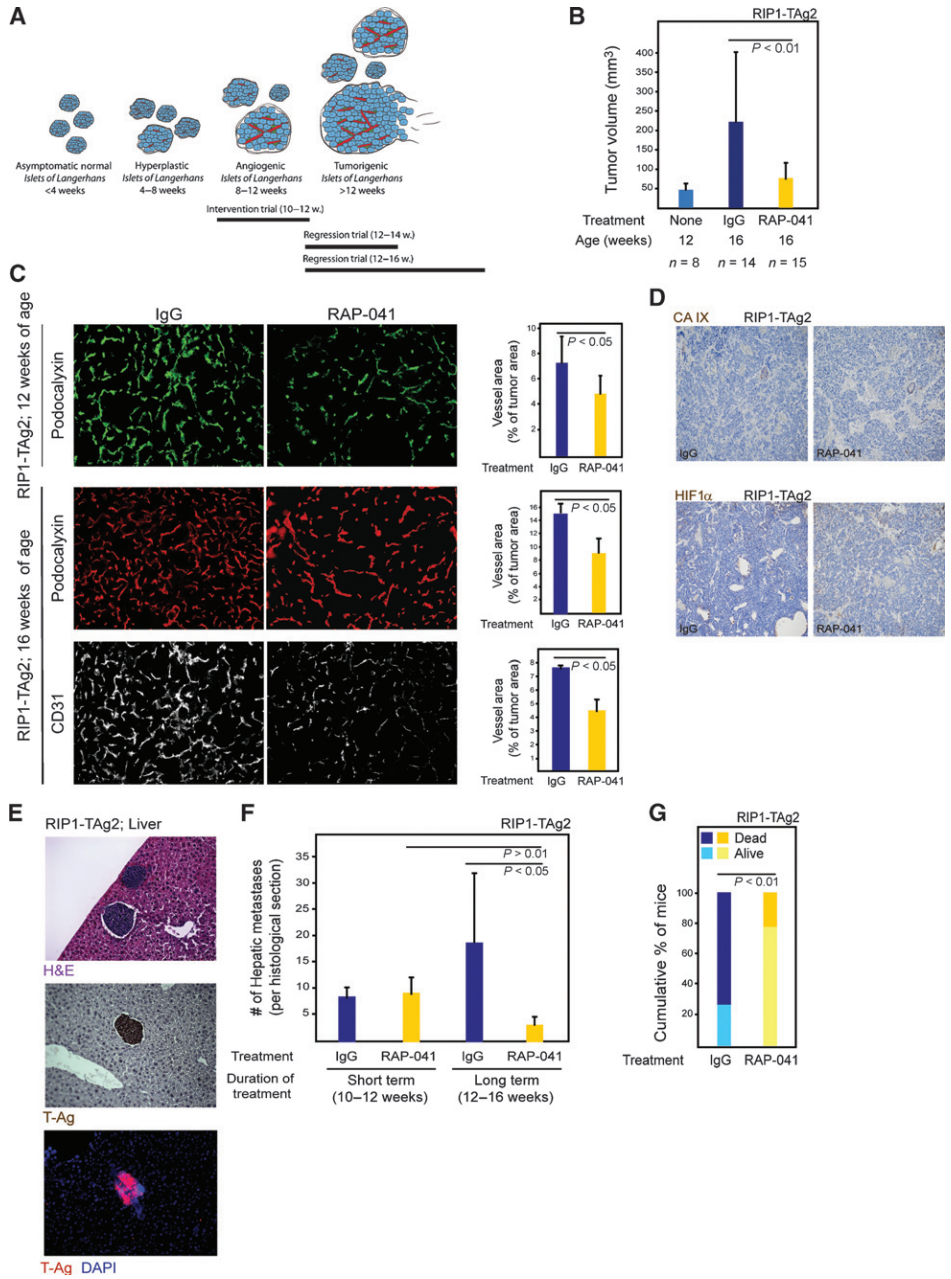
A
Asymptomatic normal Islets of Langerhans <4 weeks
Hyperplastic Islets of Langerhans 4–8 weeks
Angiogenic Islets of Langerhans 8–12 weeks
Tumorigenic Islets of Langerhans >12 weeks
Intervention trial (10–12 w.)
Regression trial (12–14 w.)
Regression trial (12–16 w.)
B
RIP1-TAg2
Tumor volume (mm3)
P < 0.01
Treatment None IgG RAP-041
Age (weeks) 12 16 16
n = 8 n = 14 n = 15
C
RIP1-TAg2; 12 weeks of age
RIP1-TAg2; 16 weeks of age
Podocalyxin
CD31
IgG
RAP-041
Vessel area (% of tumor area)
P < 0.05
Treatment IgG RAP-041
D
CA IX
HIF1α
RIP1-TAg2
IgG
RAP-041
E
RIP1-TAg2; Liver
H&E
T-Ag
T-Ag DAPI
F
RIP1-TAg2
# of Hepatic metastases (per histological section)
P > 0.01
P < 0.05
Treatment IgG RAP-041 IgG RAP-041
Duration of treatment
Short term (10–12 weeks)
Long term (12–16 weeks)
G
RIP1-TAg2
Dead
Alive
Cumulative % of mice
P < 0.01
Treatment IgG RAP-041

tractable ALK1 inhibitor and analysis of gene-expression patterns relating to metastatic spread in breast cancer patient specimens.

Materials and Methods

Cell culture

MDA-MB-231 were maintained in culture in DMEM (Invitrogen), supplemented with 10% FCS. EO771 breast cancer cells were cultured in DMEM supplemented with 20% FCS.

Animal care and tumor establishment

All animal experiments were approved by the local ethical committee for animal care in Stockholm and Lund (permits N96/11 and M142/13). The RIP-TAg2 mice (C57Bl6/J background) received water supplemented with 5% sugar to alleviate hypoglycemia from 10 weeks of age. Total tumor burden per mouse was calculated as the sum of the volume of each individual tumor dissected from a RIP-TAg2 mouse pancreas. The MMTV-PyMT mice (FVB/n strain background) were followed for tumor growth from 8 to 12 weeks in early-stage trials and from 11 to 15 weeks of age in late stage trials. Primary tumor burden was determined by caliper measurements on live sedated mice once a week and the total tumor burden per mouse was calculated as the sum of the volume of each individual mammary tumor. To establish EO771 tumors, 5×10^5 cells were injected orthotopically into the fourth mammary fat pad of isofluran-anesthesized wildtype C57Bl6/J females. 1×10^6 cells of the human metastatic breast cancer cell line MDA-MB-231 were transplanted s.c. to immunocompromised SCID mice. In all cases, tumor volume was calculated as length $\times$ width^2 $\times$ $\pi/6$.

Therapeutic trials

Control IgG or RAP-041 (Acceleron Pharma) was diluted in TBS and administered twice weekly by i.p. injection at 12 mg/kg per injection. Mice carrying orthotopic EO771 mammary carcinomas were treated with either RAP-041 or IgG2a for 2 weeks starting 7 days following tumor establishment. Treatment with docetaxel (Taxotere, Sanofi-Aventis) was administered once weekly at 20 mg/kg by i.p. injection.

Tissue preparation, histology, and immunostaining

Mice were heart-perfused with PBS followed by 4% paraformaldehyde. For paraffin-embedding, organs were post-fixed in 4% paraformaldehyde for 2 hours before proceeding to embedding. Paraffin-embedded sections were deparaffinized and rehydrated followed by antigen retrieval in low pH buffer (pH 6; DAKO) for 20 min at 95°C. Blocking was performed in 10% normal goat serum in TNB buffer (PerkinElmer). The primary antibody against the PyMT oncogene (1:100; Abcam ab15085) was incubated in blocking buffer overnight at 4°C. For SV40 T-Ag staining, a high pH antigen retrieval buffer (pH 10; DAKO) was used, followed by washes and quenching of endogenous peroxidase activity with 50% methanol/3% H_2O_2 in PBS for 10 minutes in room temperature. A wash in PBS preceded blocking with 10% normal goat serum in TNB for 1 hour. The primary antibody against T-Ag (1:1,000; a kind gift from Douglas Hanahan, EPFL) was incubated at 4°C overnight. After washes with PBS containing 0.1% Tween-20, a suitable biotinylated secondary antibody was incubated for 45 minutes in room temperature.

For cryopreservation, tumors, livers and/or lungs were kept in 30% sucrose at 4°C overnight, followed by embedding in cryosectioning media. Frozen sections were fixed in ice-cold acetone, followed by blocking using serum free protein block (DAKO) for >90 minutes at room temperature. Primary antibodies directed against CD31 (dilution 1:100; Pharmingen MEC13.3), podocalyxin (dilution 1:100; R&D Systems, AF1556), and BMP9 (dilution 1:500; Abcam; ab35088) were incubated overnight at 4°C. Appropriate Alexa 594 and Alexa 488–flourochrome-conjugated secondary antibodies (Invitrogen) were used and sections were finally mounted using 4′,6-diamidino-2-phenylindole-containing mounting media (Vector Laboratories).

Quantification of metastases

The right lateral liver lobe from RIP-TAg2 mice or the left lung lobes of MMTV-PyMT or EO771-bearing mice were embedded in paraffin upon tissue fixation. The metastatic burden was assessed by serial sectioning of the entire lung/liver lobe. Following hematoxylin and eosin (H&E) staining on every 25th section, the number of metastatic foci (>8 cells in diameter) was determined in >15 sections per mouse and >5 mice per group.

RNA isolation and quantitative RT-PCR

Total RNA of 12-weeks-old MMTV-PyMT mice mammary tissue was isolated using TRIzol extraction (Invitrogen), followed by the RNeasy Mini Kit (Qiagen) according to the manufacturer's instructions. A 1 μg total RNA was subsequently used to generate cDNA using the iScript cDNA Synthesis Kit (Bio-Rad). Quantitative reverse transcription PCR was performed using the KAPA SYBR Fast qPCR Kit (Kapa Biosystems) on a Rotorgene 6000 (Qiagen) in triplicates using primers purchased from Qiagen: RPL19, TGFβ, BMP9/GDF2, BMP10, and GDF5 (QuantiTect Primer Assays QT00166145, QT00145250, QT00307587, QT00259847, and QT00250523, respectively). Primers for analysis of Id1 and Id3 as in ref. 18.

Tumor grade assessment

To assess the tumor grade of lesions from MMTV-PyMT mice, tumor tissue was classified into different degrees of progression by quantifying the area of transformed glands occupied by each

Figure 1.

Long-term ALK1 inhibition does not give rise to evasive resistance. A, cartoon depicting stage-specific therapeutic trials in the RIP-TAg2 mouse model of pancreatic neuroendocrine tumorigenesis. Short-term trials (10–12 weeks of age and 12–14 weeks of age) have been presented previously (18). B, long-term treatment of RIP-TAg2 mice with twice-weekly administration of control IgG or RAP-041 for 4 weeks starting at the age of 12 weeks. C, visualization of endothelial cells in tumors from RIP1-Tag2 mice by immunostaining for podocalyxin or CD31. Quantitation of vessel area was performed by assessing >15 images/mouse in a total of at least 5 mice per group. D, assessment of hypoxia in tumors from RIP-TAg2 mice by immunostaining for CA IX and HIF1α. E, representative image of hepatic metastatic lesion from RIP-TAg2 mice, as demonstrated by H&E staining (top) and immunostaining for the oncogene T-Ag (middle and bottom). F, quantitation of the number of metastatic foci in the liver of RIP-TAg2 mice. Analysis was performed on at least 5 mice per group. G, representation of the survival rate of RIP1-TAg2 mice included in therapeutic trials (Control, $n = 41$; RAP-041, $n = 14$; $P < 0.01$, χ^2-test).

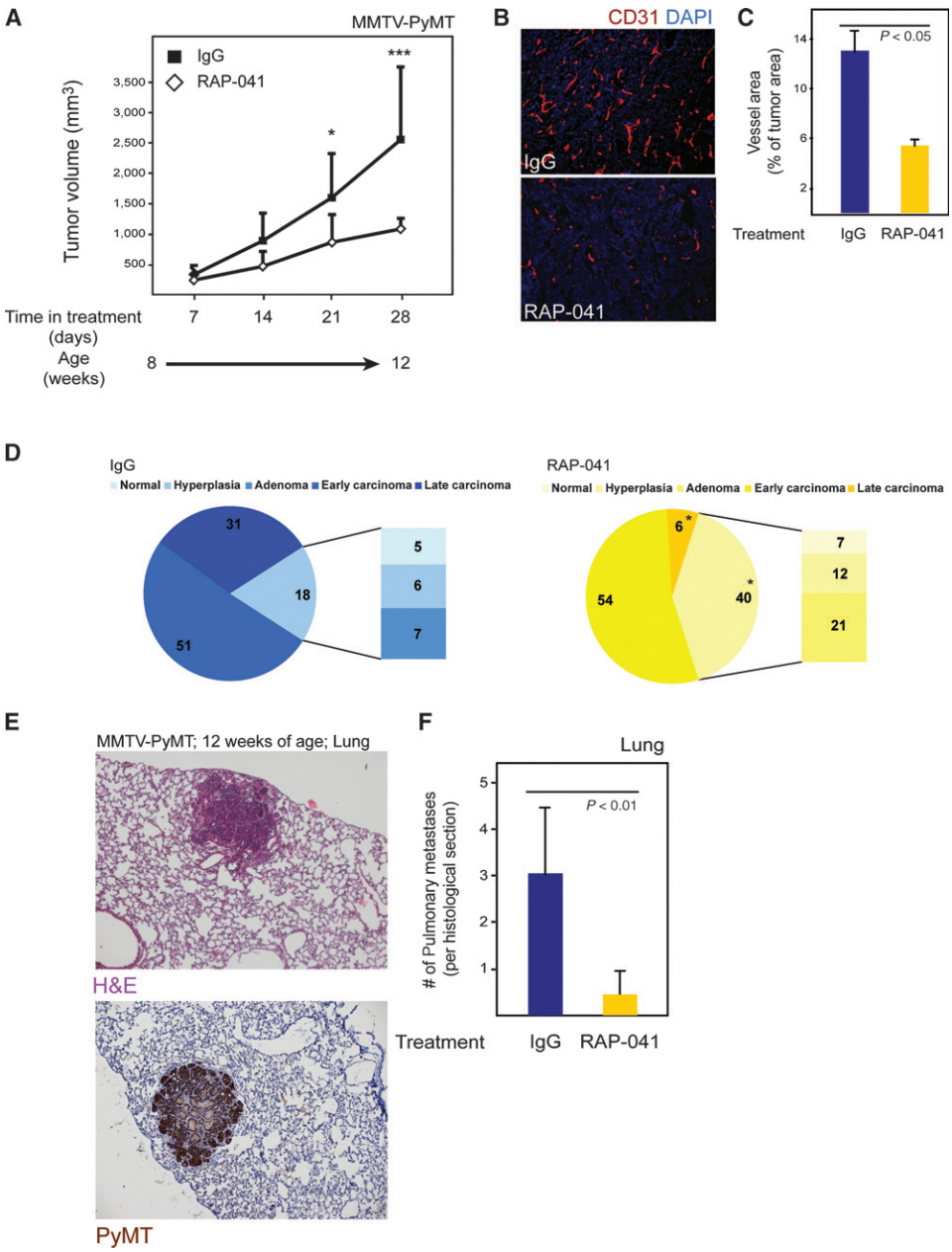
A
MMTV-PyMT
IgG
RAP-041
Tumor volume (mm3)
3,500
3,000
2,500
2,000
1,500
1,000
500
*
***
Time in treatment (days)
7
14
21
28
Age (weeks)
8
12
B
CD31 DAPI
IgG
RAP-041
C
Vessel area (% of tumor area)
14
10
6
2
P < 0.05
Treatment
IgG
RAP-041
D
IgG
Normal Hyperplasia Adenoma Early carcinoma Late carcinoma
31
18
51
5
6
7
RAP-041
Normal Hyperplasia Adenoma Early carcinoma Late carcinoma
6*
54
40*
7
12
21
E
MMTV-PyMT; 12 weeks of age; Lung
H&E
PyMT
F
Lung
# of Pulmonary metastases (per histological section)
5
4
3
2
1
P < 0.01
Treatment
IgG
RAP-041

stage. Progression follows from normal fat tissue to a "precancerous stage" characterized by premalignant hyperplasia and adenoma (with the retention of some normal ductal and acinar mammary gland morphology), to a more epithelial cell—dense "early carcinoma" with stromal invasion, and finally to an invasive, very dense, high—mitotic index "late-stage carcinoma."

Tumors were evaluated for the proportion of mammary fat tissue, hyperplastic tissue, adenoma, early carcinoma, and late carcinoma.

Clinical datasets

Expression data from The Cancer Genome Atlas (TCGA; http://cancergenome.nih.gov/) were downloaded in November 2013. The data were $\log_2$ transformed after addition of 1 to each normalized value. Clinical and follow-up data were downloaded in May 2014. All analyses were done with R using the basic and survival packages. Breast cancer subtypes were determined using nearest correlations with the PAM50 centroids.

The nested case–control study gained approval by the ethics committee at Karolinska Institutet, Stockholm, Sweden. The full details of the study design, collection of clinical-pathologic information, gene-expression profiling of fresh frozen tumor tissue and subsequent preprocessing and normalization of microarray gene-expression data, and finally conditional logistic regression modeling of the nested case–control study have been reported elsewhere (array data deposited at the Gene Expression Omnibus Database under accession number GSE48091; ref. 21), and is the subject of a separate report (Lindström and colleagues; submitted for publication). Gene-expression data were collapsed to gene level using a nonspecific filter keeping only the probe sets with highest interquartile range in the case of multiple mappings to the same Entrez Gene ID. As in the original publication, out of seven considered clinical-pathologic variables—estrogen receptor (ER), progresterone receptor and HER2 status, histologic grade, proliferation, tumor size, and lymph node status—three variables, namely lymph node status, tumor size, and HER2 status, were considered significant and included in multivariable conditional logistic regression models. A missing category was used to handle missing values in clinical-pathologic data. All gene-expression data analysis and statistical analysis were done in R/Bioconductor.

Statistical analysis

Unless specifically stated, all measurements are depicted as mean $\pm$ SD. Statistical analyses for tumor volume were performed using an unpaired, two-tailed Student t test. Statistical analyses for tumor characteristics were performed using a Mann–Whitney U test. Statistical significance was considered using $\alpha = 0.05$.

Results

Long-term inhibition of ALK1 impairs metastatic dissemination and prolongs survival in an experimental model of neuroendocrine tumorigenesis

We, and others, have previously documented the emergence of therapeutic resistance toward anti-VEGF therapy using various pharmacologic agents (14–16). Evasive resistance to VEGF-inhibitory modalities is accompanied by a hypoxia-driven malignization, that is, enhanced local invasion and increased rate of metastatic seeding, of tumors in the prototypical RIP-TAg2 mouse model of angiogenesis-dependent pancreatic neuroendocrine tumorigenesis (NET). To investigate whether antiangiogenic therapy by inhibition of ALK1 signaling gives rise to a similar exacerbation of systemic dissemination, we contrasted previously performed short-term therapeutic trials (18) with a long-term regimen of single-agent neoadjuvant therapy using ALK1-Fc, a ligand trap that neutralizes BMP9 and BMP10 (RAP-041, mouse counterpart of dalantercept; Fig. 1A). Regardless of the length or timing of the treatment of RIP-TAg2 mice, single-agent RAP-041 gave rise to a state of stable disease during the course of the trials, in contrast with tumors in control-treated mice that consistently presented with overt progressive disease (Fig. 1B and ref. 18). Despite inducing a demonstrable reduction in vessel area, average vessel length and the number of vessel endpoints, as judged by immunostaining for the endothelial cell markers podocalyxin or CD31 (Fig. 1C and data not shown), RAP-041 did not provoke widespread hypoxia, using CA IX or HIF1α expression as proxies for low tissue oxygenation (Fig. 1D). Pancreatic NETs of RIP-TAg2 mice disseminate predominantly to sentinel lymph nodes in the mesentery and to the liver, similar to the corresponding human disease (Fig. 1E; ref. 22). The incidence of hepatic metastases in RIP-TAg2 mice was not changed following short-term therapy with RAP-041 (Fig. 1F). Strikingly, however, upon long-term administration of neoadjuvant therapy with RAP-041 to mice harboring advanced disease, the rate of metastatic dissemination to the liver decreased by 86% compared with treatment with control IgG (Fig. 1F). In sharp contrast with anti-VEGF therapy, which induced an increased rate of metastasis (14, 16), ALK1 inhibition caused regression of preformed hepatic NET foci during the course of the therapeutic trial in RIP-TAg2 mice from an average of 8.1 to 2.8 foci per histologic section (Fig. 1F). In line with the substantial reduction in both primary tumor burden and metastatic manifestation in RIP-TAg2 mice following ALK1 inhibition, the rate of OS at 16 weeks of age was also increased from 27% (11/41) to 79% (11/14; Fig. 1G).

ALK1-Fc reduces metastatic dissemination to the lung in a genetically engineered mouse model of breast cancer

Given the failure of anti-VEGF therapy to affect OS in breast cancer, we extended our analyses on the role of ALK1 signaling in

Figure 2.
Inhibition of ALK1 reduces the growth, angiogenic response, and metastatic dissemination of early-stage experimental breast cancer. A, MMTV-PyMT mice treated for 4 weeks with twice-weekly administration of control IgG ($n = 13$) or RAP-041 (ALK1-Fc; $n = 15$) beginning at 8 weeks of age; *, $P < 0.05$; ***, $P < 0.001$. B, visualization of endothelial cells in tumors from MMTV-PyMT mice using immunostaining for CD31 (red) counterstained for cell nuclei (blue; DAPI). C, quantitation of vessel area in tumors from MMTV-PyMT mice. Each analysis was performed by assessing >15 images/mouse in at least 5 mice per group. D, assessment of the grade of primary tumors from MMTV-PyMT mice. The percentage of the total lesion area that displays each grade is depicted. Quantitation represents the average of 5 mice per group; *, $P < 0.05$; χ^2-test. E, representative image of pulmonary metastatic lesion from MMTV-PyMT mice, as demonstrated by H&E staining (top) and immunostaining for the oncogene PyMT (bottom). F, quantitation of the number of metastatic foci in the lungs of MMTV-PyMT mice. Analysis was performed on 20 images/mouse in at least 5 mice per group.

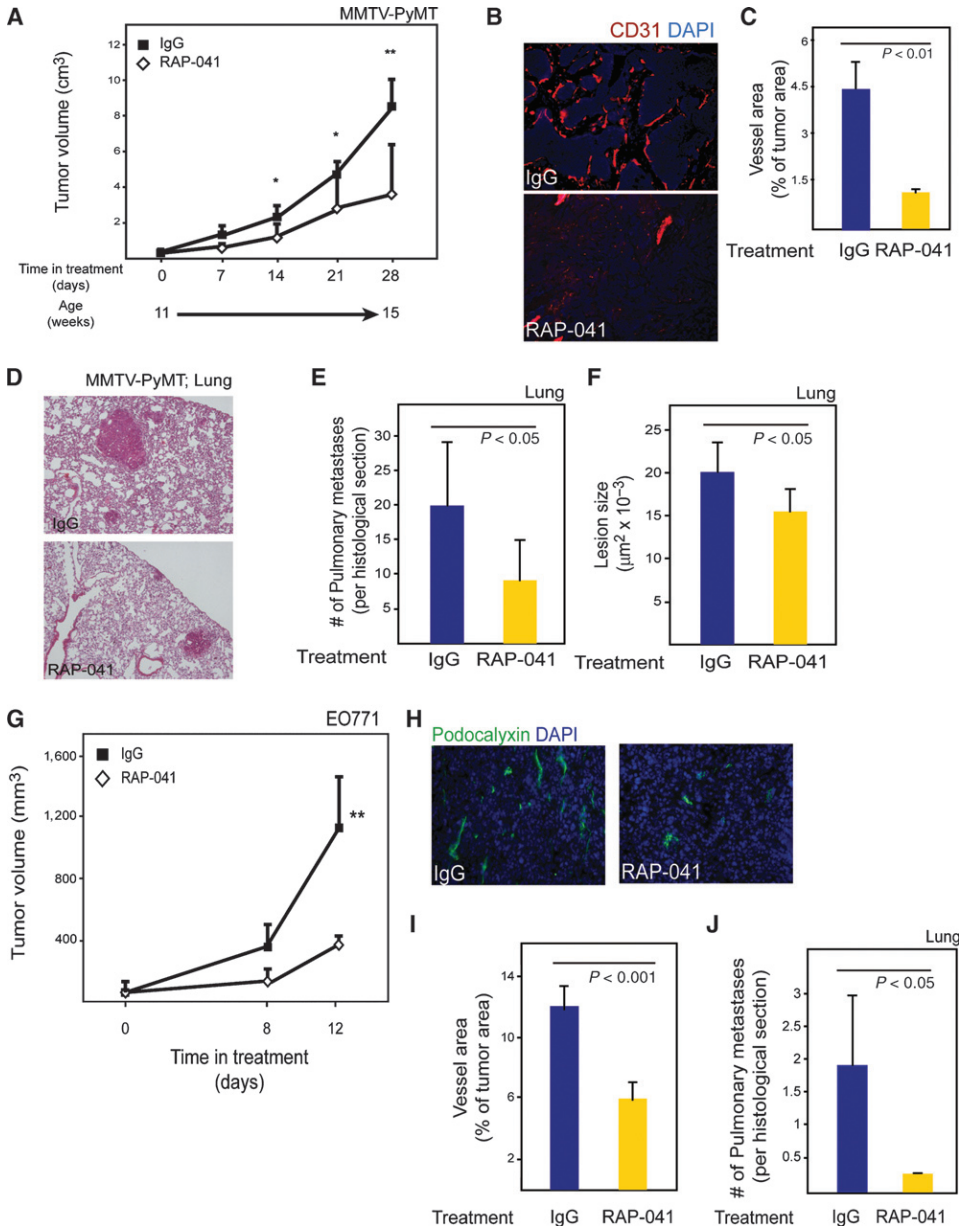
A
MMTV-PyMT
IgG
RAP-041
Tumor volume (cm3)
Time in treatment (days)
Age (weeks)
B
CD31 DAPI
IgG
RAP-041
C
P < 0.01
Vessel area (% of tumor area)
Treatment
IgG RAP-041
D
MMTV-PyMT; Lung
IgG
RAP-041
E
Lung
P < 0.05
# of Pulmonary metastases (per histological section)
Treatment
IgG RAP-041
F
Lung
P < 0.05
Lesion size (μm2 x 10−3)
Treatment
IgG RAP-041
G
EO771
IgG
RAP-041
Tumor volume (mm3)
Time in treatment (days)
H
Podocalyxin DAPI
IgG
RAP-041
I
P < 0.001
Vessel area (% of tumor area)
Treatment
IgG RAP-041
J
Lung
P < 0.05
# of Pulmonary metastases (per histological section)
Treatment
IgG RAP-041

metastatic dissemination to this disease by studying the MMTV-PyMT genetically engineered mouse model of mammary carcinoma; a mouse model faithfully recapitulating many aspects of the human disease, including dissemination pattern to the lung and lymph nodes (23). Initial characterization of mammary tumors from MMTV-PyMT mice demonstrated an endothelial cell–exclusive expression of ALK1 and readily detectable expression levels of its ligands BMP9, BMP10, and TGF-β (Supplementary Fig. S1A–S1C). Next, MMTV-PyMT mice were administered RAP-041 from 8 to 12 weeks of age in a preclinical neoadjuvant trial. Consistent with the effects in pancreatic NETs, inhibition of ALK1 significantly delayed the growth and reduced the vessel area of primary mammary carcinomas (Fig. 2A–C). The observed action of RAP-041 was a result of on-target effects, as demonstrated by diminished expression of the ALK1 target genes *Id1* and *Id3* in tumor lysates (Supplementary Fig. S2A and S2B). Treatment with RAP-041 had no discernible direct effect on the proliferation or apoptosis of malignant cells isolated from MMTV-PyMT tumors *in vitro* (Supplementary Fig. S2C and S2D), indicating that the therapeutic benefit was derived from indirect targeting of tumor cells by impinging on the neoangiogenic process. Notably, treatment with ALK1-Fc impeded the tumor progression pathway, as evidenced by a shift in the tumor grade from predominant malignant and invasive lesions observed in the control group (31% late carcinoma vs. 18% normal/hyperplasia/adenoma) to a higher degree of premalignant lesions in the treated group (6% late carcinoma vs. 40% normal/hyperplasia/adenoma; Fig. 2D). Importantly, the impaired tumor progression also translated into an 87% decrease in metastatic colonization of the lung (Fig. 2E and F). Tumor growth rate and vessel area were similarly compromised following neoadjuvant treatment with ALK1-Fc of older MMTV-PyMT mice already presenting with fully established disease (Fig. 3A–C). Again, inhibition of ALK1 expressed solely by the tumor endothelium significantly reduced the rate of metastasis by 55% (Fig. 3D and E). Furthermore, in addition to reducing the number of metastatic foci, RAP-041 treatment also significantly moderated the average size of the pulmonary metastatic lesions (Fig. 3F).

ALK1 inhibition induces angiogenic and metastatic blockade in experimental mammary carcinoma

To corroborate our findings of a role for endothelial ALK1 signaling in the metastatic cascade in breast tumors, we transplanted the ER-expressing mouse mammary carcinoma cell line EO771 orthotopically into the mammary fat pad of mice. The expression of BMP9 and TGF-β in EO771 tumor tissue was confirmed by quantitative PCR or immunostaining (Supplementary Fig. S1B and S1C). Consistent with our previous observations, administration of ALK1-Fc significantly delayed the growth of EO771 tumors (Fig. 3G) with concomitant reduction of vessel area (Fig. 3H and I). Importantly, neoadjuvant treatment of EO771-bearing mice with RAP-041 reduced the metastatic success rate to the lung by 87% (Fig. 3J), further demonstrating the involvement of ALK1 ligands and the tumor endothelium in the process of tumor cell dissemination to distant sites.

A combined therapeutic regimen of ALK1-Fc and docetaxel reduces tumor growth and metastatic dissemination

Neoadjuvant therapy of breast cancer is increasingly being used in order to reduce the primary tumor bulk, enable breast-conserving surgery and prevent metastatic manifestation (1). Therefore, we investigated the utility of combining inhibition of ALK1 with commonly used pharmacologic treatment strategies for breast cancer in a series of preclinical trials enrolling MMTV-PyMT mice in the neoadjuvant setting. Combined administration of RAP-041 with trastuzumab or the VEGFR2-neutralizing antibody DC101 did not yield any, or only marginal, therapeutic benefit compared with either treatment alone (data not shown). Strikingly, however, concomitant inhibition of ALK1 with neoadjuvant docetaxel gave rise to improved control of tumor growth (Fig. 4A). The addition of RAP-041 to the docetaxel regimen resulted in partial responses in 5 of 13 (38%) mice, compared with 0 of 10 (0%) in mice treated with single-agent docetaxel (Fig. 4B). Interestingly, treatment with single-agent docetaxel afforded a significant reduction of tumor vascularity; an effect that was exacerbated by combination treatment with RAP-041 (Fig. 4C and D). Most notably, the combination of ALK1-Fc and chemotherapy brought about a further 63% decrease in the metastatic index of the lung compared with docetaxel alone and prevented colonization of pulmonary metastases by 93% compared with control therapy (Fig. 4E).

ALK1 is an independent biomarker for metastatic recurrence of human breast cancer

Comparative studies demonstrated widespread expression of BMP9 protein, but not BMP10 protein, by malignant cells in human breast carcinomas (Fig. 5A). Functionality of the ALK1 paracrine signaling network and therapeutic utility of ALK1-Fc in the human setting was demonstrated by near-complete retardation of the growth of orthotopic xenografts of the aggressive triple-negative human breast carcinoma cell line MDA-MB-231 by treatment with ACE-041/dalantercept (the human counterpart of RAP-041; Fig. 5B). Next, to explore whether the expression of ALK1 (gene name *ACVRL1*) holds prognostic capability for metastatic disease in human patients, we analyzed gene-expression patterns in tumor material from a population-based nested case–control study encompassing 768 subjects with complete clinical follow-up (21). Briefly, 190 breast cancer patients that developed distant metastatic disease (cases) were selected from a consecutive

Figure 3.
Inhibition of ALK1 reduces the growth, angiogenic response, and metastatic dissemination of advanced experimental breast cancer. A, MMTV-PyMT mice treated for 4 weeks with twice-weekly administration of control IgG ($n = 5$) or RAP-041 (ALK1-Fc; $n = 6$) beginning at 11 weeks of age; *, $P < 0.05$; **, $P < 0.01$. B, visualization of endothelial cells in tumors from MMTV-PyMT mice using immunostaining for CD31 (red) and counterstaining for cell nuclei (blue; DAPI). C, quantitation of vessel area in tumors from MMTV-PyMT mice. Each analysis was performed by assessing >15 images/mouse in at least 5 mice per group. D, representative image of pulmonary metastatic lesions from MMTV-PyMT mice, as demonstrated by H&E staining. E and F, quantitation of the number (E) and size (F) of metastatic foci in the lungs of MMTV-PyMT mice. Analysis was performed on at least 5 mice per group. G, mice bearing orthotopically implanted syngeneic mouse mammary carcinoma EO771 tumors treated with twice-weekly administration of control IgG ($n = 7$) or RAP-041 (ALK1-Fc; $n = 7$). **, $P < 0.01$. H, visualization of endothelial cells in EO771 tumors by immunostaining for podocalyxin (green) and counterstaining for cell nuclei (blue; DAPI). I, quantitation of vessel density in EO771 tumors. Each analysis was performed by assessing >15 images/mouse in a total of at least 5 mice per group. J, quantitation of the number of metastatic foci in the lungs of mice bearing EO771 tumors. Analysis was performed on at least 5 mice per group.

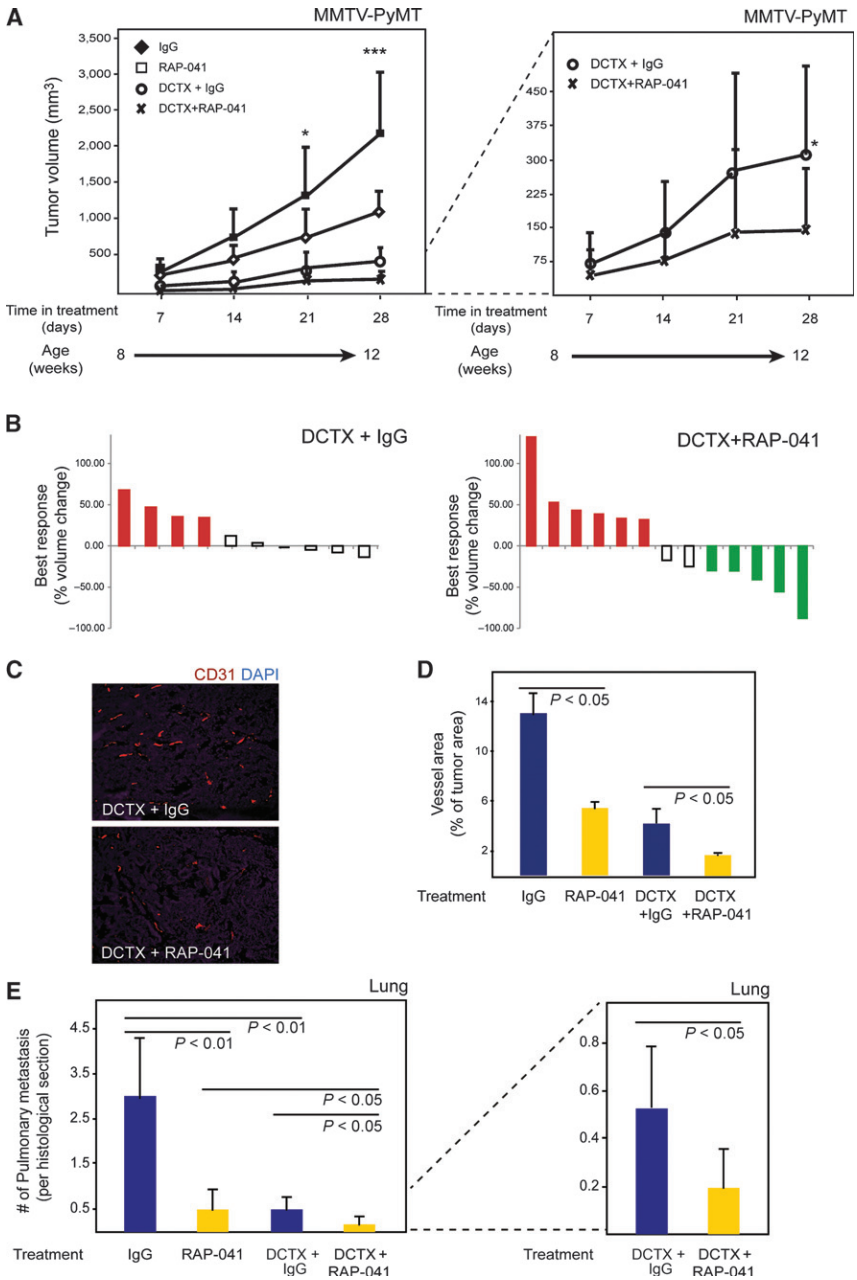
A
MMTV-PyMT
IgG
RAP-041
DCTX + IgG
DCTX+RAP-041
Tumor volume (mm3)
Time in treatment (days)
Age (weeks)
MMTV-PyMT
B
DCTX + IgG
DCTX+RAP-041
Best response (% volume change)
C
CD31 DAPI
DCTX + IgG
DCTX + RAP-041
D
Vessel area (% of tumor area)
P < 0.05
Treatment
IgG
RAP-041
DCTX +IgG
DCTX +RAP-041
E
Lung
# of Pulmonary metastasis (per histological section)
P < 0.01
P < 0.05
Treatment
IgG
RAP-041
DCTX + IgG
DCTX + RAP-041

series of individuals and three random control patients (free from metastasis) for each case were closely matched by adjuvant therapy, age and calendar period at diagnosis (21). Expression of *ACVRL1* was found to correlate significantly with prototypical endothelial cell genes, further corroborating the predominant vascular expression of ALK1 in human breast cancers (Supplementary Table S1). In addition, *ACVRL1* expression was significantly correlated to the expression of its target gene *Id1*, implying activation of the pathway (data not shown). In strong support of our functional data, abundant expression of *ACVRL1* was highly significantly associated with the incidence of metastatic disease (Table 1). Similarly, expression of *SMAD6*, a known downstream target gene of ALK1 activation was linked to recurrent disease (Table 1). In sharp contrast, the expression of the canonical TGFβ type I receptor ALK5 (*TGFBRI*) and its ligands $TGF\beta_{1\text{-}3}$, that are implicated in promotion of metastasis through induction of epithelial-to-mesenchymal transition (EMT), was equally distributed between cases and controls, with the exception of $TGF\beta_1$, expression of which was marginally associated with metastatic disease (Table 1). Importantly, in a multivariate analysis of risk factors for presenting with metastatic disease, expression of both *ACVRL1* (HR, 3.59; 95% CI, 2.52–5.15) and *SMAD6* (HR, 1.43; 95% CI, 1.15–1.77) remained as statistically significant and independent prognostic factors, alongside well-known clinical risk factors such as lymph node status, tumor size, and HER2 amplification (Table 1). Intriguingly, the known ligands for ALK1, that is, BMP9 (GDF2) and BMP10, were only weakly associated to metastasis, even when their expression was combined (Table 1).

High expression of endothelial ALK1 is an independent prognostic factor for poor survival in human breast cancer

To further validate our finding of a functional association between ALK1 signaling and metastatic colonization in human breast cancer, we analyzed breast cancer gene-expression data from TCGA. The validation set revealed that expression of *ACVRL1* was indeed correlated with the expression of well-known endothelial markers (Supplementary Table S1). Next, a Cox proportional hazards model was applied to gene-expression data from TCGA with event-free survival as the endpoint. Univariate models did not demonstrate any significant prognostic information held by either *ACVRL1* itself (data not shown) or by a general vascular index (normalized average expression of the prototypical endothelial cell markers *PECAM1*, *CDH5*, and *CD34*; hereafter referred to as the endothelial metagene). Strikingly, however, in a multivariate model (Table 2), both the *ACVRL1* expression level (HR, 2.35; 95% CI, 1.34–4.09) and the endothelial metagene (HR, 0.46; 95% CI, 0.28–0.74) were independent prognostic factors for event-free survival, also after adjustment for lymph node status and stratification for the molecular subtype of the disease according to the PAM50 profile. The opposing HRs of the vascular index and the *ACVRL1* expression level in this dataset suggested that the

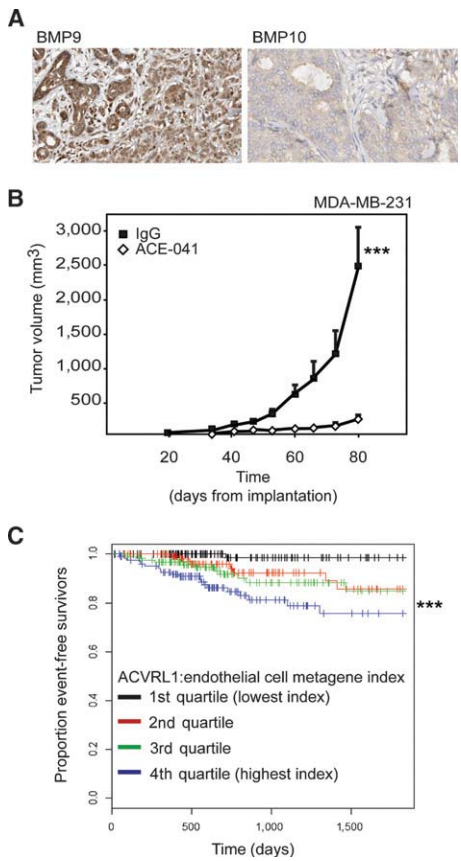

Figure 5.
ALK1 is functionally implicated in human breast carcinoma. A, representative pictures of immunostaining of human breast carcinoma for BMP9 (left) or BMP10 (right). Images taken from www.proteinatlas.org (33). B, SCID mice bearing orthotopically implanted MDA-MB-231 tumors and treated with control IgG or human ALK1-Fc (ACE-041); ***, $P < 0.001$. C, Kaplan–Meier curve of the event-free survival of breast cancer patients divided in quartiles by the ratio of *ACVRL1* expression and an endothelial cell metagene (*CDH5*, *PECAM1*, and *CD34*) with the first and fourth quartile exhibiting the lowest and highest ratio, respectively; ***, $P < 0.00038$, log-rank test.

Figure 4.
Neoadjuvant combination therapy with ALK1-Fc and docetaxel produces objective responses and reduced metastatic dissemination of experimental breast cancer. A, MMTV-PyMT mice treated for 4 weeks with the combination of twice-weekly administration of control IgG ($n = 13$) or RAP-041 (ALK1-Fc; $n = 15$) with weekly docetaxel alone ($n = 10$) or docetaxel in combination with RAP-041 ($n = 13$) beginning at 8 weeks of age; *, $P < 0.05$; ***, $P < 0.001$. B, waterfall plot of best response during the course of a preclinical trial of MMTV-PyMT mice treated with docetaxel alone ($n = 10$) or in combination with RAP-041 ($n = 13$). Red, white, and green bars represent mice with progressive disease, stable disease, and partial response, respectively, according to RECIST criteria. C, visualization of endothelial cells in tumors from MMTV-PyMT mice using immunostaining for CD31 (red) and counterstaining for cell nuclei (blue; DAPI). D, quantitation of vessel area in tumors from MMTV-PyMT mice. Each analysis was performed by assessing >15 images/mouse in at least 5 mice per group. E, quantitation of the number of metastatic foci in the lungs of MMTV-PyMT mice. Analysis was performed on at least 5 mice per group.

Table 1. Univariate and multivariable conditional logistic regression models comparing patients developing metastatic disease with patients free from disseminating disease in a nested case–control study[a]

Variable[b]	*n*	Univariate models		Multivariable model A		Multivariable model B	
		HR[c] (95% CI)	*P*	HR[c] (95% CI)	*P*	HR[c] (95% CI)	*P*
ACVRL1 (ALK1)		1.92 (1.58–2.34)	<0.001	3.59 (2.51–5.15)	<0.001		
Endothelial metagene[d]		1.14 (0.96–1.35)	0.124	0.44 (0.32–0.62)	<0.001		
ACVRL1:endothelial metagene index[e]		2.17 (1.78–2.66)	<0.001			2.01 (1.62–2.50)	<0.001
GDF2 (BMP9)		1.11 (0.95–1.30)	0.196				
BMP10		1.20 (1.01–1.41)	0.037				
ALK1 ligands [*GDF2* (*BMP9*) + *BMP10*]		1.20 (1.02–1.42)	0.033	1.28 (1.05–1.56)	0.013	1.16 (0.96–1.40)	0.120
SMAD6		1.60 (1.33–1.91)	<0.001	1.43 (1.15–1.77)	0.001	1.54 (1.26–1.89)	<0.001
TGFBR1 (*ALK5*)		1.07 (0.91–1.26)	0.390				
TGFB1		1.24 (1.05–1.47)	0.012				
TGFB2		1.03 (0.87–1.21)	0.766				
TGFB3		0.88 (0.73–1.05)	0.155				
Lymph node status			<0.001		0.063		0.064
Negative	304	1 (ref.)		1 (ref.)		1 (ref.)	
Positive	442	2.52 (1.69–3.77)		1.72 (1.09–2.71)		1.70 (1.09–2.65)	
Unknown	22	1.11 (0.36–3.41)		1.46 (0.37–5.87)		1.45 (0.38–5.54)	
Tumor size, mm			0.008		0.032		0.063
≤20	354	1 (ref.)		1 (ref.)		1 (ref.)	
>20	398	1.73 (1.22–2.44)		1.73 (1.15–2.60)		1.62 (1.08–2.42)	
Unknown	16	0.98 (0.27–3.59)		1.08 (0.22–5.25)		1.11 (0.24–5.12)	
HER2 status			<0.001		0.005		<0.001
Negative	519	1 (ref.)		1 (ref.)		1 (ref.)	
Positive	145	2.60 (1.74–3.88)		2.05 (1.28–3.30)		2.36 (1.48–3.75)	
Unknown	104	0.75 (0.44–1.31)		0.80 (0.43–1.49)		0.83 (0.46–1.53)	

Abbreviation: ref., reference.

[a]Controls randomly matched to cases by age, adjuvant therapy, and calendar period at diagnosis.

[b]Numerical variables are centered and scaled (SD set to one) in the models. Gene-expression values are normalized $\log_2$ summarized microarray probe intensity values.

[c]For numerical variables, HR is the relative hazard when increasing the variable one SD.

[d]Average expression of the prototypical endothelial cell markers PECAM1, CDH5, and CD34.

[e]Difference between ACVRL1 expression and endothelial metagene expression; corresponds to ($\log_2$ of) the ratio of ACVRL1 probe intensity over average endothelial metagene probe intensity.

molecular characteristics, rather than the absolute extent of vascularization, hold prognostic information. The ratio between *ACVRL1* expression and the endothelial metagene (i.e., the relative expression of ACVRL1 per endothelial cell) was, therefore, evaluated and found to serve as a highly specific prognostic biomarker for recurrent disease; breast cancer patients within the quartile of highest *ACVRL1*:endothelial metagene ratio were subject to an exceedingly poor event-free survival, compared with those patients with the lowest ratio (Fig. 5C). Reassuringly, the independent prognostic capability of the *ACVRL1*:endothelial metagene index was confirmed by analysis of gene-expression data from the nested case–control study (Table 1). Further analysis revealed that the association between the *ACVRL1*:endothelial metagene index and distant metastases was robust regardless of treatment received and was not a feature of any particular molecular subtype or size of breast tumor (Supplementary Fig. S3A–S3C).

Discussion

Taken together, we have combined mechanism-based studies of ALK1 signaling in advanced genetically engineered mouse models of breast cancer with preclinical efficacy trials of a clinically tractable pharmacologic inhibitor of ALK1 and expression analysis of *ACVRL1* in human patient materials in relation to relevant clinical parameters for metastatic disease. The present studies strongly suggest an independent role for endothelial ALK1 signaling in the process of metastatic dissemination and colonization of distant organs in breast cancer. On the basis of our findings, pharmacologic inhibitors of the ALK1 pathway, thus, present as attractive and realistic partners with chemotherapy in the management of metastatic breast cancer.

Table 2. Multivariable analysis of the impact of prognostic parameters on event-free survival in the TCGA dataset for breast cancer

Parameter	HR (95% CI)	*P*
ACVRL1	2.62 (1.53–4.5)	0.00046
Endothelial metagene	0.36 (0.23–0.56)	0.0000064
Lymph node status, positive	4.94 (2.18–11.19)	0.00013

ALK1-blocking agents are currently being developed clinically for various malignancies (17). Dalantercept (ACE-041), the human counterpart of RAP-041, is an ALK1 ligand trap comprising the extracellular domain of ALK1 fused to the Fc portion of IgG. Phase I clinical trials demonstrate the safety and tolerability of dalantercept; the most common and dose-limiting side effects include peripheral edema and fluid retention (24). Likewise, the fully human ALK1-neutralizing antibody PF-03446962 has concluded phase I clinical trials with grade 3 thrombocytopenia and increase in pancreatic enzymes as the dose-limiting toxicities (25). Both compounds show evidence for on-target effects on the neoangiogenic vasculature in functional imaging modalities, such as ^{18}FDG-PET and contrast-enhanced ultrasound imaging (24, 25). Notably, the side effect profile of the ALK1 targeting agents is distinct from that of anti-VEGF compounds, such as bevacizumab, sunitinib, and sorafenib, indicating a unique mechanism of action. In our preclinical trials, we found that, unlike VEGF pathway inhibitors, prolonged administration of ALK1-Fc did not give rise to widespread tissue hypoxia, rebound of tumor growth, increased local invasion or augmented seeding of distant

metastases (14–16, 26). In sharp contrast, neutralization of ALK1 ligands in the neoadjuvant setting resulted in a substantial reduction in metastatic colonization and in some cases even regression of preexisting metastatic lesions. It is interesting to note that the ALK1 target gene Id1, which we found to be substantially downregulated following treatment with RAP-041 and significantly correlated to ALK1 expression in human breast tumors, is part of a gene-expression signature predictive of breast cancer lung metastasis (27) and suppression of Id1 impairs metastatic colonization in a mouse model of lung carcinoma (28). The fact that ALK1 inhibition did not provoke tissue hypoxia is the most likely cause for the observed discrepancy with anti-VEGF therapy, as hypoxia has been suggested to be the main driving force for the malignization of tumors following VEGF blockade in preclinical studies (14, 26). The relative lack of hypoxia, despite reduced vessel area, implicitly suggests that ALK1 inhibition improves the exchange of oxygen and nutrients across the abnormal neovasculature in tumors. Further mechanistic studies of the distinct effects of ALK1-Fc on the tumor vasculature are warranted.

Herein, we provide compelling evidence from a population-based nested case–control study encompassing 768 subjects (23) that high expression of *ACVRL1* in the tumor vasculature serves as a highly significant biomarker for a metastatic phenotype in breast cancer, alongside traditional risk factors such as lymph node status, tumor size and HER2 amplification. This finding was corroborated by analysis of the independent TCGA dataset, in which the expression of endothelial *ACVRL1* was found to be strongly associated with event-free survival. Our findings should be confirmed at the protein level, but we have been unable to do so in the current study despite substantial efforts, due to a lack of specific reagents to detect the ALK1 protein in human tissues (data not shown). Intriguingly, ALK1 expression was closely linked to prototypical endothelial cell marker genes, providing further evidence that the endothelium takes an active part as a key regulator of the metastatic process; an aspect of the vascular wall that has been highlighted also in recent studies of signaling pathways emanating from endoglin, CCL2/CCR2 and HIF1α/2α in the tumor endothelium (16, 29, 30). Signaling by TGFβ in malignant cells promotes many aspects of the metastatic process, most notably migration and invasion, through induction of EMT (31). We recently demonstrated that the action of TGFβ on the vasculature weakens the endothelial cell barrier to tumor cell intravasation, thus endorsing malignant cell escape from the primary site into the bloodstream through an analogous mesenchymal transition of endothelial cells (16). Hence, the mechanism behind the antimetastatic effect of single-agent ALK1-Fc conceivably involves sealing the endothelial cell barrier to cancer cell transmigration, thereby confining malignant cells within the primary tumor. Furthermore, combined neoadjuvant treatment with RAP-041 and docetaxel eradicated the vast majority of pulmonary metastases. Docetaxel treatment gives rise to a well-documented reduction in vessel area (32), and the synergistic interaction with ALK1 inhibition is, thus, likely to take place at the level of the tumor endothelium.

Taken together, our mechanism-based therapeutic studies, combined with gene-expression analysis of patient specimens designed to investigate prometastatic factors, thus strongly support further development of ALK1-targeting agents, such as dalantercept and PF-03446962, as clinically tractable combination partners for chemotherapy to reduce the incidence of distant metastases in breast cancer.

Disclosure of Potential Conflicts of Interest

R. Kumar is a Chief Scientific Officer and has ownership interest (including patents) in Acceleron Pharma. K. Pietras has ownership interest in a patent pertaining to ALK1 antagonism held by the Ludwig Institute for Cancer Research Ltd and licensed to Acceleron Pharma. No potential conflicts of interest were disclosed by the other authors.

Authors' Contributions

Conception and design: S.I. Cunha, L. Lindström, R.S. Pearsall, J. Bergh, K. Pietras

Development of methodology: S.I. Cunha, P. Roswall

Acquisition of data (provided animals, acquired and managed patients, provided facilities, etc.): S.I. Cunha, M. Bocci, N. Eleftheriou, P. Roswall, E. Cordero, L. Lindström, M. Bartoschek, B.K. Haller, R.S. Pearsall, R. Kumar, J. Bergh

Analysis and interpretation of data (e.g., statistical analysis, biostatistics, computational analysis): S.I. Cunha, M. Bocci, J. Lövrot, N. Eleftheriou, L. Lindström, M. Bartoschek, B.K. Haller, A.W. Mulivor, C. Larsson, K. Pietras

Writing, review, and/or revision of the manuscript: S.I. Cunha, M. Bocci, J. Lövrot, L. Lindström, R.S. Pearsall, A.W. Mulivor, R. Kumar, K. Pietras

Administrative, technical, or material support (i.e., reporting or organizing data, constructing databases): S.I. Cunha, P. Roswall, L. Lindström

Study supervision: S.I. Cunha, K. Pietras

Acknowledgments

The results presented herein are in part based upon data generated by the TCGA Research Network: http://cancergenome.nih.gov/.

Grant Support

Kristian Pietras is the Göran & Birgitta Grosskopf Professor at Lund University. This research is supported by a Consolidator Grant from the European Research Council (the TUMORGAN project), the Swedish Research Council, the Swedish Cancer Society, the STARGET consortium (a Swedish Research Council Linnaeus network), BioCARE and Lund University. The research group of Jonas Bergh is supported by the Swedish Cancer Society, BRECT, Karolinska Institutet and Stockholm County Council, the research funds at Radiumhemmet, Karolinska Institutet & Karolinska University Hospital.

The costs of publication of this article were defrayed in part by the payment of page charges. This article must therefore be hereby marked *advertisement* in accordance with 18 U.S.C. Section 1734 solely to indicate this fact.

Received December 19, 2014; revised March 17, 2015; accepted April 1, 2015; published online June 15, 2015.

References

1. Sledge GW, Mamounas EP, Hortobagyi GN, Burstein HJ, Goodwin PJ, Wolff AC. Past, present, and future challenges in breast cancer treatment. J Clin Oncol 2014;32:1979–86.
2. Nguyen DX, Bos PD, Massague J. Metastasis: from dissemination to organ-specific colonization. Nat Rev Cancer 2009;9:274–84.
3. Chiang AC, Massague J. Molecular basis of metastasis. N Engl J Med 2008;359:2814–23.
4. Walters S, Maringe C, Butler J, Rachet B, Barrett-Lee P, Bergh J, et al. Breast cancer survival and stage at diagnosis in Australia, Canada, Denmark, Norway, Sweden and the UK, 2000–2007: a population-based study. Br J Cancer 2013;108:1195–208.
5. Kerbel RS. Tumor angiogenesis. N Engl J Med 2008;358:2039–49.
6. Ferrara N, Kerbel RS. Angiogenesis as a therapeutic target. Nature 2005; 438:967–74.

7. Weidner N. Tumoural vascularity as a prognostic factor in cancer patients: the evidence continues to grow. J Pathol 1998;184:119–22.
8. Escudier B, Eisen T, Stadler WM, Szczylik C, Oudard S, Siebels M, et al. Sorafenib in advanced clear-cell renal-cell carcinoma. N Engl J Med 2007;356:125–34.
9. Hurwitz H, Fehrenbacher L, Novotny W, Cartwright T, Hainsworth J, Heim W, et al. Bevacizumab plus irinotecan, fluorouracil, and leucovorin for metastatic colorectal cancer. N Engl J Med 2004;350:2335–42.
10. Motzer RJ, Hutson TE, Tomczak P, Michaelson MD, Bukowski RM, Rixe O, et al. Sunitinib versus interferon alfa in metastatic renal-cell carcinoma. N Engl J Med 2007;356:115–24.
11. Raymond E, Dahan L, Raoul JL, Bang YJ, Borbath I, Lombard-Bohas C, et al. Sunitinib malate for the treatment of pancreatic neuroendocrine tumors. N Engl J Med 2011;364:501–13.
12. Kumler I, Christiansen OG, Nielsen DL. A systematic review of bevacizumab efficacy in breast cancer. Cancer Treat Rev 2014;40:960–73.
13. Mackey JR, Kerbel RS, Gelmon KA, McLeod DM, Chia SK, Rayson D, et al. Controlling angiogenesis in breast cancer: a systematic review of anti-angiogenic trials. Cancer Treat Rev 2012;38:673–88.
14. Paez-Ribes M, Allen E, Hudock J, Takeda T, Okuyama H, Vinals F, et al. Antiangiogenic therapy elicits malignant progression of tumors to increased local invasion and distant metastasis. Cancer Cell 2009;15:220–31.
15. Ebos JM, Lee CR, Cruz-Munoz W, Bjarnason GA, Christensen JG, Kerbel RS. Accelerated metastasis after short-term treatment with a potent inhibitor of tumor angiogenesis. Cancer Cell 2009;15:232–9.
16. Anderberg C, Cunha SI, Zhai Z, Cortez E, Pardali E, Johnson JR, et al. Deficiency for endoglin in tumor vasculature weakens the endothelial barrier to metastatic dissemination. J Exp Med 2013;210:563–79.
17. Cunha SI, Pietras K. ALK1 as an emerging target for antiangiogenic therapy of cancer. Blood 2011;117:6999–7006.
18. Cunha SI, Pardali E, Thorikay M, Anderberg C, Hawinkels L, Goumans MJ, et al. Genetic and pharmacological targeting of activin receptor-like kinase 1 impairs tumor growth and angiogenesis. J Exp Med 2010;207:85–100.
19. Mitchell D, Pobre EG, Mulivor AW, Grinberg AV, Castonguay R, Monnell TE, et al. ALK1-Fc inhibits multiple mediators of angiogenesis and suppresses tumor growth. Mol Cancer Ther 2010;9:379–88.
20. Hu-Lowe DD, Chen E, Zhang L, Watson KD, Mancuso P, Lappin P, et al. Targeting activin receptor-like kinase 1 (ALK1) inhibits angiogenesis and tumorigenesis through a mechanism of action complementary to anti-VEGF therapies. Cancer Res 2011;71:1362–73.
21. Lindstrom L, Jauhiainen A, Wilking U, Foukakis T, Åström G, Czene K, et al. Abstract P6-06-17: gene signature model predicts metastatic onset better than standard clinical markers—Nested case–control design uniquely enables enrichment for biologically relevant features. Cancer Res 2013;73 Suppl 24:P6-06-17.
22. House MG, Schulick RD. Endocrine tumors of the pancreas. Curr Opin Oncol 2006;18:23–9.
23. Fluck MM, Schaffhausen BS. Lessons in signaling and tumorigenesis from polyomavirus middle T antigen. Microbiol Mol Biol Rev 2009;73:542–63.
24. Bendell JC, Gordon MS, Hurwitz HI, Jones SF, Mendelson DS, Blobe GC, et al. Safety, pharmacokinetics, pharmacodynamics, and antitumor activity of dalantercept, an activin receptor-like kinase-1 ligand trap, in patients with advanced cancer. Clin Cancer Res 2014;20:480–9.
25. Necchi A, Giannatempo P, Mariani L, Fare E, Raggi D, Pennati M, et al. PF-03446962, a fully-human monoclonal antibody against transforming growth-factor beta (TGFbeta) receptor ALK1, in pre-treated patients with urothelial cancer: an open label, single-group, phase 2 trial. Invest New Drugs 2014;32:555–60.
26. Casanovas O, Hicklin DJ, Bergers G, Hanahan D. Drug resistance by evasion of antiangiogenic targeting of VEGF signaling in late-stage pancreatic islet tumors. Cancer Cell 2005;8:299–309.
27. Minn AJ, Gupta GP, Siegel PM, Bos PD, Shu W, Giri DD, et al. Genes that mediate breast cancer metastasis to lung. Nature 2005;436:518–24.
28. Gao D, Nolan DJ, Mellick AS, Bambino K, McDonnell K, Mittal V. Endothelial progenitor cells control the angiogenic switch in mouse lung metastasis. Science 2008;319:195–8.
29. Wolf MJ, Hoos A, Bauer J, Boettcher S, Knust M, Weber A, et al. Endothelial CCR2 signaling induced by colon carcinoma cells enables extravasation via the JAK2-Stat5 and p38MAPK pathway. Cancer Cell 2012;22:91–105.
30. Branco-Price C, Zhang N, Schnelle M, Evans C, Katschinski DM, Liao D, et al. Endothelial cell HIF-1alpha and HIF-2alpha differentially regulate metastatic success. Cancer Cell 2012;21:52–65.
31. Pardali K, Moustakas A. Actions of TGF-beta as tumor suppressor and pro-metastatic factor in human cancer. Biochim Biophys Acta 2007;1775:21–62.
32. Sweeney CJ, Miller KD, Sissons SE, Nozaki S, Heilman DK, Shen J, et al. The antiangiogenic property of docetaxel is synergistic with a recombinant humanized monoclonal antibody against vascular endothelial growth factor or 2-methoxyestradiol but antagonized by endothelial growth factors. Cancer Res 2001;61:3369–72.
33. Ponten F, Jirstrom K, Uhlen M. The Human Protein Atlas—a tool for pathology. J Pathol 2008;216:387–93.

Cancer Research

Correction: Endothelial ALK1 Is a Therapeutic Target to Block Metastatic Dissemination of Breast Cancer

In this article (Cancer Res 2015;75:2445–56), which appeared in the June 15, 2015, issue of *Cancer Research* (1), the authors present translational studies supporting a causal link between the expression of the endothelial cell–expressed TGFβ family receptor ALK1 and metastatic dissemination of breast cancer. For a subsection of their studies, the authors utilized data from gene expression analysis of patient samples from a clinical cohort designed as a nested case–control study (data presented in Table 1). In subsequent follow-up studies, the authors have uncovered a potential bias in this dataset. Importantly, however, the analyses included in the article are unaffected, and the conclusions of the work are not in question.

As background, a metastatic breast cancer cohort study was first designed (2). Thereafter, a case–control study nested in the corresponding primary breast cancer cohort was designed by selecting distant metastasis–free controls to each case. Tumor RNA was extracted in the same order. All RNAs were profiled on microarrays in randomized order. For quality control, RNA was also reextracted in a randomized order for randomly selected cases–controls sets and profiled with the rest. The potential bias of the data from the nested case–control study is due to apparent RNA extraction batch effects confounded with case–control status. Reassuringly, gene expression data for endothelial ALK1 are consistent for a substudy in which RNA has been reextracted from a new tumor piece in a randomized order.

The correlation between gene expression data for original and reextracted RNA is excellent for key breast cancer genes, for example, *ESR1* ($r = 0.95$) and *ERBB2* ($r = 0.96$). Bridging the primary comparison, case–control set differences ($n = 40$) for *ACVRL1* and the *ACVRL1*:endothelial metagene index that we reported are consistent between the two extractions (Fig. 1). A case–control set difference is the value for the case minus the (average) value of the matched control(s).

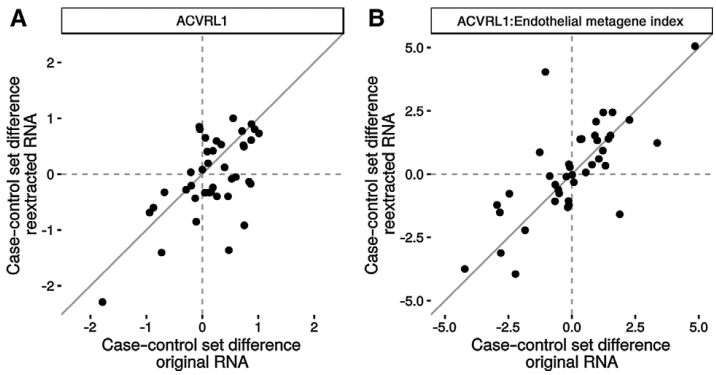

Figure 1.
Case–control set differences in the original RNA extraction and in the reextracted RNA confirms a close correlation between datasets for both *ACVRL1* gene expression (left) and for the *ACVRL1*:endothelial metagene index (right).

Although the potential bias of the dataset does not affect the outcome of the current study, the authors recommend careful scrutiny of the data and inclusion of proper controls when attempting other analyses based on these data. Microarray data for the reextracted RNA are deposited at the Gene Expression Omnibus database under accession number GSE81954.

All authors have been informed of and agree to this correction.

References

1. Cunha SI, Bocci M, Lövrot J, Eleftheriou N, Roswall P, Cordero E, et al. Endothelial ALK1 is a therapeutic target to block metastatic dissemination of breast cancer. Cancer Res 2015;75:2445–56.
2. Falato C, Tobin NP, Lorent J, Lindström LS, Bergh J, Foukakis T. Intrinsic subtypes and genomic signatures of primary breast cancer and prognosis after systemic relapse. Mol Oncol 2016;10:517–25.

Published online October 14, 2016.
doi: 10.1158/0008-5472.CAN-16-2220

Paper II

Compound genetically engineered mouse models of cancer reveal dual targeting of ALK1 and endoglin as a synergistic opportunity to impinge on angiogenic TGF-β signaling

Nikolas M. Eleftheriou[1], Jonas Sjölund[1], Matteo Bocci[1], Eliane Cortez[1], Se-Jin Lee[2], Sara I. Cunha[3,*], Kristian Pietras[1,*]

[1]Division of Translational Cancer Research, Department of Laboratory Medicine, Lund University, Medicon Village, Lund, Sweden

[2]Department of Molecular Biology and Genetics, Johns Hopkins University School of Medicine, Baltimore, MD, USA

[3]Department of Immunology, Genetics and Pathology, Uppsala University, Uppsala, Sweden

[*]These authors contributed equally to this work

Correspondence to: Sara I. Cunha, **email:** Sara.Cunha@igp.uu.se
Kristian Pietras, **email:** Kristian.Pietras@med.lu.se

Keywords: *angiogenesis, targeted therapy, BMP9, ALK1, endoglin*

Received: *June 04, 2016* ***Accepted:*** *October 03, 2016* ***Published:*** *October 12, 2016*

ABSTRACT

Angiogenesis occurs early in tumor development, sustains primary tumor growth and provides a route for metastatic escape. The TGF-β family receptors modulate angiogenesis via endothelial-cell specific pathways. Here we investigate the interaction of two such receptors, ALK1 and endoglin, in pancreatic neuroendocrine tumors (PanNET). Independently, ALK1 and endoglin deficiencies exhibited genetically divergent phenotypes, while both highly correlate to an endothelial metagene in human and mouse PanNETs. A concurrent deficiency of both receptors synergistically decreased tumor burden to a greater extent than either individual knockdown. Furthermore, the knockout of *Gdf2* (BMP9), the primary ligand for ALK1 and endoglin, exhibited a mixed phenotype from each of ALK1 and endoglin deficiencies; overall primary tumor burden decreased, but hepatic metastases increased. Tumors lacking BMP9 display a hyperbranching vasculature, and an increase in vascular mesenchymal-marker expression, which may be implicit in the increase in metastases. Taken together, our work cautions against singular blockade of BMP9 and instead demonstrates the utility of dual blockade of ALK1 and endoglin as a strategy for anti-angiogenic therapy in PanNET.

INTRODUCTION

Induction of neo-angiogenesis is a compulsory hallmark of cancer and an early event during tumor progression [1]. Substantial efforts to develop angiogenesis inhibitors to treat cancer have resulted in a set of clinically approved drugs with blockade of vascular endothelial growth factor (VEGF) signaling as a common mechanism of action [2, 3]. Despite the fact that VEGF inhibitors are included in the first-line therapy against advanced and metastatic cancer of the colon, kidney, lung, liver and neuroendocrine pancreas, among others, the search for alternative and/or complementary targets for drug development is highly warranted due to a lack of persistent efficacy or substantial improvements of overall survival with currently used compounds.

The transforming growth factor (TGF)-β family consists of more than 30 ligands that bind and signal through serine/threonine kinase receptors (TGF-β type I and type II receptors) and accessory transmembrane proteins (TGF-β type III receptors) [4]. Evidence for a profound role for TGF-β signaling in angiogenesis comes from studies demonstrating that family ligands, such as TGF-β and bone morphogenetic protein (BMP) 9, activate receptor complexes on many cell types relevant to angiogenesis, including endothelial cells and

perivascular cells. Moreover, genetic ablation of various receptors or ligands from the TGF-β family, most notably the TGF-β type I receptors activin receptor-like kinase (ALK)1 and ALK5, results in embryonic lethality due to vasculogenic or angiogenic defects [5]. In addition, gene knock-out for endoglin, an endothelial-cell selective TGF-β type III receptor, gives rise to a phenotype with close similarities to that of ALK1 ablation, in line with their analogous expression patterns, similar upregulation during active angiogenesis both in development and pathological conditions, and causal role in the genetic vascular deficiency syndrome hereditary hemorrhagic telangiectasia [6, 7]. However, the precise role for these signaling partners and their ligands during the complex process of angiogenesis has proven difficult to pinpoint, as their actions appear highly concentration and context dependent [8].

In the setting of tumor angiogenesis, genetic or pharmacologic targeting of ALK1 (gene name *Acvrl1*) results in a significant growth delay and angiogenic blockade [9–13]. In addition, ALK1 inhibition substantially impacts on metastatic dissemination by reducing the colonization of distant organs in a range of mouse models of cancer, including mammary carcinoma and pancreatic neuroendocrine tumor (PanNET)[12]. Conversely, in our comparative studies, genetic targeting of endoglin (gene name *Eng*), either globally or in an endothelial cell-restricted manner, only transiently impacts on tumor growth and angiogenesis [14]. Surprisingly, a reduced dosage of the endoglin gene gives rise to an increase in metastatic spread due to adoption of a mesenchymal phenotype by endothelial cells, which in turn leads to enhanced tumor cell intravasation [14, 15]. The divergent results on tumor parameters following targeting of ALK1 or endoglin, both thought to act in concert in the same endothelial cell regulatory pathway, begs the questions of which signaling event is dominant and whether combinatorial targeting would be beneficial. Also, it is still unclear what role BMP9, the most prominent ligand for both ALK1 and endoglin, plays in the regulation of tumor angiogenesis through its receptors.

Herein, we have aimed to further elucidate the functional dependence between ALK1 and endoglin in determining hallmark capabilities of tumorigenesis through targeting studies in compound genetically engineered mice. Furthermore, we have utilized mice deficient for BMP9 (gene name *Gdf2*) to investigate the impact of ligand binding to ALK1 and endoglin on tumor parameters. Our studies demonstrated a specific correlation of the expression of *ACVRL1* and *ENG* with an endothelial metagene in human PanNETs. In mechanistic studies, combined deficiency for one allele each of *Acvrl1* and *Eng* resulted in severe retardation of the development of experimental PanNETs in mice, in conjunction with suppression of angiogenesis and metastatic dissemination. In contrast, despite reducing tumor volume, deficiency for *Gdf2* gave rise to an enhanced incidence of micrometastatic lesions in the liver. Taken together, we have demonstrated the utility of combinatorial targeting of TGF-β family signaling to impair tumor growth and metastatic dissemination, although caution is warranted in the choice of target molecule.

RESULTS

Concomitant *Acvrl1* and *Eng* deficiency synergistically decreases pancreatic neuroendocrine tumor volume

Our previous studies indicate that genetic ablation of *Acvrl1* or *Eng* in the context of pancreatic neuroendocrine tumorigenesis in RIP1-TAg2 mice [16] gives rise to divergent phenotypes, despite the fact that the two receptors both bind the predominant ligand BMP9, but also TGF-β [9, 12, 14]. The apparent contextual manner in which TGF-β family signaling functions depending on the activity of other receptors and/or ligands, led us to further investigate the extent of interaction within the endothelial TGF-β signaling pathways. Analysis of the expression of *ACVRL1* and *ENG*, either alone or combined, in 20 human PanNETs and 9 metastases (cohort previously reported in [17]) was demonstrated to be highly correlated to an endothelial cell metagene consisting of *CD34*, *CDH5* and *PECAM1* (Figure 1A–1C), indicating an exclusive endothelial cell expression within the tumor neovasculature. In addition, the expression of *ACVRL1* and *ENG* were significantly correlated to each other, suggesting that the two receptors act in concert (Figure 1D). The abundance of transcript for *ACVRL1* and *ENG* in primary tumors and metastatic lesions was similar (Figure 1A–1D). All correlations were confirmed in mouse PanNETs from RIP1-TAg2 mice, where expression of *Acvrl1* and *Eng* was found to be highest during the angiogenic phase of tumor development, compared to pre-malignant lesions (normal or hyperplastic islets), primary tumors (islet tumors or metastasis-like primary tumors), or hepatic metastases (Figure 1E–1H).

We next sought to explore the utility of a dual targeting strategy for *Acvrl1* and *Eng* by generating RIP1-TAg2 mice with loss of one copy of each gene. While the global homozygous knockout of *Acvrl1* or *Eng* is each embryonic lethal due to vascular malformations [6, 18], the double heterozygous deficient mice ($Acvrl1^{+/-}Eng^{+/-}$) were viable, fertile, generated offspring in Mendelian ratios and did not display any obvious impairment in growth. Our previous studies have explored the individual heterozygous deficiencies in RIP-TAg2 mice, showing that receptor expression decreases proportionately, and further describes consequential phenotypes in vascularity, dissemination and changes in downstream target gene induction [9, 14]. Vessels of PanNET in compound RIP1-TAg2 mice were visualized by immunostaining for the

luminal endothelial cell marker podocalyxin. In line with our previous report [9], single deficiency for *Acvrl1* gave rise to a significantly reduced total vessel area, total vessel length and total number of junctions compared to PanNET from wildtype RIP1-TAg2 mice, characteristic of an overall impairment in angiogenesis (Figure 2A–2E). In addition, and as demonstrated by our previous study [14], deficiency for *Eng* did not impact on vessel parameters in PanNET from RIP1-TAg2 mice at 12 weeks of age (Figure 2A–2E). Double deficiency for *Acvrl1* and *Eng* reduced vessel area and length, but did not further exacerbate the phenotype of single *Acvrl1* deficiency (Figure 2A–2E).

In agreement with our previous reports, ablation of one copy of *Acvrl1* delayed tumor growth, while reducing the *Eng* gene dosage by half did not affect the growth rate of PanNET in RIP1-TAg2 mice (Figure 3A). Interestingly, 12-week old compound RIP1-TAg2; $Acvrl1^{+/-}Eng^{+/-}$ mice presented with a significantly reduced overall tumor burden by 57% and 39%, compared to RIP1-TAg2; $Acvrl1^{+/+}Eng^{+/+}$ mice or RIP1-TAg2; $Acvrl1^{+/-}Eng^{+/+}$ mice, respectively (Figure 3A). In addition, a trend towards fewer hepatic micrometastatic lesions was observed in RIP1-TAg2; $Acvrl1^{+/-}Eng^{+/-}$ mice compared to RIP1-TAg2; $Acvrl1^{+/+}Eng^{+/+}$ mice at 12 weeks of age (Figure 3B).

Taken together, our analyses of compound RIP1-TAg2; $Acvrl1^{+/-}Eng^{+/-}$ mice illustrates the utility of combinatorial targeting of ALK1 and endoglin in reducing hallmark parameters of tumor growth and progression.

Ablation of BMP9 reduces the growth of primary PanNETs, while increasing the rate of metastasis

To understand the contribution of BMP9 ligand binding to the outcome of targeting each of its receptors ALK1 and endoglin, we made use of *Gdf2*-deficient mice. Knock-out mice for *Gdf2* are viable and fertile with no overt defect in blood vessel development, *e.g.* in neonatal vascularization of the retina, due to redundant signaling by the homologous ligand BMP10 [19]. However, *Gdf2*-deficient mice present with abnormal lymphatic vessel maturation and deficiency in lymphatic valve formation and lymph drainage, consistent with ALK1 expression in lymphatic endothelial cells [20, 21].

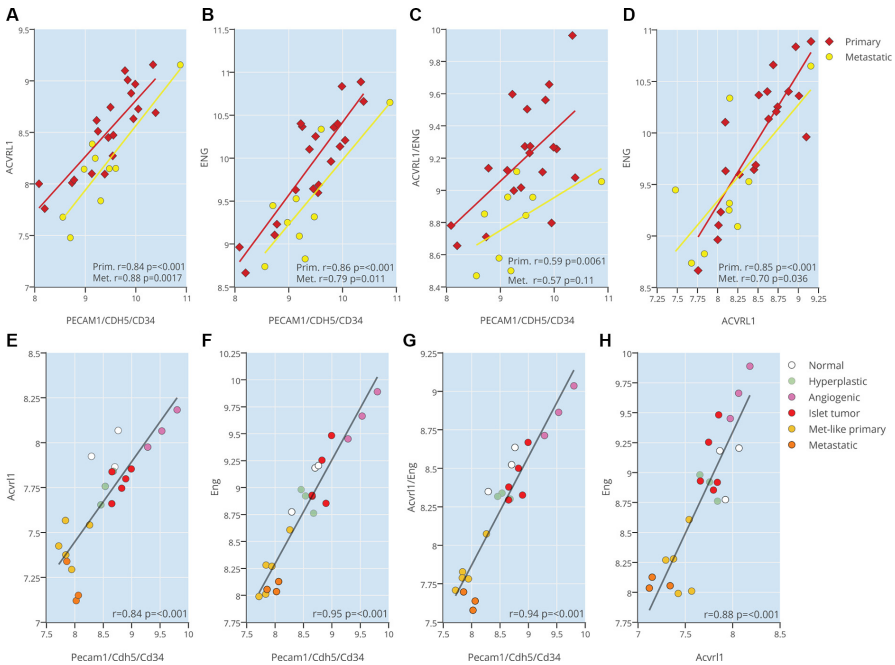

Figure 1: ACVRL1 and ENG expression are correlated to tumor neovasculature. (**A–C**) Expression correlation of ACVRL1 and ENG against an endothelial metagene (*CD34*, *CDH5*, *PECAM1*) (A–C), and against each other (**D**) from a human dataset of pancreatic neuroendocrine tumors and metastases (**E–H**) Expression correlation of *Acvrl1* and *Eng* against an endothelial metagene (*Cd34*, *Cdh5*, *Pecam1*) (A-C), and against each other (D) from a mouse dataset of pancreatic neuroendocrine RIP1-TAg2 islets, tumors and metastases.

Here, we investigated whether the expression of the closely related family members BMP10 or GDF5 was altered in PanNETs from RIP1-TAg2; *Gdf2*$^{-/-}$ mice, but no compensatory upregulation was found in the tumors in the absence of BMP9 (Figure 4A). Similarly, there were no statistically significant changes in the expression of *Acvrl1, Eng* or *Tgfbr1*, although a trend towards elevated levels of all genes was discerned (Figure 4A). Charting of the tumorigenic progression demonstrated that RIP1-TAg2; *Gdf2*$^{-/-}$ mice presented with a 44% reduction in the number of tumors (Figure 4B, 5.2 ± 0.5 tumors / mouse in *Gdf2*-deficient mice, compared to 9.3 ± 0.8 for wildtype RIP1-TAg2 mice), and a 49% reduction in total tumor volume (Figure 4C, 19.9 ± 2.9 mm^3/mouse in *Gdf2*-deficient mice, compared to 39.4 ± 8.2 for wildtype RIP1-TAg2 mice). The tumor volume and number for RIP1-TAg2; *Gdf2*$^{+/-}$ mice were intermediate between the wildtype and knockout phenotypes, demonstrating a gene dosage effect (Figure 4B–4C). In contrast, the number of angiogenic islets was not dependent on *Gdf2* deficiency, indicating little influence of BMP9 signaling in activating the angiogenic switch (Figure 4D). In support of a lack of direct effect of BMP9, or the related ligand BMP10, in the regulation of angiogenic vessel growth within human

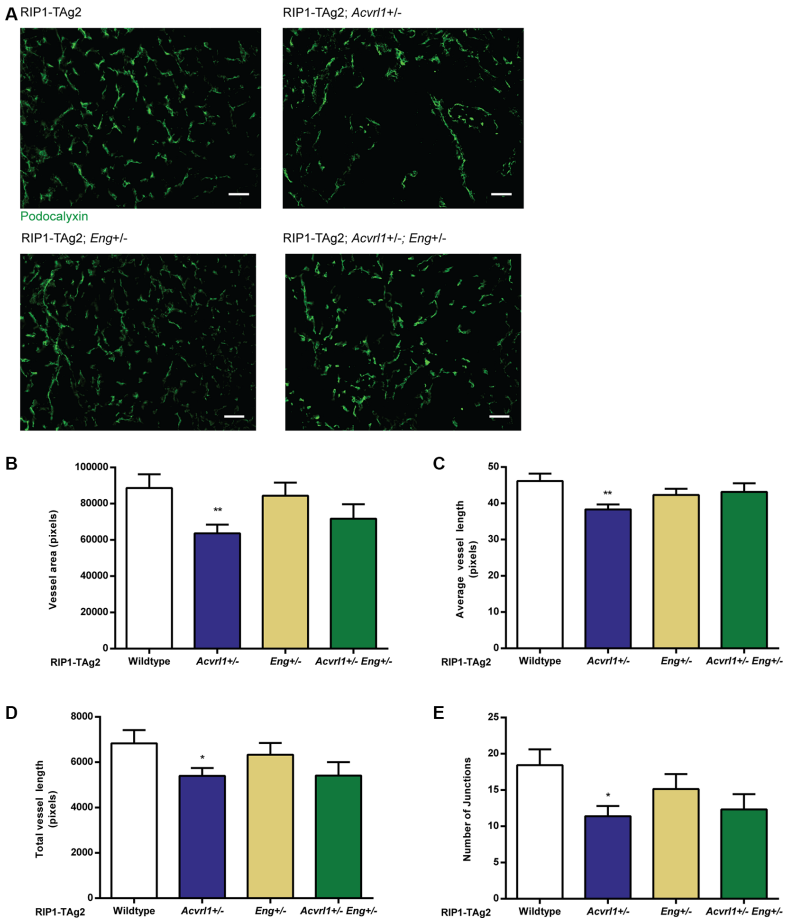

Figure 2: Deficiency of Acvrl1 alone reduces tumor angiogenesis. (**A**) Representative images of Podocalyxin-stained vessels in PanNETs of 12-week old RIP-TAg2 mice. Scale bar 50 μm. B-E Vessel analysis of Podocalyxin-stained vessels in PanNETs of 12-week old RIP-TAg2 mice; total vessel area (**B**), average vessel length (**C**), total vessel length (**D**), and total number of junctions (**E**). n = 2–3 mice Data are mean ± SEM. *$P < 0.05$; **$P < 0.01$ vs. Wildtype with Student's t-test

primary or metastatic PanNETs, the expression of *GDF2*, *BMP10* (Figure 4E–4J) or *GDF5* (data not shown) was neither correlated to an endothelial cell metagene, nor to the expression of their receptors *ACVRL1* or *ENG*. Notably, *GDF2* and *BMP10* expression was significantly correlated to each other (Figure 4J). Finally, in mouse PanNETs from RIP1-Tag2 mice, the expression of *Gdf2* was even found to be inversely correlated to its receptors *Acvrl1* and *Eng*, as well as to the vascular metagene (Figure 4K–4N).

Next, to assess quantitative and qualitative differences in the angiogenic response due to the lack of BMP9, we performed a careful automated image analysis of the vessel tree, as detected by immunostaining for the endothelial cell marker podocalyxin and for tomato lectin used to visualize functional vessels (Figure 5A–5C). The total vessel area and the average vessel length were not affected by the absence of BMP9 (Figure 5D–5E). Notably, however, the number of vessel junctions and the branching density was significantly higher in tumors from *Gdf2*-deficient mice (Figure 5A–5G). In addition, the lacunarity of the vasculature, *i.e.* the irregularity and size of the gaps between blood vessels, was significantly lower in PanNET from RIP1-TAg2; *Gdf2*$^{-/-}$ mice (Figure 5H). Finally, analysis of the proportion of functional vessels as visualized by injection with FITC-conjugated tomato lectin demonstrated no difference between groups (Figure 5I).

Exploration of specific changes in gene expression in endothelial cells associated with deficiency for BMP9 demonstrated a dramatically impaired activity of the ALK1 signaling pathway, as assessed by the expression of the prototypical target genes *Id1*, *Id3* and *Smad6* in isolated PanNET endothelial cells, indicative of a non-redundant function for BMP9 in activating signaling in endothelial cells downstream of BMP receptors (Figure 6A). In contrast, the expression of ALK5 target genes in endothelial cells was inconsistently and relatively less regulated, effectively resulting in an increased ratio of ALK5/ALK1 activity (Figure 6A). ALK1 signaling has previously been implicated in the regulation of endothelial stalk cell/tip cell identity [19]. Intriguingly, the transcripts for both endothelial stalk cell-related genes, such as *Hey1* and *Flt1* (VEGFR1), and for the tip cell-related gene *Kdr* (VEGFR2), were increased in abundance in an isolated pool of endothelial cells from PanNET lesions in RIP1-TAg2; *Gdf2*$^{-/-}$ mice, suggesting that both stalk cell and tip cell identity were reinforced in the absence of BMP9 (Figure 6B).

Finally, we characterized the support from vessel-associated mesenchymal cells by immunostaining for α-smooth muscle actin (α-SMA) in tumors from RIP1-TAg2 mice. Similar to *Eng*-deficient mice, RIP1-TAg2; *Gdf2*$^{-/-}$ mice presented with PanNET harboring a greater investment of mesenchymal cells in the peri-vascular niche compared to their wildtype counterpart, with evidence for co-localization of podocalyxin and α-SMA, suggestive of ongoing EndMT (Figure 6C–6D). In our previous studies, loss of endoglin in the tumor endothelium was found to be functionally linked to a facilitated transmigration of malignant cells across the vessel wall, and thereby an increased metastatic seeding, through the process of EndMT [14]. Similarly, loss of BMP9, and the concomitantly intensified EndMT, was associated with a 66% rise in metastatic colonization of the liver in mice with one deficient copy of the *Gdf2* gene, and a 188% rise in the incidence of hepatic metastases in mice with ablation of both alleles of *Gdf2* (Figure 6E).

DISCUSSION

A schematic representation of the contrasting phenotypes resulting from genetic perturbation of endothelial TGF-β family members in the context of the RIP1-TAg2 mouse model of PanNETs is shown in Figure 7. While targeting of ALK1 gives rise to suppression of key parameters, including tumor volume, vessel density and metastatic dissemination,

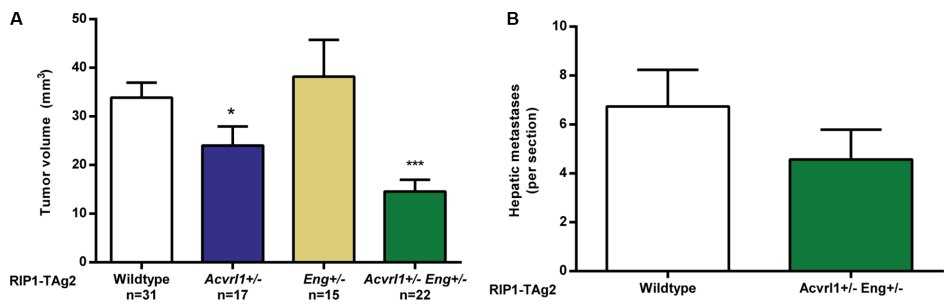

Figure 3: Acvrl1 and Eng deficiency synergistically decrease pancreatic neuroendocrine tumor volume. (**A**) Total PanNET tumor volumes from RIP1-TAg2 wildtype, *Acvrl1*- and *Eng*-deficient mice at 12 weeks of age. (**B**) Number of individual liver micrometastases from RIP1-TAg2 mice, $n = 5$ mice per group Data are mean ± SEM. ***$P < 0.001$ vs. Wildtype with Student's *t*-test

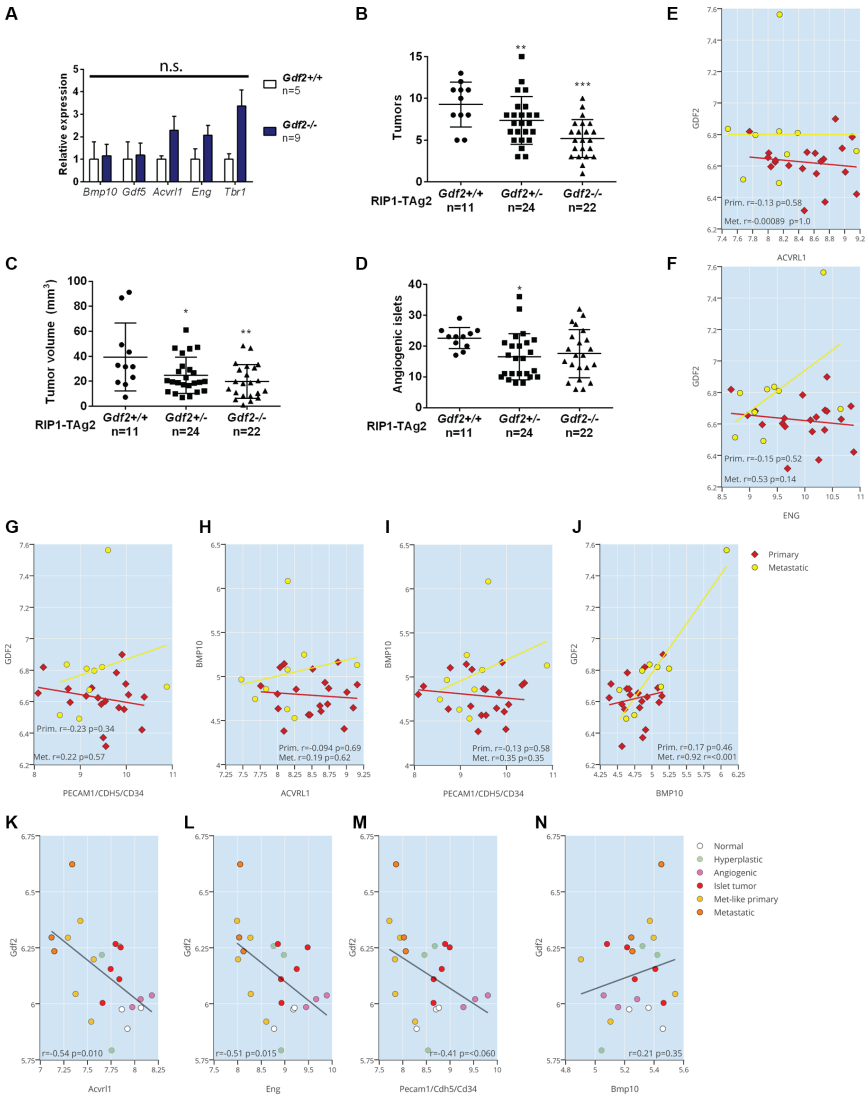

Figure 4: Ablation of BMP9 reduces the growth of primary PanNETs. (**A**) qRT-PCR expression levels of ligands BMP10 and GDF5, and receptors ALK1, Endoglin and ALK5 in whole PanNET tumors from RIP1-TAg2 wildtype, and *Gdf2* knockout mice at 12 weeks. (**B**–**D**) Total PanNET tumor volume (B), number of tumors (C) and number of angiogenic islets (D) from RIP1-TAg2 mice at 12 weeks. (**E**–**J**) Expression correlation of *GDF2* and *BMP10* against ACVRL1, ENG and an endothelial metagene (CD34, CDH5, PECAM1), (E–I), and of *GDF2* against *BMP10* (J) from a human dataset of pancreatic neuroendocrine tumors and metastases (**K**–**N**) Expression correlation of *Gdf2* against *Acvrl1*, *Eng*, an endothelial metagene (*CD34*, *CDH5*, *PECAM1*), and Bmp10 (K-N) from a mouse dataset of pancreatic neuroendocrine RIP1-TAg2 islets, tumors and metastases Data are mean ± SEM. *$P < 0.05$; **$P < 0.01$; ***$P < 0.001$ vs. Wildtype with Student's *t*-test.

suppression of endoglin enhances seeding of metastases [9, 12, 14]. Dual targeting of ALK1 and endoglin resulted in further inhibition of tumor growth, indicating that the most effective means to achieve repression of TGF-β signaling in endothelial cells is by blocking both receptors. Deficiency for BMP9 was accompanied by reduced growth of the primary tumor, in agreement with blockade of ALK1 signaling, combined with enhanced metastatic colonization, suggesting impairment of signaling via endoglin. The composite phenotype in RIP1-TAg2; *Gdf2*$^{-/-}$ mice also implies that the inhibitory effect of ALK1 blockade cannot simply be explained by neutralization of BMP9. Thus, despite the fact that the activity of the canonical Smad1/5/8-mediated ALK1 pathway is mitigated in mice lacking BMP9, further studies to identify additional ligands that bind and activate atypical signaling through ALK1 may be warranted.

Our current and previous work shows that signaling by TGF-β family members in endothelial cells governs the rate of metastatic escape from the primary tumor.

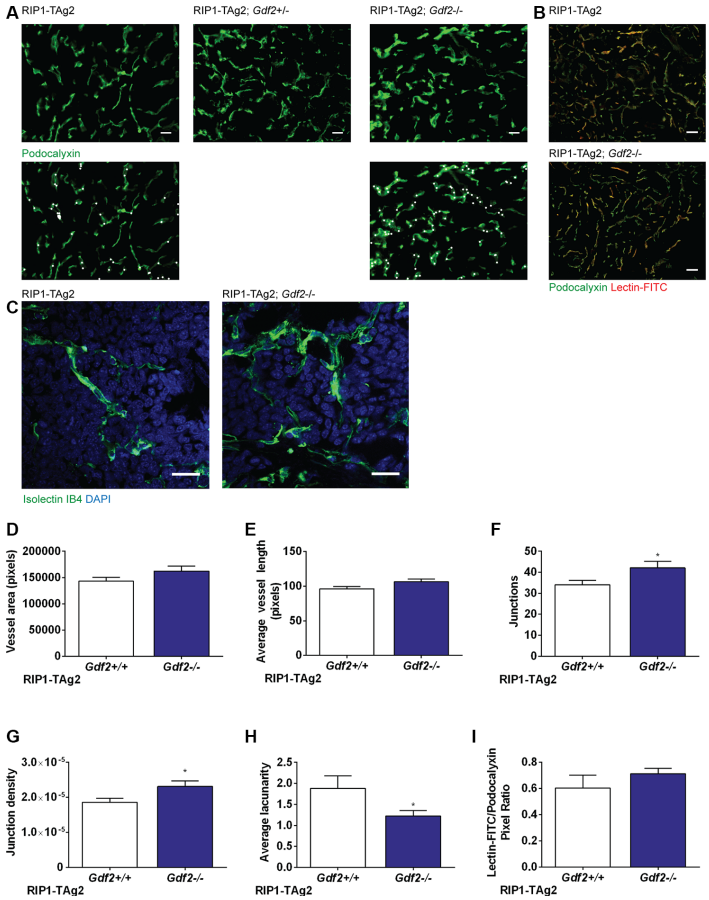

Figure 5: Ablation of BMP9 increases the number of vessel junctions and reduces lacunarity in primary tumor vasculature. (**A**) Representative images of Podocalyxin-stained vessels in PanNETs of 12-week old RIP-TAg2 mice. Vessel junctions are highlighted in second row with white dots. Scale bar 20 μm. (**B**) Representative images of Lectin-FITC perfused vessels in PanNETs of 12-week old RIP-TAg2 mice. Scale bar 50 μm. (**C**) High-magnification vessel details in PanNETs stained with Isolectin GS-IB4. Scale bar 20 μm. (**D**–**H**) Analysis of vessel features in Podocalyxin-stained PanNETs from RIP1-TAg2 mice; total vessel area (C), average vessel length (D), total number of junctions (E), junction density (F), and lacunarity (G). (**I**) Quantification of immunofluorescence of FITC-conjugated Lectin perfusion relative to Podocalyxin expression. Data are mean ± SEM. *$P < 0.05$ vs. Wildtype with Student's *t*-test.

Deficiency for endoglin or BMP9 results in a shift towards a mesenchymal phenotype of endothelial cells, thus endorsing malignant cell transmigration across the vessel wall. In contrast, inhibition of ALK1 reduces EndMT in mouse models of breast cancer (unpublished observation). Endothelial-to-mesenchymal transition in endothelial cells is correlated to the activity of the ALK5 type I receptor pathway, such that during conditions of increased EndMT and metastatic spread (targeting of endoglin or BMP9), ALK5 target genes are increasingly transcribed compared to ALK1 target genes. Conversely, during conditions of reduced EndMT and impaired systemic dissemination (targeting of ALK1), ALK5 target genes exhibit a reduced expression. A recent study demonstrated stable complex formation between ALK1, endoglin and the TGF-β type II receptor, even in the absence of any ligand [22]. Interestingly, endoglin was shown to promote ALK1-dependent Smad1/5 signaling, consistent with our finding that reduced levels of endoglin shifts the balance towards the ALK5-induced Smad2/3 pathway and with previous studies demonstrating a requirement of endoglin for BMP9-induced ALK1 signaling [23]. Presumably, in the absence of ALK1 activity, endoglin may still sequester BMP9 and/or TGF-β from binding to ALK5, thereby explaining why ALK1 targeting does not promote mesenchymal transformation of the endothelium. The relative activation status of the ALK1 and ALK5 pathways appear to be an important determinant of the endothelial cell phenotype in relation to EndMT and endorsement of tumor cell transmigration; future studies should therefore explore this parameter as a potential biomarker of prognostic significance. Also, high resolution exploration

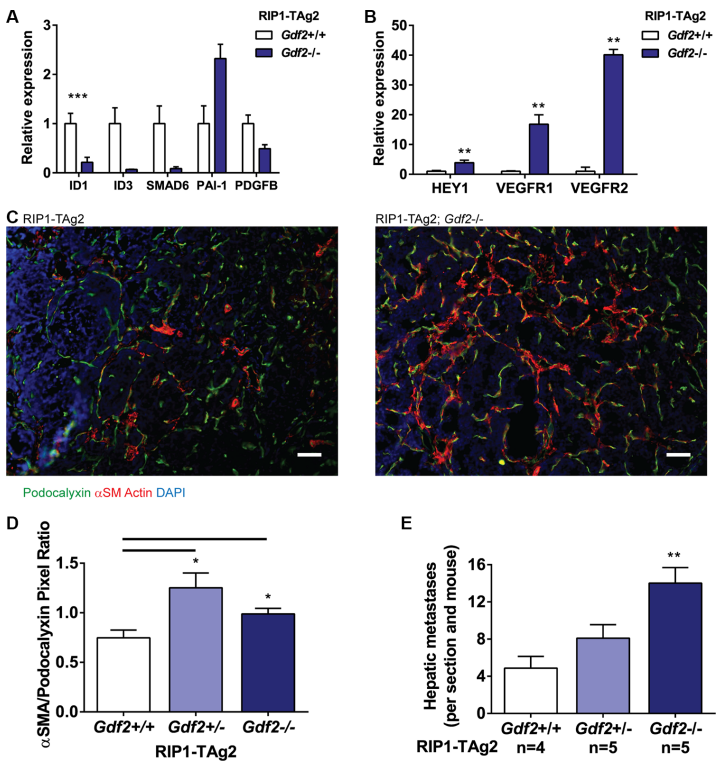

Figure 6: Ablation of BMP9 increases hepatic metastases and affects downstream ALK1 and Notch signaling. (**A**–**B**) qRT-PCR expression levels of downstream products of ALK1 and ALK5 signaling (A), and Notch signaling (B) from LYVE1-/CD31+ endothelial cells isolated from PanNET tumors. Expression levels are relative to L19 housekeeping gene. (**C**) Representative images of labelled PanNET tumors from RIP1-TAg2 mice, showing Podocalyxin (green), α-Smooth Muscle Actin (red) and nuclei (DAPI, blue). Scale bar 50 μm. (**D**) Quantification of positively-stained pixels of α-Smooth Muscle Actin relative to Podocalyxin in PanNET tumors. $n = 4$ mice per group. (**E**) Number of individual hepatic micrometastases in RIP1-TAg2 mice at 12 weeks. SEM. $^{*}P < 0.05$; $^{**}P < 0.01$; $^{***}P < 0.001$ vs. Wildtype with Student's t-test.

of the complex formation between the different type I, type II and type III receptors of the TGF-β family expressed by endothelial cells should be pursued to determine the mechanism for their interdependence of activity.

Canonical ALK1 signaling cooperates with Notch to suppress VEGF-driven sprouting and tip-cell formation during physiological angiogenesis [24]. Moreover, reduced ALK1 signaling by targeting of BMP9 and BMP10 induces a hypersprouting phenotype both *in vitro* and *in vivo*, resembling Notch inhibition [19, 24, 25]. Mechanistically, ALK1- and ALK5-mediated activation of Smad 2/3 is triggered by Notch to drive the stalk cell phenotype required for resolution of the angiogenic cascade [26]. The lack of BMP9 in the context of physiological angiogenesis is moderated to some extent by upregulation of BMP10 [19, 27]. In contrast, in our studies of pathological tumor angiogenesis, we did not observe a compensatory increase in expression of BMP10 (or the close family member GDF5) within tumor lysates. However, while the absence of BMP9 did cause significant hyperbranching, it did not reduce vessel density to the same extent as targeting of ALK1, again suggesting activation of ALK1 by alternative ligand(s) or by compensatory production of ligands at distant sites. Whether the increased density of vessel branches in tumors from RIP1-TAg2; *Gdf2*$^{-/-}$ mice is consequential to enhanced sprouting, similar to the situation during developmental angiogenesis, remains to be determined, but appears plausible. Our findings illustrate the added complexity of tumor angiogenesis compared to physiological angiogenesis, and the need for more refined studies of the intricate mechanisms of blood vessel growth within the malignant tissue.

There are currently several anti-cancer drugs targeting TGF-β family signaling, including dalantercept and PF-03446962 blocking ALK1, and TRC-105 neutralizing endoglin, in Phase II/III of clinical development for a range of indications [28–31]. Our comprehensive charting of the outcome of targeting ALK1, endoglin or BMP9 to achieve anti-angiogenic and therapeutic efficacy highlights the importance of performing detailed mechanistic studies prior to commencing clinical testing of drugs presumably impinging on the same signaling pathway, since the outcome may be diverse even when targeting closely related proteins. Specifically, our studies suggest that ALK1 would be the target of choice for the TGF-β signaling system in endothelial cells to best reduce angiogenesis [9, 12, 14]. Nevertheless, drugs for cancer indications are rarely used as monotherapy, therefore targeting of endoglin and/or BMP9 may still be pursued as partners in combinatorial treatments. Indeed, several phase II clinical trials are already in motion for combinations of inhibitors of TGF-β family signaling and well-established VEGF-targeting drugs, some of which have presented promising interim analyses [32]. The added value of combining anti-angiogenic therapies with different mechanisms of action is consistent with previous work, by us and others, identifying ALK1 or endoglin blockade as synergistic partners to VEGF inhibition in pre-clinical

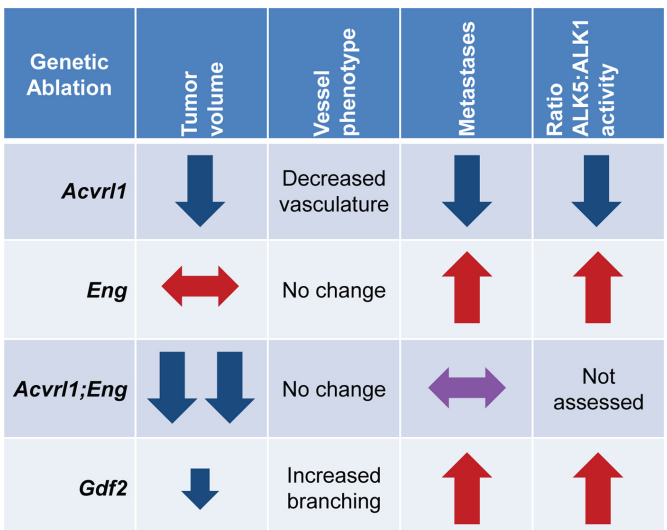

Figure 7: Representative RIP-TAg2 phenotypes for genetic ablation of *Acvrl1*, *Eng*, and *Gdf2*. Red and blue arrows are representative of the *Acvrl1* and *Eng* deficient phenotypes, respectively.

studies [11, 14]. Furthermore, the current study indicates dual targeting of ALK1 and endoglin as a promising additional possibility for combinatorial targeting of neoangiogenesis and tumor growth.

MATERIALS AND METHODS

Animal work and primary tumors

All animal experiments were approved by the ethical committees for animal care in Stockholm and Lund (permits N96/11 and M142/13, respectively). C57BL/6 RIP-TAg2 mice receive water supplemented with 5% sucrose at 10 weeks of age to counteract hypoglycemia. Mice were sacrificed at 12 weeks of age, and pancreatic neoplasms with diameter ≥ 1 mm were measured as tumors, and smaller angiogenic islets were quantified using a stereological microscope. The tumor burden was calculated as the total volumes of all tumors from the pancreas, where individual volumes were calculated as . length × 2width × $\pi/6$.

Analysis of gene expression data

Human patient data (GSE73339) and RIP1-TAg2 data (GSE73514) were downloaded from the Gene Expression Omnibus (GEO) [17]. The human data set contained 20 primary and 9 metastatic PanNETs and the mouse PanNET data set consisted of a total of 22 samples (normal (n = 3), hyperplastic (n = 3), angiogenic (n = 3), islet tumor (n = 5), met-like primary (n = 5), and metastatic (n = 3) samples)). The data were accessed on January 8, 2016. Gene expression data generated by Sadanandam et al. [17] were obtained using the Affymetrix GeneChip human Gene 1.0 ST and Affymetrix GeneChip Mouse Gene 1.0 ST arrays and were normalized using RMA. Analysis was conducted with R Studio, and the Pearson method was used to analyze correlations. All P-values reported are two-tailed.

Immunofluorescence and histology

At time of sacrifice, mice were heart perfused with 10 mL each PBS and 4% paraformaldehyde or buffered zinc formalin. The left liver lobes were post-fixed in formaldehyde overnight at 4°C, paraffin embedded and serially sectioned. Each mouse contained 8 or 15 sections (Gdf2 and Acvril1/Eng experiments respectively) and 4–5 mice per group. Paraffin-embedded sections were de-paraffinized and stained with hemotoxylin and eosin, and metastatic foci were counted if they were at least > 6 cells in diameter. The pancreas and embedded tumors were cryopreserved; stored in 30% sucrose overnight at 4°C, then embedding in cryostat sectioning matrix. Cryosections were fixed in acetone, blocked with serum-free blocking solution (DAKO) for 90 min at ambient temperature and stained with primary antibody overnight at 4°C. Sections were then stained with Alexa fluorchrome 488 and 594 nm secondary antibodies (dilution 1:1000, Invitrogen) for 90 min at ambient temperature, and mounted with 4′,6-diamidino-2-phenylindole-containing media (Vector Laboratories). Primary antibodies used in this study were Podocalyxin (dilution 1:100; R&D Systems, AF1556), αSMA-Cy3 (Clone 1A4; dilution 1:100; Cy3 conjugated; Sigma, C6198), and Isolectin IB4 (dilution 1:50; AF488 conjugated; Thermo Fisher, I21411). Vessel perfusion was evaluated by retro-orbital injection of FITC-conjugated tomato lectin allowed to circulate for 4 min prior to sacrificed (50 µl at 0.5 mg/ml; Vector Laboratories), and sections subsequently stained with anti-podocalyxin and anti-FITC antibody (dilution 1:100, Thermo Fisher, 71–1900).

Immunofluorescence-stained sections were imaged and acquired using a Nikon Eclipse E800 microscope (Nikon Instruments), SPOT RTKE camera and SPOT advanced software (SPOT Imaging), or an Olympus BX63 microscope and DP80 camera and cellSens Dimension v 1.12 software (Olympus Corporation). Analysis of podocalyxin-positive vessel features in immunostained RIP-TAg2 tumors was performed using Angiotool semi-automated software [33], with 10 or more high-power images from each mouse. Quantification of αSMA and Lectin-FITC immunostaining was performed by quantifying positively-stained pixels relative to podocalyxin-stained pixels in Adobe Photoshop CS5.1. Confocal fluorescence imaging was performed with Zeiss LSM 710 system and ZEN Black software (Carl Zeiss AG).

Endothelial cell isolation

RIP-TAg2 mice were perfused with PBS, and isolated PNET were finely cut and incubated with stirring in in 0.05 g collagenase type II (Worthington), 0.05 g collagenase IV (Invitrogen), 0.01 g DNase I (Sigma) for 15 min at 37°C with stirring. The mixture was passed through a 70-µm strainer, mixed with 20 mL ice-cold isolation buffer (DMEM supplemented with 0.2% BSA, 5% enzyme-free cell dissociation buffer [Gibco]), and centrifuged at 3400 rpm at 4°C for 5 min. The pellet was resuspended in 10 mL PharmLyse buffer and remained for 10 min at ambient temperature, and then added to 40 mL of DMEM-dissociation buffer. The pellet was resuspended in 1 ml isolation buffer and 50 µL Lyve-1 coated beads (eBiosciences 13-0443-82 ; CELLection biotin binder kit Invitrogen), and were incubated in an end-over-end shaker at 4°C for 45 mins. Magnetic separation was used, and the supernatant was then mixed and incubated with 50 µL CD31 coated beads (BD Pharmigen, 553371) Following magnetic separation and washing of the CD31+ fraction with isolation buffer, RNA isolation was completed using the RNeasy kit (Qiagen).

Real-time qPCR

Preparation of cDNA was done using iScript cDNA Synthesis kit (Biorad). QPCR was done using a KAPA Sybr Fast qPCR kit (Kapa Biosystems) on an Agilent Technologies Stratagene Mx3005P, using the following primers: RPL19, ID1, ID3 PAI-1, PDGFB, CD31, VE-cadherin (Cunha et al., 2010), VEGFR2 (Hagberg et al., 2010), and SMAD6 (F: CCACCAACTCCCTCATCACT, R: CTGGTCGTACACCGCATAGA). The following pre-validated primers were obtained from Qiagen: RPL19 (Mm_Rpl19_2_SG), BMP10 (Mm_BMP10_1_SG), GDF5 (Mm_Gdf5_1_SG), HEY1 (Mm_Hey1_1_SG), VEGFR1 (Mm_Flt1_1_SG), and VEGFR2 (Mm_Kdr_1_SG).

Statistical analysis

All measurements are depicted as mean ± SEM, and statistical analyses were performed using an unpaired two-tailed Student's *t* test. Statistical significance was considered using $\alpha = 0.05$.

ACKNOWLEDGMENTS AND FUNDING

KP is the Göran & Birgitta Grosskopf Professor at Lund University. The research presented herein was supported by a Consolidator Grant from the European Research Council (the TUMORGAN project), the Swedish Research Council, the Swedish Cancer Society, the STARGET consortium (a Swedish Research Council Linnaeus network), BioCARE, ALF-funding, and Lund University. SJL is supported by NIH grant R01AR060636.

CONFLICTS OF INTEREST

NME, JS, MB, EC, SJL and SIC have no conflicts of interest to declare. KP is named as inventor on a patent describing targeting of the ALK1 pathway in tumor angiogenesis.

Authors' contributions

NME, SIC and KP conceived the study. NME, JS, MB, EC, and SIC performed experiments and collected the data. NME, SIC, JS, MB, EC and KP analyzed the data. SJL provided exclusive reagents. NME, SIC and KP wrote the manuscript.

REFERENCES

1. Hanahan D, Weinberg RA. Hallmarks of cancer: the next generation. Cell. 2011; 144:646–674.
2. Ferrara N, Hillan KJ, Novotny W. Bevacizumab (Avastin), a humanized anti-VEGF monoclonal antibody for cancer therapy. Biochem Biophys Res Comm. 2005; 333:328–335.
3. Raymond E, Dahan L, Raoul JL, Bang YJ, Borbath I, Lombard-Bohas C, Valle J, Metrakos P, Smith D, Vinik A, Chen JS, Horsch D, Hammel P, et al. Sunitinib malate for the treatment of pancreatic neuroendocrine tumors. N Engl J Med. 2011; 364:501–513.
4. Derynck R, Feng XH. TGF-beta receptor signaling. Biochim Biophys Acta Rev Cancer. 1997; 1333:F105–F150.
5. ten Dijke P, Arthur HM. Extracellular control of TGFbeta signalling in vascular development and disease. Nat Rev Mol Cell Biol. 2007; 8:857–869.
6. Bourdeau A, Dumont DJ, Letarte M. A murine model of hereditary hemorrhagic telangiectasia. J Clin Invest. 1999; 104:1343–1351.
7. Arthur HM, Ure J, Smith AJ, Renforth G, Wilson DI, Torsney E, Charlton R, Parums DV, Jowett T, Marchuk DA, Burn J, Diamond AG. Endoglin, an ancillary TGFbeta receptor, is required for extraembryonic angiogenesis and plays a key role in heart development. Dev Biol. 2000; 217:42–53.
8. Cunha SI, Pietras K. ALK1 as an emerging target for antiangiogenic therapy of cancer. Blood. 2011; 117: 6999–7006.
9. Cunha SI, Pardali E, Thorikay M, Anderberg C, Hawinkels L, Goumans MJ, Seehra J, Heldin CH, Ten Dijke P, Pietras K. Genetic and pharmacological targeting of activin receptor-like kinase 1 impairs tumor growth and angiogenesis. J Exp Med. 2010; 207:85–100.
10. Mitchell D, Pobre EG, Mulivor AW, Grinberg AV, Castonguay R, Monnell TE, Solban N, Ucran JA, Pearsall RS, Underwood KW, Seehra J, Kumar R. ALK1-Fc inhibits multiple mediators of angiogenesis and suppresses tumor growth. Mol Cancer Ther. 2010; 9:379–388.
11. Hu-Lowe DD, Chen E, Zhang L, Watson KD, Mancuso P, Lappin P, Wickman G, Chen JH, Wang J, Jiang X, Amundson K, Simon R, Erbersdobler A, et al. Targeting Activin Receptor-Like Kinase 1 (ALK1) Inhibits Angiogenesis and Tumorigenesis Through a Mechanism of Action Complementary to Anti-VEGF Therapies. Cancer Res. 2011; 71:1362–1373.
12. Cunha SI, Bocci M, Lovrot J, Eleftheriou N, Roswall P, Cordero E, Lindstrom L, Bartoschek M, Haller BK, Pearsall RS, Mulivor AW, Kumar R, Larsson C, et al. Endothelial ALK1 Is a Therapeutic Target to Block Metastatic Dissemination of Breast Cancer. Cancer research. 2015; 75:2445–2456.
13. Hawinkels LJ, de Vinuesa AG, Paauwe M, Kruithof-de Julio M, Wiercinska E, Pardali E, Mezzanotte L, Keereweer S, Braumuller TM, Heijkants RC, Jonkers J, Lowik CW, Goumans MJ, et al. Activin Receptor-like Kinase 1 Ligand Trap Reduces Microvascular Density and Improves Chemotherapy Efficiency to Various Solid Tumors. Clinical cancer research. 2016; 22:96–106.

14. Anderberg C, Cunha SI, Zhai Z, Cortez E, Pardali E, Johnson JR, Franco M, Paez-Ribes M, Cordiner R, Fuxe J, Johansson BR, Goumans MJ, Casanovas O, et al. Deficiency for endoglin in tumor vasculature weakens the endothelial barrier to metastatic dissemination. J Exp Med. 2013; 210:563–579.
15. Park S, Dimaio TA, Liu W, Wang S, Sorenson CM, Sheibani N. Endoglin regulates the activation and quiescence of endothelium by participating in canonical and non-canonical TGF-beta signaling pathways. Journal of cell science. 2013; 126:1392–1405.
16. Hanahan D. Heritable formation of pancreatic beta-cell tumours in transgenic mice expressing recombinant insulin/simian virus 40 oncogenes. Nature. 1985; 315:115–122.
17. Sadanandam A, Wullschleger S, Lyssiotis CA, Grotzinger C, Barbi S, Bersani S, Korner J, Wafy I, Mafficini A, Lawlor RT, Simbolo M, Asara JM, Blaker H, et al. A Cross-Species Analysis in Pancreatic Neuroendocrine Tumors Reveals Molecular Subtypes with Distinctive Clinical, Metastatic, Developmental, and Metabolic Characteristics. Cancer Discov. 2015; 5:1296–1313.
18. Oh SP, Seki T, Goss KA, Imamura T, Yi Y, Donahoe PK, Li L, Miyazono K, ten Dijke P, Kim S, Li E. Activin receptor-like kinase 1 modulates transforming growth factor-beta 1 signaling in the regulation of angiogenesis. Proc Natl Acad Sci USA. 2000; 97:2626–2631.
19. Ricard N, Ciais D, Levet S, Subileau M, Mallet C, Zimmers TA, Lee SJ, Bidart M, Feige JJ, Bailly S. BMP9 and BMP10 are critical for postnatal retinal vascular remodeling. Blood. 2012; 119:6162–6171.
20. Levet S, Ciais D, Merdzhanova G, Mallet C, Zimmers TA, Lee SJ, Navarro FP, Texier I, Feige JJ, Bailly S, Vittet D. Bone morphogenetic protein 9 (BMP9) controls lymphatic vessel maturation and valve formation. Blood. 2013; 122:598–607.
21. Yoshimatsu Y, Lee YG, Akatsu Y, Taguchi L, Suzuki HI, Cunha SI, Maruyama K, Suzuki Y, Yamazaki T, Katsura A, Oh SP, Zimmers TA, Lee SJ, et al. Bone morphogenetic protein-9 inhibits lymphatic vessel formation via activin receptor-like kinase 1 during development and cancer progression. Proceedings of the National Academy of Sciences of the United States of America. 2013; 110:18940–18945.
22. Pomeraniec L, Hector-Greene M, Ehrlich M, Blobe GC, Henis YI. Regulation of TGF-beta receptor hetero-oligomerization and signaling by endoglin. Molecular biology of the cell. 2015; 26:3117–3127.
23. Nolan-Stevaux O, Zhong W, Culp S, Shaffer K, Hoover J, Wickramasinghe D, Ruefli-Brasse A. Endoglin requirement for BMP9 signaling in endothelial cells reveals new mechanism of action for selective anti-endoglin antibodies. PloS one. 2012; 7:e50920.
24. Larrivee B, Prahst C, Gordon E, del Toro R, Mathivet T, Duarte A, Simons M, Eichmann A. ALK1 signaling inhibits angiogenesis by cooperating with the Notch pathway. Developmental cell. 2012; 22:489–500.
25. Kerr G, Sheldon H, Chaikuad A, Alfano I, von Delft F, Bullock AN, Harris AL. A small molecule targeting ALK1 prevents Notch cooperativity and inhibits functional angiogenesis. Angiogenesis. 2015; 18:209–217.
26. Aspalter IM, Gordon E, Dubrac A, Ragab A, Narloch J, Vizan P, Geudens I, Collins RT, Franco CA, Abrahams CL, Thurston G, Fruttiger M, Rosewell I, et al. Alk1 and Alk5 inhibition by Nrp1 controls vascular sprouting downstream of Notch. Nature communications. 2015; 6:7264.
27. Chen H, Brady Ridgway J, Sai T, Lai J, Warming S, Roose-Girma M, Zhang G, Shou W, Yan M. Context-dependent signaling defines roles of BMP9 and BMP10 in embryonic and postnatal development. Proceedings of the National Academy of Sciences of the United States of America. 2013; 110:11887–11892.
28. Gordon MS, Robert F, Matei D, Mendelson DS, Goldman JW, Chiorean EG, Strother RM, Seon BK, Figg WD, Peer CJ, Alvarez D, Adams BJ, Theuer CP, et al. An open-label phase Ib dose-escalation study of TRC105 (anti-endoglin antibody) with bevacizumab in patients with advanced cancer. Clinical cancer research. 2014; 20:5918–5926.
29. Makker V, Filiaci VL, Chen LM, Darus CJ, Kendrick JE, Sutton G, Moxley K, Aghajanian C. Phase II evaluation of dalantercept, a soluble recombinant activin receptor-like kinase 1 (ALK1) receptor fusion protein, for the treatment of recurrent or persistent endometrial cancer: an NRG Oncology/Gynecologic Oncology Group Study 0229N. Gynecologic oncology. 2015; 138:24–29.
30. Necchi A, Giannatempo P, Mariani L, Fare E, Raggi D, Pennati M, Zaffaroni N, Crippa F, Marchiano A, Nicolai N, Maffezzini M, Togliardi E, Daidone MG, et al. PF-03446962, a fully-human monoclonal antibody against transforming growth-factor beta (TGFbeta) receptor ALK1, in pre-treated patients with urothelial cancer: an open label, single-group, phase 2 trial. Invest New Drugs. 2014; 32:555–560.
31. Goff LW, Cohen RB, Berlin JD, de Braud FG, Lyshchik A, Noberasco C, Bertolini F, Carpentieri M, Stampino CG, Abbattista A, Wang E, Borghaei H. A Phase I Study of the Anti-Activin Receptor-Like Kinase 1 (ALK-1) Monoclonal Antibody PF-03446962 in Patients with Advanced Solid Tumors. Clinical cancer research. 2016; 22:2146–2154.
32. Voss MH, Plimack ER, Rini BI, Atkins MB, Alter R, Bhatt RS, Beck JT, Mutyaba M, Pappas KM, Wilson D, Zhang XS, Sherman ML, Pandya SS. The DART Study: Part 1 results from the dalantercept plus axitinib dose escalation and expansion cohorts in patients with advanced renal cell carcinoma (RCC). J Clin Oncol. 2015; 33.
33. Zudaire E, Gambardella L, Kurcz C, Vermeren S. A computational tool for quantitative analysis of vascular networks. PloS one. 2011; 6:e27385.

Paper III

Endothelial-specific genetic modifications of TGF-β receptors in mouse models of pancreatic neuroendocrine tumors

Nikolas Eleftheriou, Matteo Bocci, Ewa Kurzejamska, Eugenia Cordero, Kristian Pietras [1]

Department of Laboratory Medicine, Lund University

[1]Corresponding author: kristian.pietras@med.lu.se

December 22 2016

Introduction

Tumors contain a complex microenvironment required to support primary tumor growth. Cells must be in close proximity to capillary vessels in order to maintain cellular function. The recruitment of new blood vessels, termed *angiogenesis*, thus becomes crucial in tumor development from the neoplasm stage onward[1,2]. Angiogenesis drives the growth of the primary tumor, as well as provides a route for metastatic dissemination, as cancer cells can intravasate into blood or lymphatic vessels. The requirement of angiogenesis in solid tumors has made targeting this process the subject of various cancer therapies.

The transforming growth factor-β (TGF- β) family of ligands and receptors are implicated in tumor development as tumors become increasingly malignant, including reprogramming fibroblasts, subverting immune response and promoting epithelial-to-mesenchymal transition[3]. Additionally, TGF-β family signaling can impact tumor angiogenesis by affecting endothelial cell proliferation and migration. The TGF-β family of ligands binds to serine/threonine kinase receptor complexes of type I and II receptors[4]. TGF-β receptor 2 (TBGFBR2) is a type II receptor that can complex with the type I receptors activin receptor-like kinase (ALK)1 and ALK5, propagating downstream Smad1/5/8 and Smad2/3 signaling respectively. ALK1 expression is endothelial cell restricted and ALK1 signaling is complimented by the type III receptor endoglin (Eng), whereas ALK5 and TGFBR2 are ubiquitously expressed. Mice with global knockouts of *Tgfbr2*, *Alk5,Alk1 or Eng* do not survive past embryonic development, displaying failure in vessel formation[5,6]. However it is unclear exactly how these receptors specifically target angiogenesis, or if signaling originating from the endothelial cell can directly impact the tumor microenvironment or metastatic disseminations.

Previously we have shown how inhibition of ALK1 can decrease tumor burden and metastatic potential in mouse pancreatic neuroendocrine tumors (PanNET)[7,8], but similar studies on ALK5 require genetically engineered mice to pinpoint genetic modifications to the vascular compartment. The RIP1-TAg2 mouse model produces PanNETs which strongly express TGF-β and are highly angiogenic[9]. We have developed RIP1-TAg2 compound mice with VE-Cadherin or NG2 promoter-linked Cre-ERT2 recombinase system to temporally induce genetic modifications upon injection of tamoxifen. These compound mice contain floxed *Alk5*, or an X chromosome-linked constitutively active ALK5 mutant (mut*Alk5*CA) preceded by a lox-STOP-lox motif[10]. By isolating these genetic modifications in endothelial ALK5 signaling we demonstrate their capacity to alter primary tumor burden, neoangiogenesis, and preferred mechanisms of metastatic dissemination.

Results

mut*Alk5*CA endothelial-specific knock-in increases tumor volume

Our previous studies focused on the ablation of the receptors *Endoglin* and *Alk1*, and the ligand *BMP9*, and their effects on the endothelial compartment of tumors from RIP1-TAg2 mice[7,8,11,12]. Here we induced endothelial-specific VE-Cadherin Cre (*Cdh5*-CreERT2) recombination of *lox*P-flanked *Alk5*, or *lox*P-STOP-*lox*P mut*Alk5*^{CA} in RIP1-TAg2 mice. Mice underwent tamoxifen-induced recombination at 5-6 weeks of age during the hyperplastic, pre-angiogenic stage of tumor development, and were sacrificed at 12 weeks of age when tumors have developed and typically display metastatic spread (Fig 1). These mice did not display any obvious impairment in development upon induction of recombination, and any deaths prior to twelve weeks was not correlated to a single phenotype. *Alk5* endothelial knockouts did not exhibit any changes in tumor burden (Fig 2 A-C), whereas endothelial mut*Alk5*^{CA}-expressing mice displayed an overall increase in tumor volume (Fig 2 D-F).

ALK5 receptor knockout drives unique angiogenic response

The angiogenic response in neuroendocrine tumors was assessed by immunostaining for the endothelial-cell marker podocalyxin and automated image analysis of the tumor vessel tree. Mice with the endothelial-specific deletion of *Alk5* exhibited higher vessel density, with increases in vessel area, number of endpoints and the number of branch points (Fig 3 A-E, L). Mice expressing endothelial-specific mut*Alk5*^{CA} do not have appear to affect the tumor vasculature, lacking qualitative or quantitative differences from wildtype RIP1-TAg2 tumors (Fig 3F-J, M).

Constitutively active endothelial *Alk5* drives liver metastases; *Alk5* deletion drives metastatic spread to lymph nodes

RIP1-TAg2 tumors have the potential to disseminate to the nearby mesenteric lymph nodes, and to the liver where they appear as micrometastases. At the time of sacrifice, 37% of RIP1-TAg2 mice (7 of 19) with the endothelial-*Alk5* deletion presented with enlarged red lymph nodes in the mesentery, whereas only one mouse had an enlarged lymph node in the control group (1 of 19);the other experimental groups had no enlarged lymph nodes present (Fig 4 A). T-antigen positive cells from the RIP1-TAg2 tumors were not uncommon in lymph nodes across experimental groups (Fig 4 B), however only the endothelial-*Alk5* knockout group consistently showed larger areas of T-antigen positive cells in lymph node cross sections (Fig 4D,E). Quantification of micrometastases from serially sectioned left lateral liver lobes of RIP1-TAg2

mice revealed a higher frequency of metastases in endothelial-mut*Alk5*CA mice, in comparison to wildtype and *Alk5* knockout RIP1-TAg2 mice (Fig 4 C).

***Alk5* knockout in perictyes decreases number or angiogeneic islets**

We prepared genetically engineered RIP1-TAg2 mice under control of pericyte-specfic Cre recombination (*NG2*-CreERT2), in effort to induce genetic changes in pericytes. These mice were induced as above for recombination of *lox*P-flanked *Alk5*, or *lox*P-STOP-*lox*P mut*Alk5*^{CA}. NG2-deletion of *Alk5* produced fewer angiogenic islets, but not changes in tumor number or volume at 12 weeks (Fig 5 A-C), and expression of mut*Alk5*^{CA} produced no detectable changes (Fig 5 D-F). The vessel properties of *Alk5*-pericyte knockouts were also analyzed; however there were no changes in any parameters (Fig 5 G-K).

Discussion

Some trends have emerged from the primary tumor, metastasis and vessel analysis completed thus far. Specifically targeting *Alk5* in endothelial cells has greatly affected vessel development. It remains unclear whether the *Alk5* deletion has affected the vessel functionality, and this should be further tested by injection of fluorescently-labelled lectin to perfuse functioning vessels. The lack of ALK5 should affect TGF-β downstream signaling of SMAD2/3, however ALK1, binding to bone morphogenetic protein (BMP)9 by complexing with BMPRII or ACTRII, may also be affected[4]. It is possible that this endothelial deletion of *Alk5* decreases the activity of the ALK1 signaling arm, leading to the over-stimulation of a tip-cell identity and the hyperbranching phenotype, similarly observed elsewhere[13].

The metastatic phenotypes observed hinge around the signaling capacity of ALK5. Mice expressing mut*Alk5*CA tend to have larger tumors and more liver micrometastases, without any obvious changes to vessel properties. The lack of endothelial ALK5 instead drives dissemination to the mesenteric lymph nodes. Tumors from RIP1-TAg2 are poorly lymphangiogenic, although tumors can be seen bordering lymphatic vessels in the pancreas, and it may possible for the neuroendocrine tumors to develop lymphatic microvessels through changes in signaling. Furthermore lymphatic endothelial cells express VE-Cadherin, and the genetic modifications will also affect these vessels. It remains to be seen if changes in lymphatic endothelial cells are impacting the growth of these PanNET tumors. In either route of dissemination to the liver or lymph nodes, the mechanism of action is not yet clear.

The deletion of *Alk5* in NG2-positive pericytes produced fewer angigogenic islets, otherwise neither the deletion of *Alk5*, or expression of mut*Alk5*^{CA} has impacted the tumor growth. It is

unclear as to when and how perycites are recruited to the tumor microenvironment, and it may be that the pericyte coverage has changed in these mice, warranting further investigations. However, there are unique phenotypes by specifically targeting endothelial cells that have not been reproduced by targeting other cells in the vessel niche.

Previously we have shown the knockdown and inhibition of ALK1 can decrease tumor volume, angiogenesis and incidence of metastasis, whereas deficiency for its ligand (BMP9) or endoglin do not have the same effects on tumor burden despite being parts of the same signaling arm[7,11,12,14]. Furthermore, deficiency of ALK1 downregulated ALK5 downstream signaling, meanwhile deficiency of endoglin upregulated ALK5 downstream signaling. Thus far, the genetically engineered RIP1-TAg2 mice described here do not phenocopy either ALK1, endoglin or BMP9 deficient mice. Both TGFBR2 and ALK5 are ubiquitously expressed, unlike ALK1 and ENG. The tumor therapies for ALK1 (dalantercept, PF-0344962) or ENG (TRC-105) are intended to target angiogenesis, whereas galunisertib, a kinase inhibitor specific to ALK5, targets all cell types expressing ALK5 including tumor and endothelial cells. It remains to be seen if specifically targeting ALK5 in endothelial cells, or if a combination of ALK5 and ALK1 inhibition are viable therapeutic approaches.

Materials and Methods

Animal work

In vivo mouse experiments were approved by Lunds ethical committees for animal care (permit M142/13). C57BL/6 RIP1-TAg2; *Cdh5*-CreERT2 mice received tamoxifen (75mg/kg body weight; Sigma, T5648) or corn oil vehicle (Sigma, C8267) for five consecutive days between five and six weeks of age, and water supplemented with 5% sucrose at ten weeks of age until sacrifice. Mice were sacrificed at 12 weeks of age. At sacrifice, mice are heart perfused with 10ml PBS followed by 10mL buffered zinc formalin (Sigma, Z2902).

Tumor measurements

Primary tumors are counted as all neoplasms ≥ 1mm in diameter, and remaining angiogenic islets are counted under a stereological microscope. The tumor volume is counted from the total volume of all tumors in one mouse pancreas, each calculated as length × 2width × $\pi/6$.

Immunofluorescence and vessel analysis

The pancreas and tumors are stored in 30% sucrose overnight at 4°C, then stored in OCT Cryomount (Histolab, 45830). Cryosections were cut at 8µm thickness, acetone fixed, and treated with Protein Block Serum-Free (DAKO, X0909) for 90min at room temperature. Sections were exposed to anti-Podocalyxin antibody (dilution 1:100; R&D Systems, AF1556) overnight at4°C, then Alexa-488nm secondary antibody (dilution 1:1000, Invitrogen) for 90min at room temperature, and treated with mounted media with DAPI (Vector Laboratories, H-1200). Fluorescent images were acquired with an Olympus BX63 microscope, DP80 camera and cellSens Dimension v 1.12 software (Olypmus Corporation. Approximately 10 or more 20x-magnification images were taken of tumors in each mouse, and analysis of the podocalyxin-positive vessel tree was processed with Angiotool semi-automated software[15].

Immunohistochemistry and metastasis identification

Mesenteric lymph nodes and the left lateral liver lobes were fixed in formalin buffer overnight at 4°C and paraffin embedded. Each entire liver lobe was serially sectioned at 5µm thickness; every 34th section was deparaffinized and underwent hematoxylin and eosin staining. A focus of at least six cells in diameter was positively counted as a single micrometastasis. Lymph nodes sections were cut at 5µm thickness, deparaffinized, treated with pH 10 antigen retrieval buffer, and endogenous peroxidase activity was quenched with 50% MeOH/3% H2O2.Sections were then blocked with 10% goat serum (DAKO, X0907), and exposed to anti-SV40 T-antigen antibody (dilution 1:10000, gift from Douglas Hanahan, EPFL) overnight at 4°C. Following primary antibody incubation, sections were incubated with appropriate biotinylated secondary,

then visualized using Vectastain ABC (Vector Laboratories, PK-6100) and DAB peroxidase substrate kits (Vector Laboratories, SK-4100)

Statistical analysis

Measurements are displayed as mean ± SEM. Statistics were performed using an unpaired two-tailed Student's *t* test, or a chi-squared test (Fig 4A only), with significance threshold at $\alpha = 0.05$

Figures

1 **Experimental setup for genetically engineered compound mice**

RIP1-TAg2 expressing VE-cadherin estrogen receptor-Cre recombinase system are induced with tamoxifen by six weeks of age. Mice may carry *lox*-flanked sites to delete *Tgfbr2* or *Alk5*, or express a constitutively active mutant *alk5*. Mice are sacrificed at 12 weeks of age for primary tumor measurements and downstream analysis.

2 **Quantification of primary pancreatic neuroendocrine tumors**

Number of angiogenic islets as detected under a stereoscopic microscope (A,D), number of tumors at least 1mm wide(B,E), and total combined tumor volume (C,F) per mouse sacrificed at 12 weeks of age, across all experimental groups.

3 **Impact of receptor modifications on dimensions of the vessel network**

PanNET tumors stained for luminal vessel marker podocalyxin and quantified by automated analysis for average vessel length (A,F), vessel area (B,G), number of vessel endpoints (C,H), number of branching junctions (D,I), and junction density (E,J). Representative images show podocalyxin-positive (green) vessel network of tumors from RIP1-TAg2 mice: unmodified (K), *Alk5* knockout (L), constitutively active *Alk5* mutant (M). Scale bar 100µm

4 **Metastatic dissemination to mesenteric lymph nodes and lateral left liver lobe**

Comparison of enlarged mesenteric lymph nodes observed in RIP1-TAg2; *Alk5*-/- mice (A), and mesenteric lymph nodes with any number of cells positively expressing T-antigen across all experimental groups (B). Number of micrometastases counted in serially sectioned left liver lobe per mouse (C). Images of SV40 T-antigen (brown) and nuclear hematoxylin (blue) staining in mesenteric lymph nodes of RIP1-TAg2 (D) and RIP1-TAg2; *Alk5*-/- mice (E). Arrow highlights area positive for T-antigen staining in panel D; bulk of lymph node in panel E are T-antigen positive. Scale bar 500µm.

5 **Primary pancreatic neuroendocrine tumors in NG2-specific genetically engineered mice**

Number of angiogenic islets as detected under a stereoscopic microscope (A,D), number of tumors at least 1mm wide(B,E), and total combined tumor volume (C,F) per mouse sacrificed at 12 weeks of age, across all experimental groups. PanNET tumors stained for luminal vessel marker podocalyxin and quantified by automated analysis for average vessel length (G), vessel area (H), number of vessel endpoints (I), number of branching junctions (J), and junction density (K).

References

1. Hanahan D, Weinberg RA (2000) The hallmarks of cancer. *Cell* **100:** 57-70
2. Hanahan D, Weinberg RA (2011) Hallmarks of cancer: the next generation. *Cell* **144:** 646-674
3. Tian M, Schiemann WP (2009) The TGF-beta paradox in human cancer: an update. *Future Oncol* **5:** 259-271
4. Derynck R, Feng XH (1997) TGF-beta receptor signaling. *Biochim Biophys Acta Rev Cancer* **1333:** F105-F150
5. Oshima M, Oshima H, Taketo MM (1996) TGF-b receptor type II deficiency results in defects of yolk sac hematopoiesis and vasculogenesis. *Dev Biol* **179:** 297-302
6. ten Dijke P, Arthur HM (2007) Extracellular control of TGFbeta signalling in vascular development and disease. *Nat Rev Mol Cell Biol* **8:** 857-869
7. Cunha SI, Bocci M, Lovrot J, Eleftheriou N, Roswall P, Cordero E, Lindstrom L, Bartoschek M, Haller BK, Pearsall RS*, et al.* (2015) Endothelial ALK1 Is a Therapeutic Target to Block Metastatic Dissemination of Breast Cancer. *Cancer research* **75:** 2445-2456
8. Cunha SI, Pardali E, Thorikay M, Anderberg C, Hawinkels L, Goumans MJ, Seehra J, Heldin CH, Ten Dijke P, Pietras K (2010) Genetic and pharmacological targeting of activin receptor-like kinase 1 impairs tumor growth and angiogenesis. *J Exp Med* **207:** 85-100
9. Hanahan D (1985) Heritable formation of pancreatic beta-cell tumours in transgenic mice expressing recombinant insulin/simian virus 40 oncogenes. *Nature* **315:** 115-122
10. Bartholin L, Cyprian FS, Vincent D, Garcia CN, Martel S, Horvat B, Berthet C, Goddard-Leon S, Treilleux I, Rimokh R*, et al.* (2008) Generation of mice with conditionally activated transforming growth factor beta signaling through the TbetaRI/ALK5 receptor. *Genesis* **46:** 724-731
11. Anderberg C, Cunha SI, Zhai Z, Cortez E, Pardali E, Johnson JR, Franco M, Paez-Ribes M, Cordiner R, Fuxe J*, et al.* (2013) Deficiency for endoglin in tumor vasculature weakens the endothelial barrier to metastatic dissemination. *J Exp Med* **210:** 563-579
12. Eleftheriou NM, Sjolund J, Bocci M, Cortez E, Lee SJ, Cunha SI, Pietras K (2016) Compound genetically engineered mouse models of cancer reveal dual targeting of ALK1 and endoglin as a synergistic opportunity to impinge on angiogenic TGF-beta signaling. *Oncotarget*, 10.18632/oncotarget.12604
13. Larrivee B, Prahst C, Gordon E, del Toro R, Mathivet T, Duarte A, Simons M, Eichmann A (2012) ALK1 signaling inhibits angiogenesis by cooperating with the Notch pathway. *Developmental cell* **22:** 489-500
14. Cunha SI, Pietras K (2011) ALK1 as an emerging target for antiangiogenic therapy of cancer. *Blood* **117:** 6999-7006
15. Zudaire E, Gambardella L, Kurcz C, Vermeren S (2011) A computational tool for quantitative analysis of vascular networks. *PloS one* **6:** e27385

Figure 1

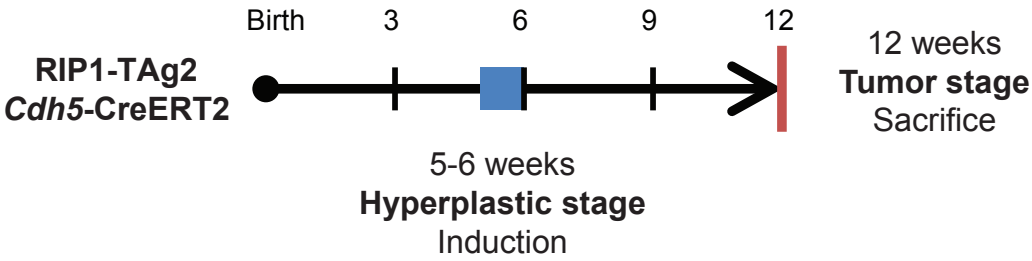
Birth
3
6
9
12
RIP1-TAg2
Cdh5-CreERT2
12 weeks
Tumor stage
Sacrifice
5-6 weeks
Hyperplastic stage
Induction

Figure 2

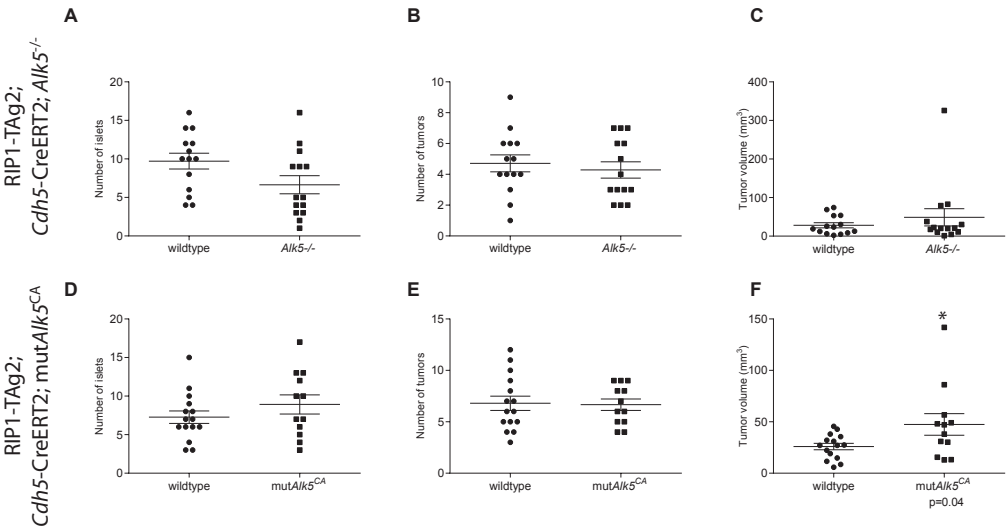
RIP1-TAg2; Cdh5-CreERT2; Alk5-/-
RIP1-TAg2; Cdh5-CreERT2; mutAlk5CA
A
B
C
D
E
F
Number of islets
Number of tumors
Tumor volume (mm3)
wildtype
Alk5-/-
mutAlk5CA
*
p=0.04

Figure 3

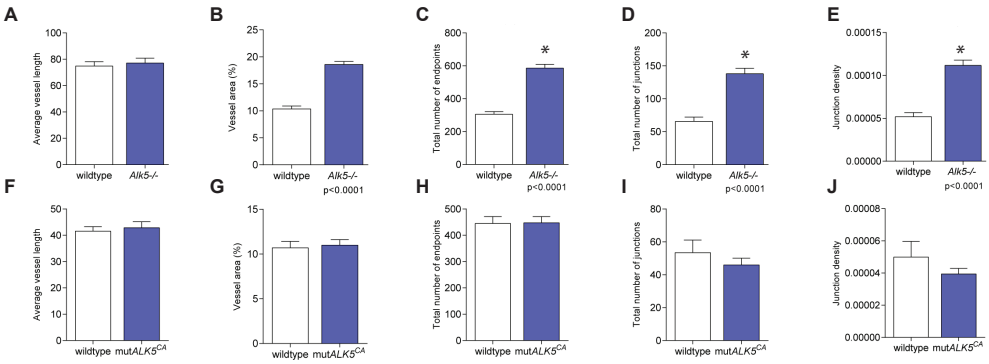

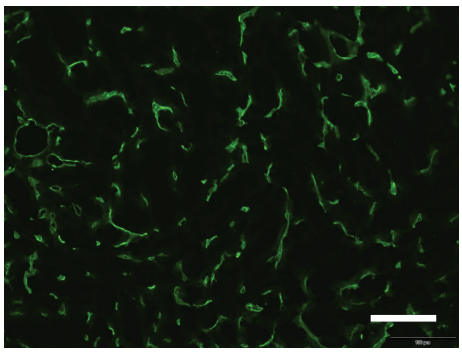

RIP1-TAg2

Podocalyxin

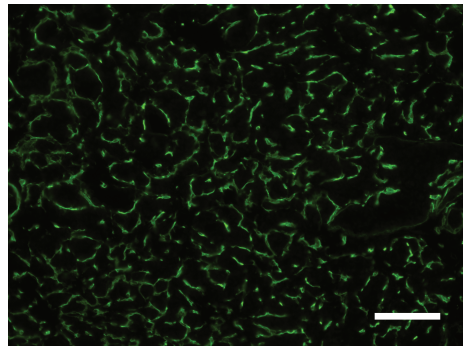

RIP1-TAg2; *Cdh5*-CreERT2; *Alk5*$^{-/-}$

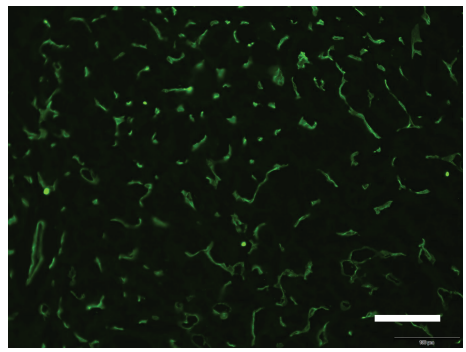

RIP1-TAg2; *Cdh5*-CreERT2; mut*Alk5*^{CA}

Figure 4

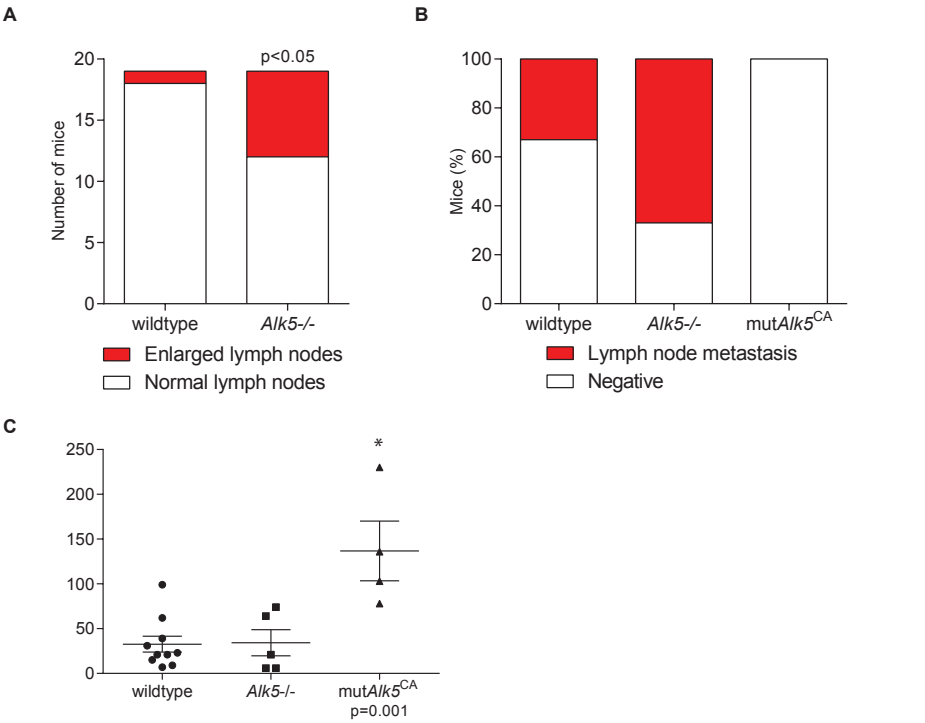

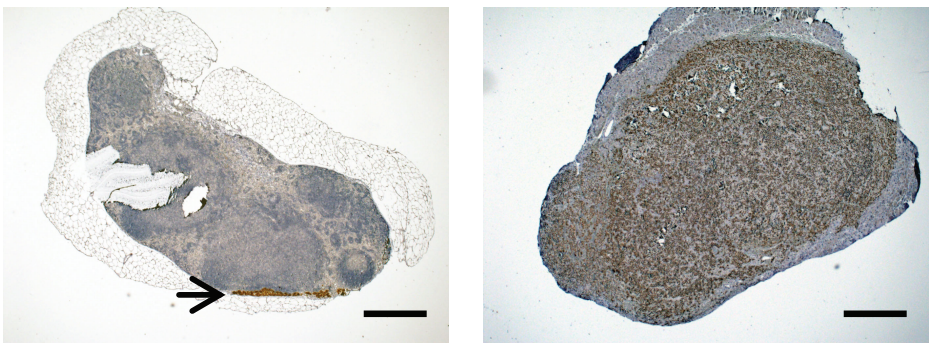

RIP1-TAg2

T-antigen Hematoxylin

RIP1-TAg2; *Cdh5*-CreERT2; mut*Alk5*^{CA}

Figure 5

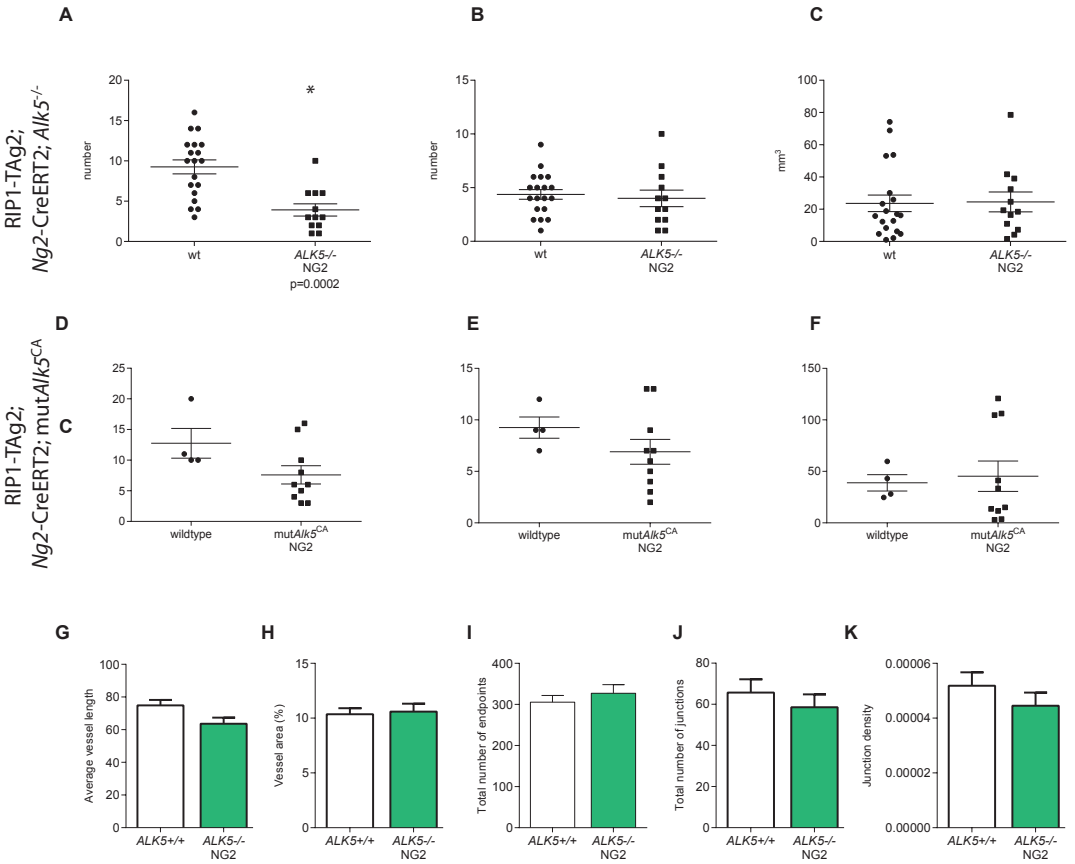
A
B
C
RIP1-TAg2; Ng2-CreERT2; Alk5-/-
number
mm3
wt
ALK5-/- NG2
p=0.0002
D
E
F
RIP1-TAg2; Ng2-CreERT2; mutAlk5CA
wildtype
mutAlk5CA NG2
G
H
I
J
K
Average vessel length
Vessel area (%)
Total number of endpoints
Total number of junctions
Junction density
ALK5+/+
ALK5-/- NG2

Paper IV

Exploring novel targeting opportunities of endothelial TGF-β signaling during tumor angiogenesis

Nikolas Eleftheriou[1,2], Matteo Bocci[1,2], Ewa Kurzejamska[1,2], Sara Cunha[3], Eugenia Cordero[2], Kristian Pietras[2,4]

[1]Shared authors
[2]Department of Laboratory Medicine, Lund University
[3]Department of Immunology, Genetics and Pathology, Uppsala University
[4]Corresponding author: kristian.pietras@med.lu.se

December 29, 2016

Introduction

Tumor initiation is fueled by genetic aberrations that cancel the physiological programs for growth control to allow unrestrained proliferation of cancer cells. However, over the past decades, it has become evident that cancer cells need a permissive environment in order to thrive [1,2]. The tumor micro-organ is populated by a host of different cell types, including cancer-associated fibroblasts, cells of the innate and the adaptive immune response, as well as endothelial cells and pericytes in the angiogenic vasculature. Blockade of the hallmark cancer cell capability of inducing neo-angiogenesis was long heralded as a major opportunity to achieve cancer cure due to interference with the delivery of oxygen and nutrients to the expanding tumor tissue [3]. Following successful pre-clinical testing, the experience from clinical trials has been sobering with improvements measured in months of progression-free survival in metastatic patients, with only minor impact on the overall survival [4,5]. Current anti-angiogenic therapies are all based on inhibition of signaling initiated by the vascular endothelial growth factor (VEGF) family, which by itself promotes endothelial cell proliferation, migration, sprouting and tube formation [6]. However, with a rapidly expanding knowledge base on the biology of tumor angiogenesis, the prospects of developing new mechanism-based drugs as partners in combination therapies are improving.

Members of the transforming growth factor (TGF)-β family of extracellular signaling proteins modulate a wide variety of cellular processes, including growth control, survival, and differentiation in mammalian cell types[7]. The more than 30 different ligands in the family bind and activate heterotetrameric complexes of TGF-β type I receptors and type II receptors. In addition, accessory TGF-β type III receptors may further modulate the outcome. Endothelial cells typically express the TGF-β type I receptors ALK1 and ALK5, which compete for binding of the prototypical TGF-β ligand in complex with the TGF-β type II receptor (TGFBR2) and the TGF-β type III receptor endoglin. Gene targeting studies in mice have revealed a critical role for TGF-β during developmental angiogenesis with deficiencies for ALK1, ALK5, TGFBR2, endoglin and TGF-β resulting in embryonic lethality due to vascular malformations and/or stunted blood vessel development [8-10]. Drug development to block tumor angiogenesis by impinging on TGF-β family signaling has focused on the development of inhibitors of ALK1 and endoglin, due to their endothelial cell-selective expression pattern. Pharmacological or genetic targeting studies of ALK1 in mouse models of cancer have demonstrated potent anti-angiogenic effects, resulting in tumor stasis and stunted metastatic colonization. While neutralizing antibodies against endoglin also reduce tumor growth in a range of tumors, caution is raised by gene

targeting studies revealing that deficiency for endoglin is associated with increased metastatic seeding [11]. Similarly, our recent study on the ALK1 ligand bone morphogenetic protein (BMP) 9 demonstrate augmented formation of metastases in the absence of BMP9 [12]. Less is known about the impact of targeting the interaction partner of TGF-β, ALK1 and endoglin, *i.e.* TGFBR2. Clearly, in depth mechanistic studies are warranted to determine the optimal targeting strategy to interfere with TGF-β induced tumor angiogenesis.

Here, using genetically engineered mouse models of cancer, we have extended the characterization of pharmacological targeting of endothelial cell TGF-β signaling by exploring the timing of inhibition, as well as the target identity. We have investigated the utility of post-surgical ALK1 inhibition in mouse models of breast cancer; an indication in which anti-VEGF therapy has not been efficacious and new anti-angiogenic treatment strategies are needed. In addition, we have generated TGFBR2-deficient mouse models of pancreatic neuroendocrine tumors (PNET); a malignant disease in which monotherapy with anti-VEGF compounds has proven efficacy and an opportunity for combinatorial therapies is evident. Finally, we have further explored the cellular and molecular mechanism behind the growth-inhibitory effects of ALK1 blockade.

Results and Discussion

ALK1 blockade is efficacious as a single agent in treating experimental breast cancer

Treatment of patients with advanced breast cancer with the VEGF receptor tyrosine kinase inhibitor sunitinib or with the VEGFA-neutralizing antibody bevacizumab does not provide an advantage in overall survival [13,14]. In our previous pre-clinical studies, we demonstrated efficacy of the ALK1-targeting agent RAP-041 in a range of different mouse models of breast cancer [15]. Here, we have extended our experimental trial scheme by exploring the combined administration of RAP-041 and the VEGFR2-targeting antibody DC101 to genetically engineered MMTV-PyMT mice. As previously reported, blockade of ALK1 delayed the growth of mammary carcinomas and at the conclusion of the trial, mice treated with RAP-041 presented with tumors that were 45% smaller than mice treated with control IgG (Fig. 1). Similarly, VEGFR2 inhibition with DC101 produced a 62% growth retardation (Fig. 1). However, while the combination of RAP-041 and DC101 proved safe and tolerable (data not shown), the tumor growth delay was only marginally longer than for each mono-therapy (Fig. 1). In contrast to our findings, previous pre-clinical studies in melanoma and renal cell carcinoma xenografts have demonstrated additive or synergistic effect of treatment with ALK1-blocking agents and anti-VEGF therapies [16,17]. A phase 2 clinical trial testing the combination of ACE-041 (dalantercept; the human counterpart of RAP-041) and the VEGF receptor tyrosine kinase inhibitor axitinib is currently underway (ClinicalTrials.gov identifier NCT01727336). The discrepancy can be partly explained by differences in the inherent sensitivity of particular malignant diseases to anti-angiogenic therapies. While the experience from several clinical trials in breast cancer suggest a high degree of resistance to anti-VEGF therapies, such as sunitinib and bevacizumab [14,18], renal cell carcinoma patients benefit from several different treatments involving drugs impinging on VEGF signaling, including sunitinib, sorafenib, axitinib and bevacizumab[19].

While pre-clinical trials are most often performed with growth of the tumor at its primary location as a readout, breast cancer patients are more likely to receive post-surgical therapy in order to reduce the risk of relapse. To more closely mimic treatment in the adjuvant setting, we established a protocol for surgical resection of tumors derived from the estrogen receptor-positive mouse mammary carcinoma E0771. Tumor cells were injected into the mammary fat pad of C57Bl/6 mice, after which they were allowed to grow until the longest diameter reached 13 mm. Next, the tumor was surgically removed and mice were started on adjuvant therapy one

week later when the incisions were fully healed (Fig. 2A). Strikingly, 4 weeks of treatment with ALK1 inhibitor reduced the number of macrometastatic lesions in the lungs from an average of 8.3±9.1 in control IgG-treated mice to 2.0±2.3 in RAP-041-treated mice (Fig. 2B). Further, the incidence of mice with more than 1 pulmonary lesion was 11/14 in the control group, but only 3/13 in mice that received RAP-041. The efficacy of ALK1-blockade in the adjuvant setting was corroborated by the use of the syngeneic 4T1 mouse model of mammary carcinoma (Fig. 2C). Thus, ALK1 inhibition appears a tolerable and promising candidate for adjuvant therapy of breast cancer with anti-metastatic efficacy even as a single agent. However, to gain approval in clinical routine, inhibition of ALK1 would have to be tested as an add-on to existing standard-of-care. We have previously evaluated the combination of RAP-041 and docetaxel in the neo-adjuvant setting, with promising results [15], but the efficacy in the adjuvant setting remains to be determined.

ALK1 blockade modulates the immune cell repertoire of experimental mammary carincomas

The cellular and molecular mechanism behind the efficacy of RAP-041 in mouse models of breast cancer remains uncertain. While ALK1 blockade readily reduces the vascular density and perfusion of tumors [15,20], treatment with RAP-041 does not provoke hypoxia, as measured by stabilization of HIF1-α [15]. In order to probe a potential immunomodulatory role of ALK1 signaling, we profiled the abundance of various immune cell types in tumors from MMTV-PyMT mice that underwent RAP-041 treatment from 11-15 weeks of age. Immunohistochemical staining of CD45, a universal leukocyte marker, did not reveal an overt difference in the overall recruitment of bone marrow-derived immune cells following ALK1 blockade (Fig. 3A-B). Similarly, the number of F4/80-positive macrophages infiltrating the tumor parenchyma was not changed by stunted ALK1 signaling (Fig. 3C-D). Next, we assessed the extent of total T-cell recruitment by immunostaining for CD3. Interestingly, tumors from MMTV-PyMT mice treated with RAP-041 were profusely infiltrated with T-cells, in contrast to mammary lesions from control-treated mice (Fig. 3E-F), raising the possibility that ALK1 signaling governs trafficking of T-cells across the endothelium and/or T-cell activation. Indeed, preliminary analysis of gene expression by use of a quantitative PCR array indicated that genes related to T-cell activation and proliferation, most notably IFN-γ, are more abundantly expressed upon blockade of ALK1 signaling (data not shown). Taken together, blockade of ALK1 signaling with RAP-041 modulates immune cell trafficking and/or activation, revealing a potential mechanism of action for the anti-tumor efficacy. Importantly, our work highlights the need for using immunocompetent

mouse models of cancer in pre-clinical testing of drugs with potential immunomodulatory action. We have previously delineated a role for the endothelial cell-restricted TGF-β type III receptor endoglin in the control of trans-endothelial migration of malignant cells in a range of different malignant diseases, including breast cancer [11]. A reduced gene dosage of endoglin resulted in spontaneous induction of endothelial-to-mesenchymal transition through enhanced signaling by ALK5, which endorsed migration of malignant cells across the endothelial monolayer. The possibility that ALK1 signaling modulates trafficking of immune cells across the tumor endothelium warrants future studies.

TGFBR2 is an alternative target for impinging on endothelial TGF-β signaling

In order to determine the optimal target within the TGF-β family for anti-angiogenic therapy, we have previously generated genetically engineered mice with global deficiencies for ALK1, endoglin and BMP9 based on the widely studied RIP1-TAg2 mouse model for multistep pancreatic neuroendocrine tumorigenesis [11,12,20]. Intriguingly, despite acting in concert within the same signaling pathway, the resulting phenotypes from gene targeting studies are very disparate. Briefly, ALK1 deficiency reduced the number of pre-malignant angiogenic lesions and overall tumor burden. In contrast, global deficiency for endoglin did not result in lasting tumor growth retardation and in addition fueled metastatic dissemination. Mice carrying a disrupted gene for BMP9 present with a mixed phenotype with stunted growth of primary tumors, while the growth of metastatic lesions is augmented. However, our efforts so far have only included mice with ubiquitous genetic deficiencies in all cell types and throughout embryonic development and adulthood. Conceivably, targeting of genes in a cell type-specific and temporally controlled manner may produce a more reliable picture of gene function.

First, we generated compound genetically engineered RIP1-TAg2 mice with conditional and temporally controllable alleles of the gene for endoglin to enable endothelial cell-specific knock-out at any time during tumorigenesis (RIP1-TAg2; Cdh5-CreERT2; Eng fl/fl). Induction of endoglin deficiency in endothelial cells of RIP1-TAg2 mice at the pre-angiogenic stage of tumor development (5-6 weeks of age) corroborated our previous studies [11]. Hence, while endoglin deficiency resulted in a reduced number of overt tumors, this did not translate into a significant reduction in the size of tumors (Fig. 4A-C). Our findings that an endothelial cell-specific knock-out of endoglin phenocopies global deficiency lend support to the notion that endoglin is predominantly expressed and functional in the vasculature.

Second, we assessed the utility of targeting TGFBR2 in endothelial cells to achieve anti-angiogenic efficacy by generating RIP1-TAg2; Cdh5-CreERT2; TGFBR2 fl/fl mice. RIP1-TAg2 mice bearing *Tgfbr2* endothelial knockouts presented with an approximately 50% reduction in the number of angiogenic islets and tumors, and total tumor volume (Fig 5A-C), demonstrating a critical impact of TGFBR2 signaling during pancreatic neuroendocrine tumorigenesis. In addition, deficiency for *Tgfbr2* in endothelial cells resulted in fewer metastatic hepatic lesions and a lower incidence of lymphatic involvement (4/12 control mice *vs* 1/6 *Tgfbr2*-deficient mice), although the differences did not reach statistical significance (Fig. 6A-B). Next, we assessed the extent of vascularization of pancreatic neuroendocrine tumors. Mice with the endothelial-specific deletion of *Tbgbr2* displayed a vessel network of disorganized and poorly defined vessels with glomeruloid features (Fig. 7A). Quantitatively, deficiency for *Tgfbr2* resulted in a statistically significant increase in the number of vessel junctions and in vessel length, as compared to control mice (Fig 7B-F). Deletion of the gene for *Tgfbr2* in fibroblasts results in promotion of *de novo* tumorigenesis in the prostate, forestomach and mammary epithelium [21,22]. Thus, while pharmacological inhibition of TGFBR2 in the tumor vasculature appears as a promising strategy to pursue further, caution is warranted due to potential contrasting effects in different cell types or tissues. Targeting of *Tgfbr2* resulted in hypersprouting and/or hyperproliferation of the endothelium. ALK1 has been reported to act in concert with Notch/DLL4 signaling to govern the balance between tip and stalk cell identity [23]. It remains to be determined whether TGFBR2 is a partner for ALK1 in the crosstalk with Notch, but the observed hypersprouting upon disruption of *Tgfbr2* would suggest this as a distinct possibility. Alternatively, the *Tgfbr2* deficiency in endothelial cells may have relieved a growth-inhibitory effect of TGF-β, resulting in hyperproliferation. Further studies to discriminate between effects on sprouting or proliferation are warranted and include analysis of tip cell markers and Ki67 by immunostaining.

Taken together, we have demonstrated the utility of targeting TGF-β signaling in the neo-vasculature of malignant disease through pre-clinical studies utilizing genetic or pharmacological tools. Our work highlights the need for careful and systematic charting of potential drug targets, even within the same signaling family, as well as combination partners in order to prepare for well-informed mechanism-based clinical trials.

Materials and Methods

Animal work

In vivo mouse experiments were approved by Lunds ethical committees for animal care (permit M142/13).

Orthotopic tumor resection

8 week old female C57BL/6 mice were injected with $5x10^5$ E0771 or $1x10^5$ 4T1 cells into the 4th mammary fat pad, and primary tumors were excised once the diameter reached 13 or 4mm, respectively. One week post-surgery mice were treated twice weekly with RAP-041 (Acceleron) or IgG2a at 12mg/kg body weight by i.p. injection for four weeks, and then sacrificed. Lung macrometastases were counted as any visible lesions presented on the lung surface.

MMTV-PyMT ALK1-Fc treatment

Female MMTV-PyMT mice at 8 weeks of age were treated with RAP-041 (12mg/kg, Accelteron), DC101 (20mg/kg, ImClone Systems) or IgG2a by i.p. injection for four weeks, and then sacrificed. At sacrifice, mice are heart perfused with 10ml PBS followed by 10mL buffered zinc formalin.

Tgfbr2 knockout

C57BL/6 RIP1-TAg2; Cdh5-CreERT2 mice received IP tamoxifen (75mg/kg body weight; Sigma) or corn oil (Sigma) at five weeks age for five consecutive days, and water supplemented with 5% sucrose at ten through twelve weeks of age. Mice were sacrificed at 12 weeks of age. At sacrifice, mice are heart perfused with 10ml PBS followed by 10mL buffered zinc formalin.

RIP1-TAg2 Tumor measurements

Primary tumors are counted as all neoplasms ≥ 1mm in diameter, and remaining angiogenic islets are counted under a stereological microscope. The tumor volume is counted from the total volume of all tumors in one mouse pancreas, each calculated as length × 2width × $\pi/6$.

Immunofluorescence and vessel analysis

Primary tumor material from RIP1-TAg2 mice were stored in 30% sucrose overnight at 4°C, then stored in OCT cryoprotectant. Sections were cut at 8µm thickness, acetone fixed, and treated with serum-free blocking for 90min at room temperature. Sections were exposed to primary antibody anti-Podocalyxin antibody (dilution 1:100; R&D Systems, AF1556) overnight at

4°C, then Alexa-488nm secondary antibody (dilution 1:1000, Invitrogen) for 90min at room temperature, and treated with mounted media containing DAPI. Fluorescent images were acquired with an Olympus BX63 microscope, DP80 camera and cellSens Dimension v 1.12 software (Olypmus Corporation). 10 or more 20x-magnification images were taken per mouse, and analysis of the vessel tree was processed with Angiotool semi-automated software[24].

Immunohistochemistry and metastasis identification

Mammary tumors from MMTV-PyMT mice, and left lateral liver lobes and mesenteric lymph nodes from RIP1-TAg2 were fixed in formalin buffer overnight at 4°C and paraffin embedded following sacrifice. Each entire liver lobe was serially sectioned at 5µm thickness; every 34th section was deparaffinized and underwent hematoxylin and eosin staining. A focus of at least six cells in diameter was positively counted as a single micrometastasis. Mammary tumor and lymph node sections were cut at 5µm thickness, deparaffinized, treated with pH 10 antigen retrieval buffer, and endogenous peroxidase activity was quenched with 50% MeOH/3% H2O2.Sections were then blocked with appropriate 10% serum, and exposed to primary antibody overnight at 4°C. Following primary antibody incubation, sections were incubated with appropriate biotinylated secondary, then visualized using Vectastain ABC (Vector Laboratories) and DAB peroxidase substrate kits (Vector Laboratories). Primary antibodies used are anti-CD45 (dilution 1:50, BD-Pharmingen, 553076), anti-F4/80 (dilution 1:50, Abcam, ab6640), anti-CD3 (dilution 1:100, Abcam, ab16669) and anti-SV40 T-antigen antibody (dilution 1:10000, gift from Douglas Hanahan, EPFL).

Statistical analysis

Measurements are displayed as mean ± SEM. Statistics were performed using an unpaired two-tailed Student's t test, with significance threshold at $\alpha = 0.05$

Figures

1 Total tumor volume of MMTV-PyMT mouse mammary tumors over four weeks of treatment with RAP-041, DC101, RAP-041 and DC101 combination, or control IgG

2 (A) Experimental setup of orthotopic tumor resection trials for E0771 cell line, including insert image of lungs with metastatic lesions (black arrow). Number of lung metastases per mouse after post-resection treatment of IgG or RAP-041 with E0771 (B) or 4T1 (C) breast cancer cell lines

3 Immunohistochemistry images of the immune compartment in MMTV-PyMT breast tumor sections of mice treated with RAP-041 or IgG control; CD45 (A,B), F4/80 (C,D) and CD3 (E,F)

4 Number of angiogenic islets (A), tumors (B) and tumor volume (C) of tumors from RIP1-TAg2; *Cdh5*-CreERT2 mice, with conditional *eng* knockout at 12 weeks of age

5 Number of angiogenic islets (A), tumors (B) and tumor volume (C) of tumors from RIP1-TAg2 mice with conditional *Tgfbr2* knockout at 12 weeks of age

6 Total number of liver micrometastases per mouse in the left lateral liver lobe (A), and incidence of T-Antigen positive cells in lymph nodes (B) of RIP1-TAg2 mice with conditional *Tgfbr2* knockout

7 Representative images of podocalyxin-positive vessels in RIP1-TAg2 mice with conditional *Tgfbr2* knockout (A), and automated vessel analysis of vessel network features (B-F)

References

1. Quail DF, Joyce JA (2013) Microenvironmental regulation of tumor progression and metastasis. *Nature medicine* **19:** 1423-1437
2. Hanahan D, Coussens LM (2012) Accessories to the crime: functions of cells recruited to the tumor microenvironment. *Cancer Cell* **21:** 309-322
3. Kerbel RS (1997) A cancer therapy resistant to resistance. *Nature* **390:** 335-336
4. Kumler I, Christiansen OG, Nielsen DL (2014) A systematic review of bevacizumab efficacy in breast cancer. *Cancer Treat Rev* **40:** 960-973
5. Helfrich I, Scheffrahn I, Bartling S, Weis J, von Felbert V, Middleton M, Kato M, Ergun S, Schadendorf D (2010) Resistance to antiangiogenic therapy is directed by vascular phenotype, vessel stabilization, and maturation in malignant melanoma. *J Exp Med* **207:** 491-503
6. Cross MJ, Claesson-Welsh L (2001) FGF and VEGF function in angiogenesis: signalling pathways, biological responses and therapeutic inhibition. *Trends Pharmacol Sci* **22:** 201-207
7. Huminiecki L, Goldovsky L, Freilich S, Moustakas A, Ouzounis C, Heldin CH (2009) Emergence, development and diversification of the TGF-beta signalling pathway within the animal kingdom. *BMC evolutionary biology* **9:** 28
8. Oshima M, Oshima H, Taketo MM (1996) TGF-β receptor type II deficiency results in defects of yolk sac hematopoiesis and vasculogenesis. *Dev Biol* **179:** 297-302
9. Arthur HM, Ure J, Smith AJ, Renforth G, Wilson DI, Torsney E, Charlton R, Parums DV, Jowett T, Marchuk DA*, et al.* (2000) Endoglin, an ancillary TGFbeta receptor, is required for extraembryonic angiogenesis and plays a key role in heart development. *Dev Biol* **217:** 42-53
10. ten Dijke P, Arthur HM (2007) Extracellular control of TGFbeta signalling in vascular development and disease. *Nature reviews. Molecular cell biology* **8:** 857-869
11. Anderberg C, Cunha SI, Zhai Z, Cortez E, Pardali E, Johnson JR, Franco M, Paez-Ribes M, Cordiner R, Fuxe J*, et al.* (2013) Deficiency for endoglin in tumor vasculature weakens the endothelial barrier to metastatic dissemination. *J Exp Med* **210:** 563-579
12. Eleftheriou NM, Sjolund J, Bocci M, Cortez E, Lee SJ, Cunha SI, Pietras K (2016) Compound genetically engineered mouse models of cancer reveal dual targeting of ALK1 and endoglin as a synergistic opportunity to impinge on angiogenic TGF-beta signaling. *Oncotarget*, 10.18632/oncotarget.12604
13. Miller K, Wang M, Gralow J, Dickler M, Cobleigh M, Perez EA, Shenkier T, Cella D, Davidson NE (2007) Paclitaxel plus bevacizumab versus paclitaxel alone for metastatic breast cancer. *The New England journal of medicine* **357:** 2666-2676
14. Bergh J, Bondarenko IM, Lichinitser MR, Liljegren A, Greil R, Voytko NL, Makhson AN, Cortes J, Lortholary A, Bischoff J*, et al.* (2012) First-line treatment of advanced breast cancer with sunitinib in combination with docetaxel versus docetaxel alone: results of a prospective, randomized phase III study. *J Clin Oncol* **30:** 921-929
15. Cunha SI, Bocci M, Lovrot J, Eleftheriou N, Roswall P, Cordero E, Lindstrom L, Bartoschek M, Haller BK, Pearsall RS*, et al.* (2015) Endothelial ALK1 Is a Therapeutic Target to Block Metastatic Dissemination of Breast Cancer. *Cancer research* **75:** 2445-2456
16. Hu-Lowe DD, Chen E, Zhang L, Watson KD, Mancuso P, Lappin P, Wickman G, Chen JH, Wang J, Jiang X*, et al.* (2011) Targeting Activin Receptor-Like Kinase 1 (ALK1) Inhibits Angiogenesis and Tumorigenesis Through a Mechanism of Action Complementary to Anti-VEGF Therapies. *Cancer research* **71:** 1362-1373
17. Wang X, Solban N, Khanna P, Callea M, Song J, Alsop DC, Pearsall RS, Atkins MB, Mier JW, Signoretti S*, et al.* (2016) Inhibition of ALK1 signaling with dalantercept combined with VEGFR TKI leads to tumor stasis in renal cell carcinoma. *Oncotarget* **7:** 41857-41869
18. Delaloge S, Perol D, Courtinard C, Brain E, Asselain B, Bachelot T, Debled M, Dieras V, Campone M, Levy C*, et al.* (2016) Paclitaxel plus bevacizumab or paclitaxel as first-line treatment for HER2-negative metastatic breast cancer in a multicenter national observational

study. *Annals of oncology : official journal of the European Society for Medical Oncology* **27:** 1725-1732
19. Rousseau B, Kempf E, Desamericq G, Boissier E, Chaubet-Houdu M, Joly C, Saldana C, Boussion H, Neuzillet C, Macquin-Mavier I*, et al.* (2016) First-line antiangiogenics for metastatic renal cell carcinoma: A systematic review and network meta-analysis. *Critical reviews in oncology/hematology* **107:** 44-53
20. Cunha SI, Pardali E, Thorikay M, Anderberg C, Hawinkels L, Goumans MJ, Seehra J, Heldin CH, Ten Dijke P, Pietras K (2010) Genetic and pharmacological targeting of activin receptor-like kinase 1 impairs tumor growth and angiogenesis. *J Exp Med* **207:** 85-100
21. Bhowmick NA, Chytil A, Plieth D, Gorska AE, Dumont N, Shappell S, Washington MK, Neilson EG, Moses HL (2004) TGF-beta signaling in fibroblasts modulates the oncogenic potential of adjacent epithelia. *Science* **303:** 848-851
22. Cheng N, Bhowmick NA, Chytil A, Gorksa AE, Brown KA, Muraoka R, Arteaga CL, Neilson EG, Hayward SW, Moses HL (2005) Loss of TGF-beta type II receptor in fibroblasts promotes mammary carcinoma growth and invasion through upregulation of TGF-alpha-, MSP- and HGF-mediated signaling networks. *Oncogene* **24:** 5053-5068
23. Larrivee B, Prahst C, Gordon E, del Toro R, Mathivet T, Duarte A, Simons M, Eichmann A (2012) ALK1 signaling inhibits angiogenesis by cooperating with the Notch pathway. *Developmental cell* **22:** 489-500
24. Zudaire E, Gambardella L, Kurcz C, Vermeren S (2011) A computational tool for quantitative analysis of vascular networks. *PloS one* **6:** e27385

Figure 1

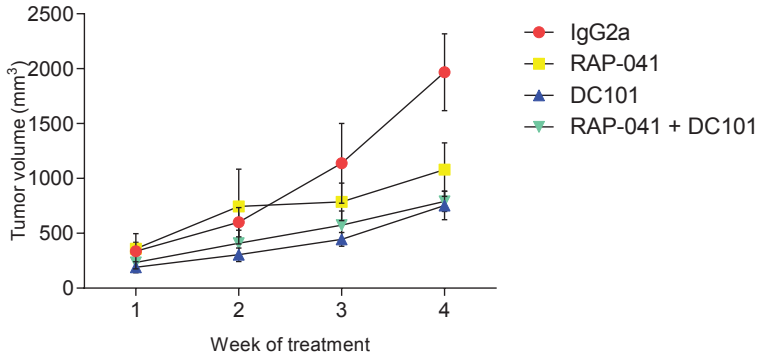
2500
2000
1500
1000
500
0
Tumor volume (mm3)
1
2
3
4
Week of treatment
IgG2a
RAP-041
DC101
RAP-041 + DC101

Figure 2

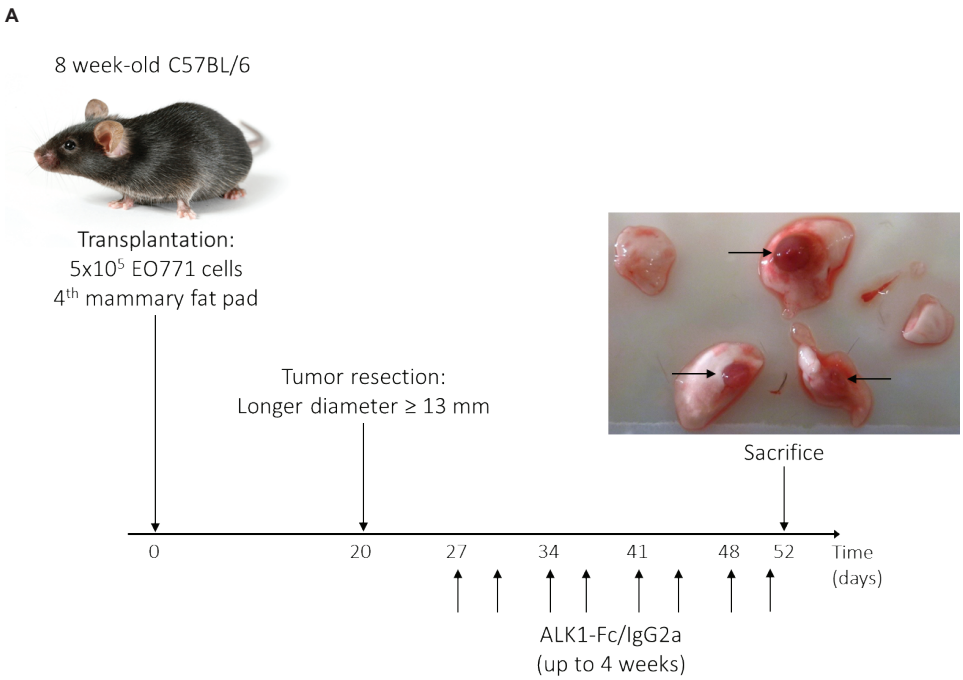
A
8 week-old C57BL/6
Transplantation:
5x10^5 EO771 cells
4th mammary fat pad
Tumor resection:
Longer diameter ≥ 13 mm
Sacrifice
0
20
27
34
41
48
52
Time
(days)
ALK1-Fc/IgG2a
(up to 4 weeks)

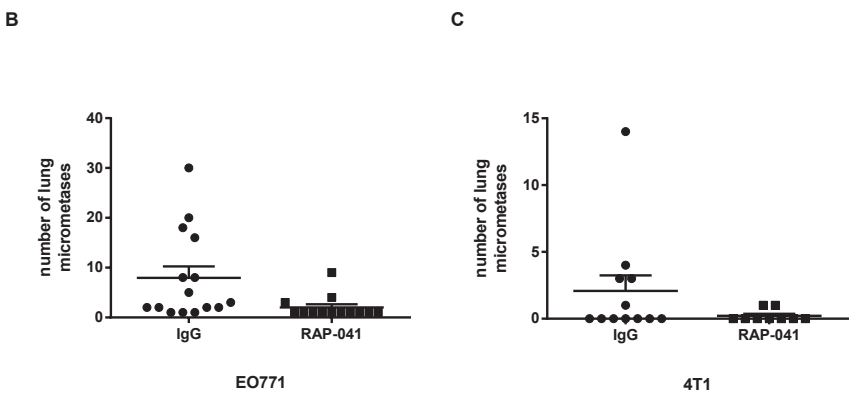
B
number of lung micrometases
40
30
20
10
0
IgG
RAP-041
EO771
C
number of lung micrometases
15
10
5
0
IgG
RAP-041
4T1

Figure 3

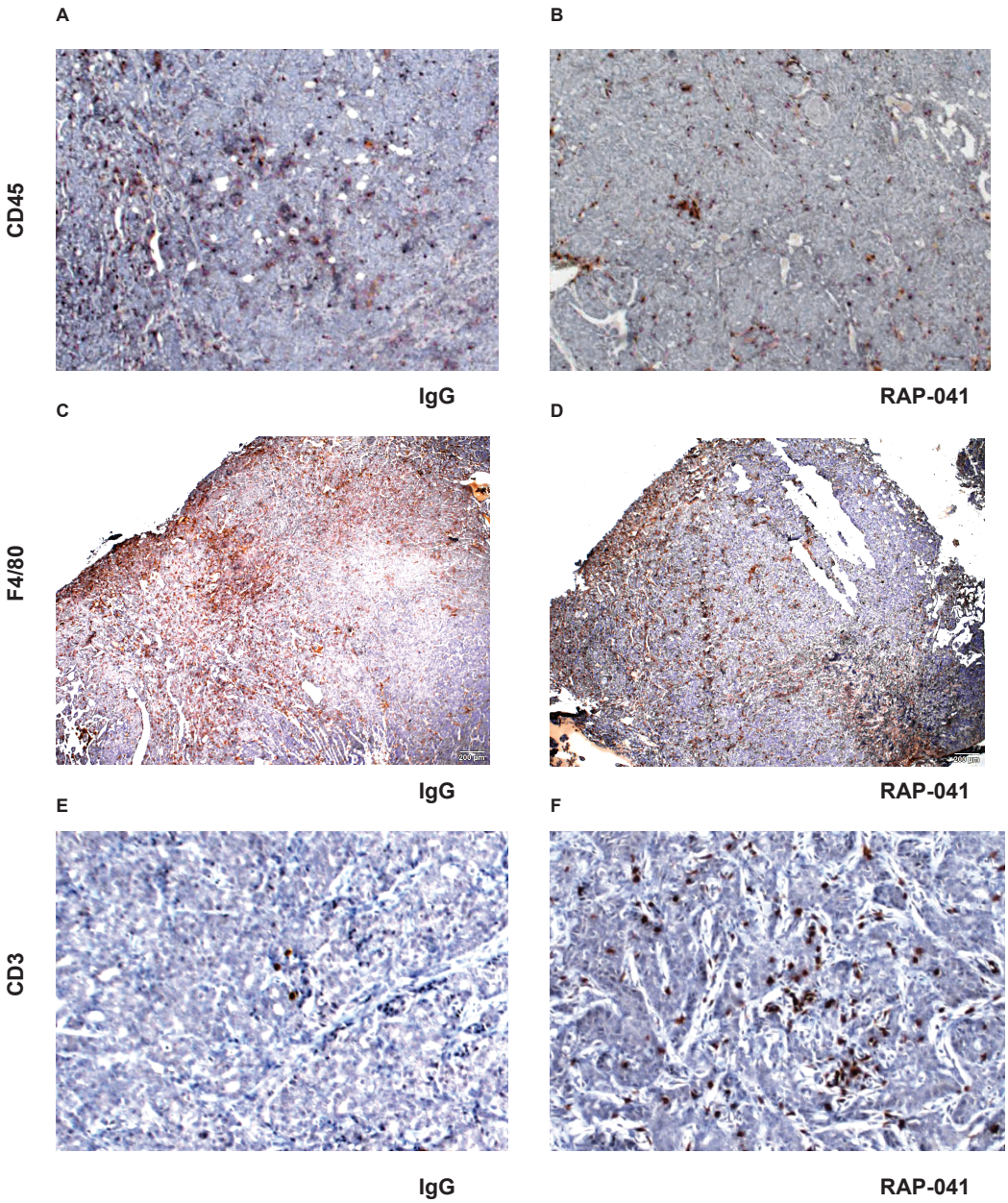

Figure 4

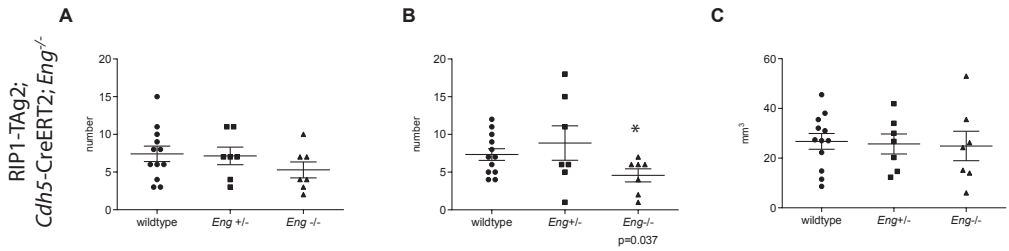
RIP1-TAg2;
Cdh5-CreERT2; Eng-/-
A
number
20
15
10
5
0
wildtype
Eng +/-
Eng -/-
B
number
20
15
10
5
0
*
wildtype
Eng+/-
Eng-/-
p=0.037
C
mm3
60
40
20
0
wildtype
Eng+/-
Eng-/-

Figure 5

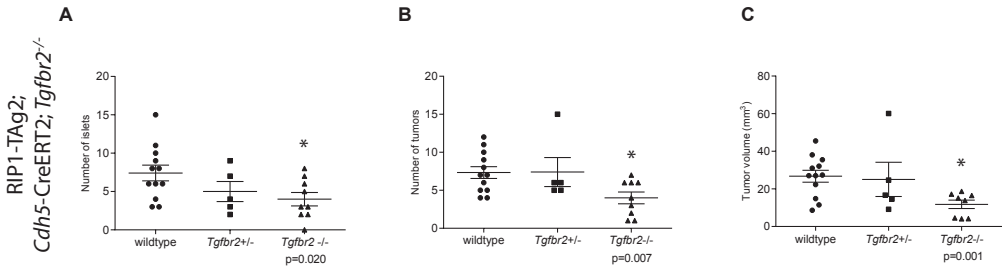
RIP1-TAg2;
Cdh5-CreERT2; Tgfbr2-/-
A
Number of islets
20
15
10
5
0
wildtype
Tgfbr2+/-
Tgfbr2 -/-
p=0.020
*
B
Number of tumors
20
15
10
5
0
wildtype
Tgfbr2+/-
Tgfbr2-/-
p=0.007
*
C
Tumor volume (mm3)
80
60
40
20
0
wildtype
Tgfbr2+/-
Tgfbr2-/-
p=0.001
*

Figure 6

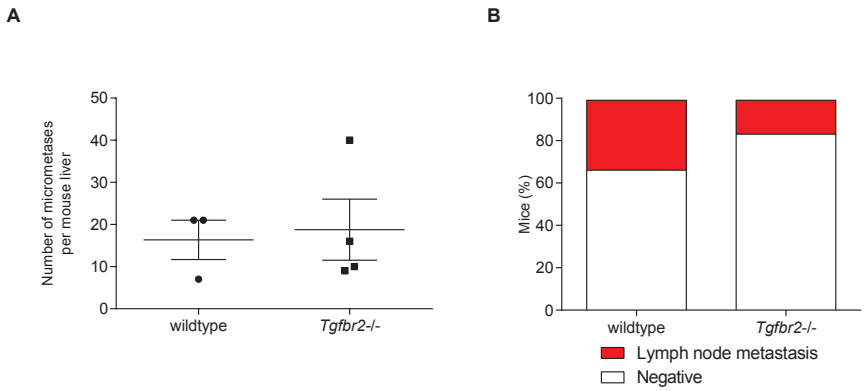
A
B
Number of micrometases per mouse liver
50
40
30
20
10
0
wildtype
Tgfbr2-/-
Mice (%)
100
80
60
40
20
0
wildtype
Tgfbr2-/-
Lymph node metastasis
Negative

Figure 7

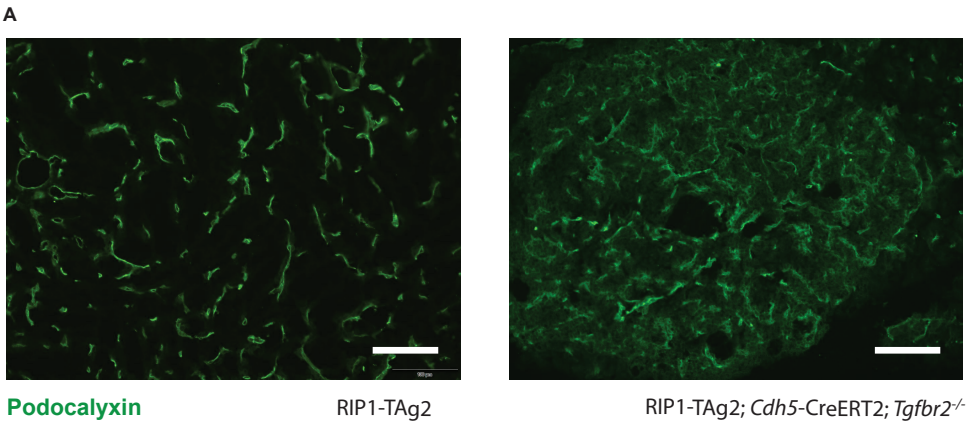
A
Podocalyxin
RIP1-TAg2
RIP1-TAg2; Cdh5-CreERT2; Tgfbr2-/-
B
Average vessel length
wildtype
TGFBR2+/-
TGFBR2-/-
p<0.001
p<0.01
C
Vessel area (%)
wildtype
TGFBR2+/-
TGFBR2-/-
D
Total number of endpoints
wildtype
TGFBR2+/-
TGFBR2-/-
p=0.001
E
Total number of junctions
wildtype
TGFBR2+/-
TGFBR2-/-
p=0.002
F
Junctions density
wildtype
TGFBRII +/+
TGFBRII -/-
p=0.001

Printed by Media-Tryck, Lund University 2017 | Nordic Ecolabel 3041 0903

LUND UNIVERSITY
Faculty of Medicine

Lund University, Faculty of Medicine
Doctoral Dissertation Series 2017:42
ISBN 978-91-7619-422-5
ISSN 1652-8220